Chalcogen-Bridged Copper Clusters

Stefanie Dehnen,[a] Andreas Eichhöfer,[b] and Dieter Fenske*[a]

Dedicated to Professor Günter Schmid on the occasion of his 65th birthday

Keywords: Copper / Sulfur / Selenium / Tellurium / Clusters

The investigation of coinage metal molecular clusters bridged by chalcogen atoms represents an area of ever increasing activity in recent chemical and material science research. This is largely due to the relatively high ionic and even higher electric conductivity of binary coinage metal chalcogenides, which leads to properties intermediate between those of semiconducting and metallic phases. In addition, the size-dependency of the chemical, physical, and structural properties of substances on going from small molecules to bulk materials is of general interest. Approaches towards the synthesis and investigation of such clusters have included the study of colloidal nanoparticles with a narrow size distribution, as well as the formation and isolation of crystalline cluster compounds amenable to structural determination by single-crystal X-ray diffraction analysis. Irrespective of the chosen synthesis route, the molecules have to be kinetically protected from decomposition to the thermodynamically favored binary phases by a suitable ligand sphere, often consisting of tertiary phosphane molecules, or a combination of phosphanes and organic groups. In this report, we concentrate on the syntheses and structural as well as physical properties of ligand-stabilized, chalcogen-bridged copper clusters, which have been comprehensively studied by means of experimental and quantum chemical investigations.

[a] Institut für Anorganische Chemie der Universität Karlsruhe (TH),
Engesserstraße, Geb. 30.45, 76128 Karlsruhe, Germany
Fax: (internat.) +49 (0)721/608-7021
E-mail: Dieter.Fenske@chemie.uni-karlsruhe.de
[b] Institut für Nanotechnologie, Forschungszentrum Karlsruhe GmbH,
Postfach 3640, 76021 Karlsruhe, Germany
Fax: (internat.) +49 (0)7247/82-6368

1. Introduction

The synthesis of chalcogen-bridged molecular clusters of the coinage metal elements represents an area of ever increasing activity in recent chemical and material science research. This can be mainly ascribed to two aspects. Firstly, binary coinage metal chalcogenides exhibit relatively high

Andreas Eichhöfer (left) was born in Hünfeld, Germany, in 1964. He received his diploma in 1991, and subsequently graduated in 1993 in the group of Prof. D. Fenske at the university of Karlsruhe with a doctoral degree on metal-phosphorous cluster complexes. He then moved to the group of Prof. G. Fritz at the same institute to work on carbosilanes as precursor compounds for the fabrication of SiC fibers. After that he returned to his previous group and became a research scientist at the Institute of Nanotechnology at the Forschungszentrum Karlsruhe in 1999, where he is currently investigating the syntheses and properties of semiconductor cluster compounds.

Stefanie Dehnen (center) was born in Gelnhausen, Germany, in 1969. She obtained her diploma from the University of Karlsruhe in 1993 and her doctoral degree in 1996 under the supervision of Prof. D. Fenske on experimental and theoretical investigations of copper sulfide and copper selenide clusters. After a postdoctoral stay with Prof. R. Ahlrichs (1997) she returned to the inorganic chemistry department at the University of Karlsruhe where she is presently preparing her Habilitation. In 1997, she was awarded a Feodor-Lynen-Stipendium of the Alexander-von-Humboldt-Stiftung, and in 1998, she received a Margarete-von-Wrangell-Habilitations-Stipendium of the state of Baden-Württemberg. Her current research interests comprise the synthesis, structural elucidation and chemical reactivity of binary or ternary polyanions of main group elements.

Dieter Fenske (right) was born in Dortmund, Germany, in 1942. He studied chemistry at the University of Münster where he also received his doctoral degree in 1973 with Prof. H. J. Becher. After the completion of his Habilitation at the University of Münster in 1978, he became Professor of Inorganic Chemistry at the University of Karlsruhe in 1981. Five years later, he was offered a Chair of Inorganic Chemistry at the University of Frankfurt, from where he returned to the University of Karlsruhe in 1988 to become Chair of Inorganic Chemistry. He received offers for the same position from the Universities of Marburg and Münster and is a laureate of the Leibniz Award and the Wilhelm Klemm Award. In 1998 he became Director of the Institute of Nanotechnology at the Forschungszentrum Karlsruhe. His research field concerns the synthesis, structures, and properties of main group element-bridged clusters of transition metals, especially group 8–10 elements.

MICROREVIEWS: This feature introduces the readers to the authors' research through a concise overview of the selected topic. Reference to important work from others in the field is included.

  1434–1948/02/0202–0279 $ 17.50+.50/0

ionic[1] and even higher electric[2] conductivity in the solid state, leading to properties intermediate between those of semiconducting and metallic phases. Secondly, the size-dependence of the chemical, physical, and structural properties of substances on going from small molecules to bulk materials is of general interest.[3] Several research groups have concentrated on the synthesis and properties of colloid nanoparticles with narrow cluster size distributions.[4] Another approach is the formation and isolation of crystalline cluster compounds suitable for single-crystal X-ray diffraction analysis. In both cases, the molecules have to be kinetically protected from further reaction to the thermodynamically favored binary phases. Therefore, a ligand sphere coordinating to the outer metal or chalcogen atoms is necessary; in most cases this consists of tertiary phosphane molecules or a combination of phosphanes and organic groups.

In this paper, we focus on ligand-stabilized, chalcogen-bridged copper clusters, which have hitherto been the most frequently studied. Experimental[5−33] and quantum chemical[34−37] investigations have been undertaken during the last decade in order to study the transition from the definitely non-metallic Cu_2E monomer (E = S, Se, Te) to the bulk Cu_2E.[38−40] From a synthetic point of view, the most important result was the elucidation of the close relationship between the chosen reaction conditions and the formation of the desired products, together with the use of this knowledge in the synthesis of different cluster types.[9−31] Furthermore, the great number of isolated and structurally characterized cluster compounds and the comprehensive computational work[34−37] in this area has allowed the delineation and rationalization of size-dependent structure principles for these molecules. Last but not least, various calculations and measurements have been carried out to obtain insights into the physical properties of the cluster materials.[32,33]

2. General Synthetic Routes

The compounds are − with some exceptions − highly air- and moisture-sensitive. Therefore, all reaction steps have to be carried out under strict exclusion of air and moisture in a high purity dried nitrogen atmosphere by employing standard Schlenk-line techniques on a double-manifold vacuum line. All solvents must be dried and freshly distilled prior to use.

Most chalcogen-bridged copper compounds have been synthesized according to the following general reaction pathway and possess one of the given formulae (Scheme 1).

The CuX-to-phosphane ratio, the counterion X of the copper salt, and especially the nature of the phosphane used, are very important. In the first step, the phosphane complexes the copper salt to generate a reactive species, the reactivity of which can be subtly regulated by the choice of X and PR_2R'. Furthermore, the driving force of the reactions is the formation of thermodynamically stable $SiMe_3X$ and can thus be controlled by the choice of X according to

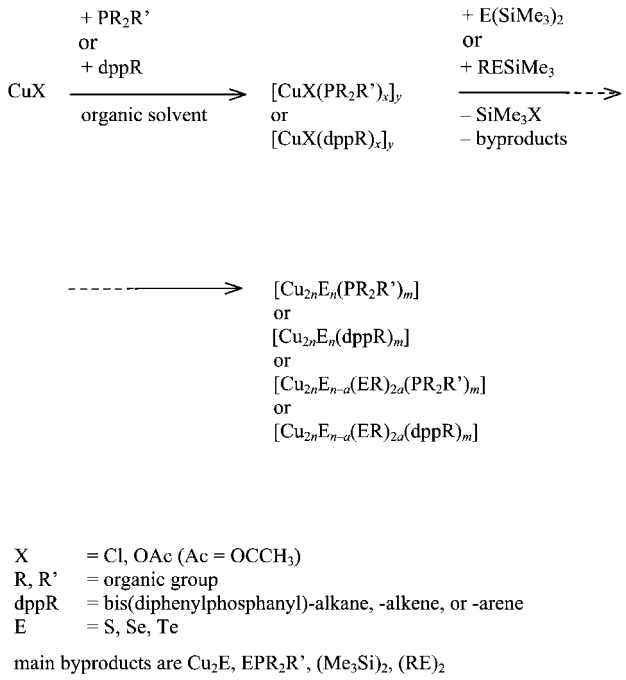

Scheme 1. General synthetic route for the formation of phosphane-ligated chalcogen-bridged copper clusters

the bond strength of the Si−X bond.[41] Finally, the steric demand of the PR_2R' molecules on the cluster surface − as measured by Tolman's cone angle θ[42] (see Table 1) − is related, although not linearly, to the final size and shape of the copper chalcogenide core.

Table 1. Values of Tolman's cone angle θ for phosphanes PR_2R' used in the syntheses of copper chalcogenide clusters (ref.[42])

PR_2R'	θ [°]
PMe_2Ph	127
PEt_3	132
$PnPr_3$	132
PEt_2Ph	136
$PPhnPr_2$	136
$PEtPh_2$	141
PPh_2nPr	141
PPh_3	145
$PMeiPr_2$	146
$PCyPh_2$	153
$PiPr_3$	160
$PtBu_2Me$	161
$PnButBu_2$	165
PCy_3	170
$PtBu_3$	182

In addition, other reaction conditions such as the chosen solvent, the reaction temperature, or the temperature program strongly influence the course of the synthesis. It has been shown that, under similar reaction conditions, the use of derivatives $RE(SiMe_3)$ (R = organic group) leads to the formation of completely different structures to those reactions employing $Se(SiMe_3)_2$. The reason for this is the different reactivity of the reactants as well as partly incomplete Se−C bond cleavage. Thus, some RE^- fragments are bound

at the periphery of the cluster framework, acting as terminal ligands in addition to the phosphane groups.

Regarding the given general formula of the products, the copper atoms can be assigned a formal charge of 1+ while the chalcogen ligands are formally viewed as E^{2-} or RE^{-} groups. However, some of the selenium-bridged species and many copper telluride clusters form non-stoichiometric compounds that display mixed-valence metal centers, leading either to an overall electron deficiency or an electron excess. This corresponds to observations made for the binary phases Cu_2S, $Cu_{2-x}Se$, and $Cu_{2-x}Te$.[38−40]

Even though most ligated copper chalcogenide clusters have been prepared as described herein, it should be mentioned that other synthetic routes to ligated or "naked" $[Cu_{2n}E_n]$ cluster compounds have been studied. Besides syntheses in solvent environments[5−31] that led to the formation of, for example, $[PhMe_3As]_4[Cu_8\{S_2C_2(CN)_2\}_6]$,[5] $(Me_4N)_2[Cu_5(SPh)_7]$,[6] $(Ph_4P)_4[Cu_{12}S_8]$,[7] or $[Cu_6\{Se(2,4,6\text{-}iPr_3C_6H_2)\}_6]$,[8] ligand-free particles have been obtained and characterized by means of laser ablation techniques in combination with mass spectrometry.[32]

3. Synthesis Details, Molecular Structures, and Stabilities

3.1. Sulfur-Bridged Copper Clusters

3.1.1. Syntheses

The reactions yielding the phosphane-ligated, sulfur-bridged copper clusters that have been isolated and structurally characterized to date are summarized in Scheme 2, in order of increasing cluster size.

Sulfur-bridged clusters could not be obtained by reactions starting from copper halides. The reason for this is the lower reactivity of primary copper acetate-phosphane complexes compared to the analogous halide complexes, as a result of the chelating acetate ligands that can be displaced in a double-step substitution of selenium ligands for oxygen.[43] Reactants of higher reactivity lead directly to the formation and precipitation of Cu_2S, even at low temperatures. The kinetic restrictions at the beginning of the synthesis are in addition to those at the end of the cluster growth. The phosphane molecules have to provide a certain minimum steric demand and it has not yet proved possible to generate sulfur-bridged copper clusters with PMe_3 ligands.

3.1.2. Structures and Stabilities

Half of the total number of known copper sulfide clusters have the general formula $[Cu_{12}S_6(PR_2R')_8]$, which represents the smallest known copper chalcogenide $[Cu_{2n}E_n]$ cluster core (**1**−**5**).[13,15,18] The respective molecular structures correspond to one of two possible isomers that can both be derived from a highly symmetric polyhedron of metal and chalcogen atoms. The highly symmetrical conformation is the reason for the strong preference for "Cu_{12}" species. An

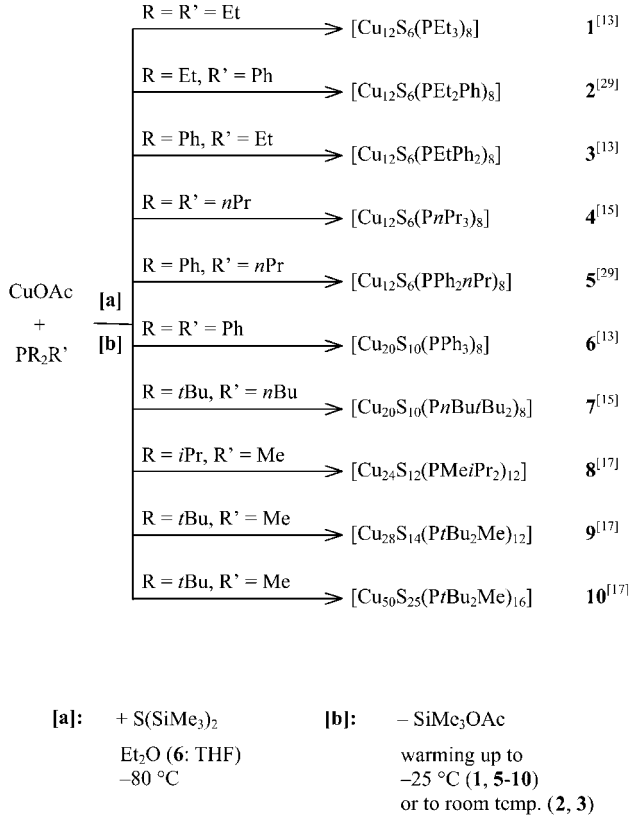

Scheme 2. Survey of the synthesis of sulfur-bridged copper clusters protected by terminal phosphane ligands

S_6 octahedron is penetrated by a Cu_{12} cubooctahedron. However, the latter is distorted as a result of the coordination of the phosphane ligands, as there is only enough space for eight rather than twelve phosphane molecules at the cluster surface within a reasonable Cu−P bond length. Different distributions of the terminal ligands with respect to the cubooctahedron atoms lead to the formation of isomers I or II, respectively. Both cluster structures, as well as a computed hypothetical "naked", undistorted $[Cu_{12}S_6]$ core,[35] are shown in Figure 1.

In the "Cu_{12}" clusters, two coordination modes of the copper atoms can be observed. The four copper atoms that are not bound by phosphane ligands are almost linearly coordinated by sulfur atoms and are positioned either in the equatorial Cu_4 ring of the cubooctahedron (I) or two each reside in the top and bottom Cu_4 planes (II). The eight remaining copper atoms bound by the PR_2R' groups are surrounded in an almost trigonal-planar manner by two sulfur neighbors and one phosphorus atom. The phosphane molecules can be thought of as "pulling" their respective metal atoms out of the basic Cu_{12} polyhedron, whereas the "naked" copper atoms are slightly displaced towards the cluster center. All the sulfur ligands act as μ_4-bridges between copper atoms. In molecules of type I, the eight phosphorus atoms are arranged around the cluster surface so as to form an approximate cube, whereas in the other isomer, if the phosphorus atoms are formally linked, a P_8 Δ-dodecahedron is obtained. Both arrangements are among the most stable polyhedra of eight points on the surface of a sphere.

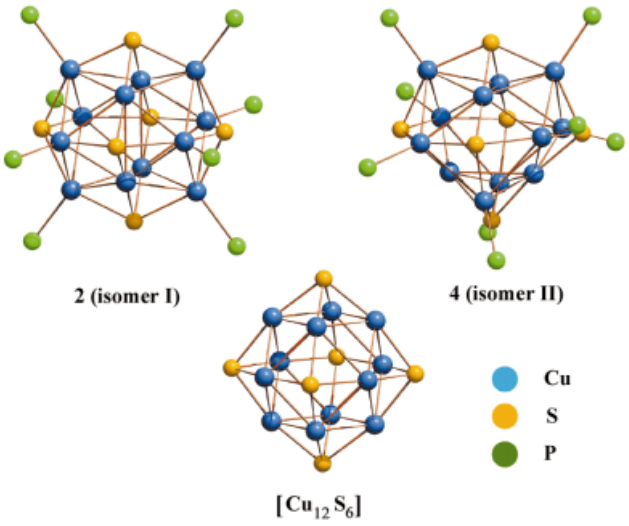

Figure 1. Molecular structures of $[Cu_{12}S_6(PEt_2Ph)_8]$ (**2**) and $[Cu_{12}S_6(PnPr_3)_8]$ (**4**) (without organic groups) and of a calculated "naked" $[Cu_{12}S_6]$ core

Quantum chemical investigations with the program system TURBOMOLE,[44,45] employing MP2[46] and DFT[47] methods, were carried out assigning the highest possible symmetry in order to explain the obvious experimental preference for type I clusters over those of type II.[36] For model ligands PH_3 (MP2 and DFT; highest possible symmetry: D_{4h} for type I or S_4 for type II), both structures representing local minima on the energy hypersurface were found to be isoenergetic within the limits of the methods used. On calculating clusters $[Cu_{12}S_6(PR_3)_8]$ with R = Et or R = Pr according to both structural isomers (DFT; highest possible symmetry: C_{4h} or S_4), i.e. one real (**1**, **4**) and one hypothetical species each, one does not find a direct correlation between the substituents on the phosphorus atoms and the thermodynamic stabilization. Thus, further kinetic effects such as solubility and mobility of the organic groups at the experimental temperatures (>> 0 K) probably play key roles in the choice of isomers. The fact that the same cone angle values are found for PEt_3 and $PnPr_3$ underlines this conclusion (see Table 1).

Another pair of isomers is formed in the presence of the sterically more demanding phosphanes PPh_3 or $PnButBu_2$, where there are 20 copper atoms in the cluster framework.[13,15] The respective molecular structures of **6** (type I) and **7** (type II) are shown in Figure 2.

Again, the positions of the eight Cu−P groups determine the shapes of the clusters, the cores of which can be regarded as distortions of the formal condensation product of two of the $Cu_{12}S_6$ units shown in Figure 1. This relationship is particularly clear when "Cu_{12}" and "Cu_{20}" clusters of type I are compared. After the loss of one apical sulfur ligand and four phosphane molecules from each, as well as one Cu_4 ring, a $[Cu_8S_5(PR_3)_4]$ and a $[Cu_{12}S_5(PR_3)_4]$ fragment are fused in such a way that two face-sharing fragments of the "Cu_{12}" cubooctahedra of cluster type I (idealized symmetry of the Cu−S−P core: D_{4h}) are obtained in

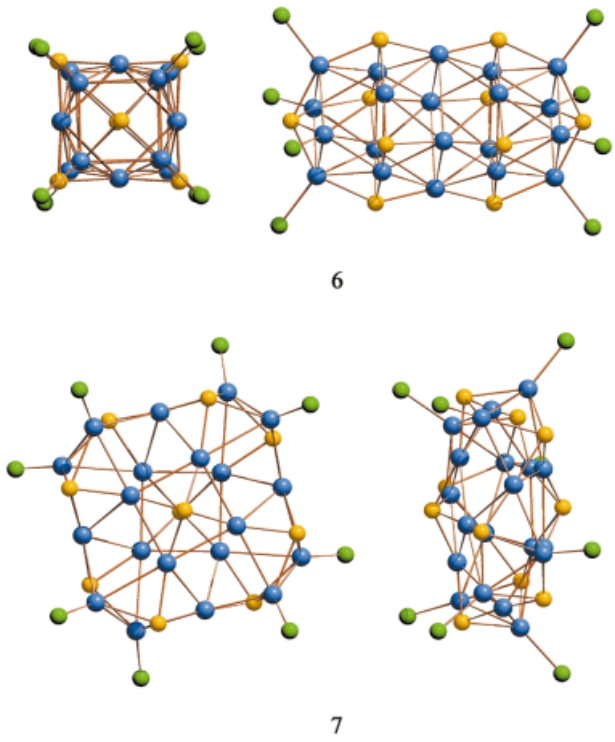

Figure 2. Molecular structures of $[Cu_{20}S_{10}(PPh_3)_8]$ (**6**) (top) and $[Cu_{20}S_{10}(PnButBu_2)_8]$ (**7**) (bottom) (without organic groups), each shown both along and perpendicular to the $S_{apical}-S_{apical}$ axis

the case of **6**. In **7** (type II, idealized symmetry of the Cu−S−P core: D_4), the ligands do not occupy coordination sites at the two outer Cu_4 rings but bind to the second and fourth rings resulting in the oblate and slightly twisted isomer. The respective S_{10} polyhedra are a bicapped tetragonal prism (**6**) and a highly compressed, bicapped tetragonal anti-prism (**7**). A tetragonal prismatic P_8 arrangement is found in **6**, while a P_8 tetragonal anti-prism is found in **7**. Coordination numbers and geometries are similar to the situation in the "Cu_{12}" species.

The structural differences between pairs of isomeric copper sulfide clusters can clearly be ascribed to the coordination sites of the phosphane groups, which are directed towards the respective copper atoms by their own steric demand to give the best protecting ligand shell around the Cu−S core. If different phosphanes display the same cone angle, isoenergetic structural isomers result, so that further kinetic aspects will dominate, as shown for the "Cu_{12}" species. If the PR_2R' groups are so small that even variation of the ligand positions does not result in a complete ligand sphere, or if the phosphane molecules are so bulky that one would have to have one fewer ligand, resulting in a non-ideal P_n polyhedron and an incomplete ligand sphere, the cluster growth continues until the optimum ratio of $[Cu_{2n}S_n]$ core and PR_2R' number and arrangement is achieved.

A continuation of the cluster growth also takes place in the presence of $PMeiPr_2$. Being too bulky for an arrangement of eight molecules around a $[Cu_{12}S_6]$ core and not generating a suitable ligand sphere with six terminal li-

gands, the phosphane groups enforce a formal dimerization of "Cu_{12}" clusters to the $[Cu_{24}S_{12}]$ core in **8**.[17] Figure 3 shows the formal dimerization of two "$[Cu_{12}S_6(PR_2R')_8]$" clusters of type II, which results in the molecular structure of **8** after the loss of four phosphane groups.

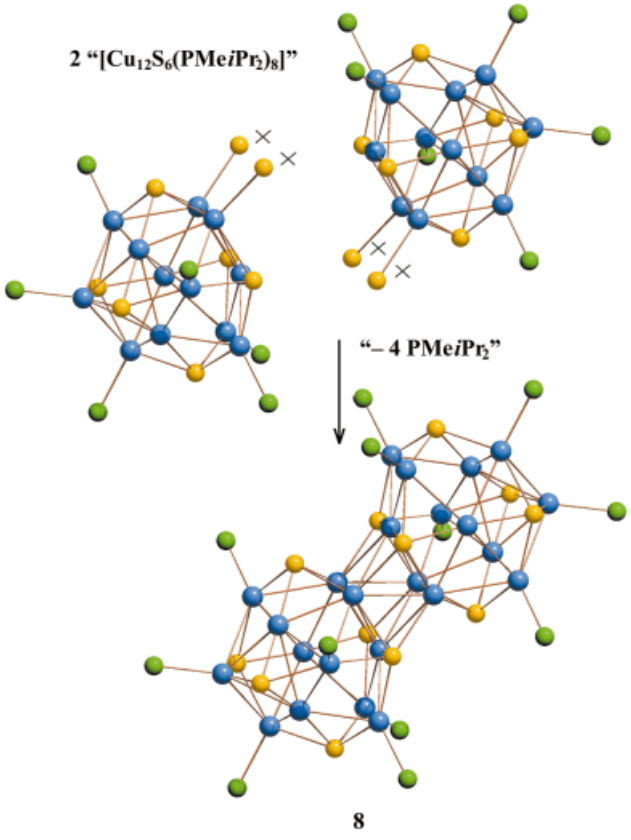

Figure 3. Formal dimerization/condensation reaction of two hypothetical clusters "$[Cu_{12}S_6(MeiPr_2)_8]$", resulting in the molecular structure of $[Cu_{24}S_{12}(PMeiPr_2)_{12}]$ (**8**) (without organic groups); phosphane ligands that are formally lost during the dimerization/condensation are drawn yellow and are marked by a cross

In contrast to the formal condensation (2 × "Cu_{12}") − 4 Cu → "Cu_{20}", which leads to the sharing of a Cu_4 rectangular face in **6**, in this case one observes a fusion of two Cu_3 triangular faces of the two basic cubooctahedra, forming a Cu_6 octahedron around the inversion center of the cluster. These six copper atoms show a novel coordination pattern. They are surrounded exclusively by sulfur neighbors in a trigonal-planar geometry. Conversely, the four sulfur atoms in the cluster center are found to act as μ_5-bridges, whereas all sulfur ligands in the clusters discussed so far and all the other ones in **8** are μ_4-bridging. The μ_5-bridges exhibit longer average Cu−S bond lengths than the μ_4-bridging sulfur ligands, as they bind to four copper neighbors with normal distances [2.159(3)−2.378(3) Å] and form one significantly longer Cu−S bond to a copper atom of the opposite asymmetric unit [2.485(3), 2.509(3) Å].

In the molecular structure of **8**, one observes the beginning of a transition from the so-called "small" copper sulfide clusters to the "middle-sized" species. Both cluster sizes possess spherical Cu−S−P frameworks with copper centers near the S_n polyhedron edges, but the "middle-sized" examples show some new structural features besides those already found for the "small" clusters: coordination numbers other than four for sulfur atoms, and copper centers that bind to more than two sulfur neighbors.

This same observation can be made for clusters **9** and **10**, particularly for the latter.[17] Unlike the species already discussed, these two clusters are topologically unrelated to the smaller examples. However, they are structurally related between themselves, and are actually formed in the same reaction. The molecular structures of **9** and **10** are shown in Figure 4, emphasizing their structural relationship by respective orientation. The basic S_{14} and S_{25} polyhedra are compared in Figure 5.

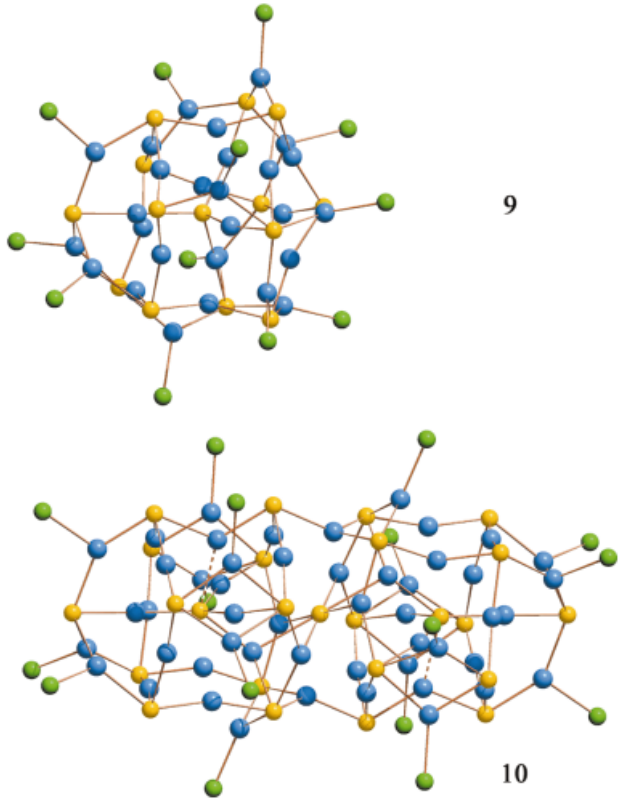

Figure 4. Molecular structures of $[Cu_{28}S_{14}(PtBu_2Me)_{12}]$ (**9**) and $[Cu_{50}S_{25}(PtBu_2Me)_{16}]$ (**10**) (without organic groups)

Besides various bridging modes of the sulfur atoms (μ_3 to μ_5 in **9**; μ_4 to μ_6 in **10**) and the greater numbers of three sulfur ligands around several of the copper atoms in **10**, both systems show another new structural feature characterizing "middle-sized" Cu−S clusters: Only for these two largest examples of copper sulfide cluster compounds does one find sulfur atoms inside an outer Cu−S shell, generating inner Cu−S units. In **9**, one sulfur ligand lies at the center of a distorted S_{13} deltahedron. Four copper atoms then bond around the central sulfur atom to yield an inner $[SCu_4]$ unit. The remaining copper centers are positioned either slightly below the surface of the S_{13} polyhedron if they show no Cu−P bonds, or slightly above if they are

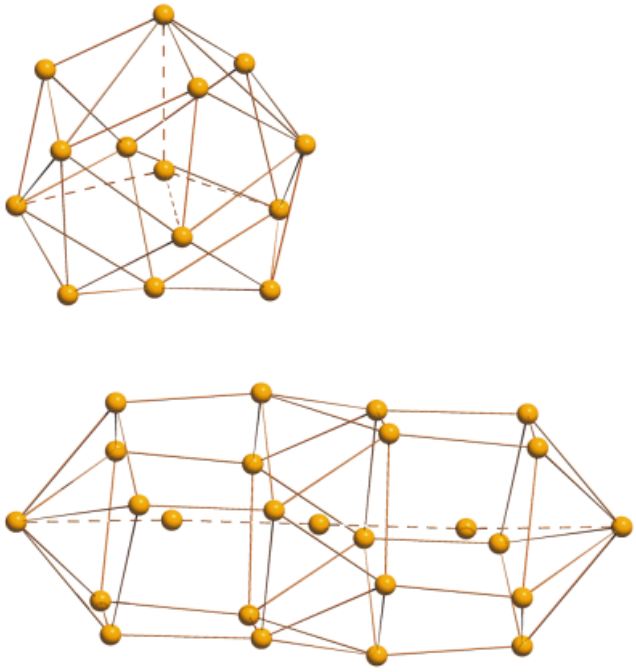

Figure 5. S_{14} (top) and S_{25} (bottom) polyhedra in **9** and **10**, respectively; the straight lines between the S atoms do not represent bonding interactions, but merely help to visualize the geometries of the polyhedra

bound by phosphane groups. A near C_3 symmetry of the Cu−S core is lost because of the "irregular" position of a single copper atom, which is also responsible for the μ_3- or μ_5-bridging mode of two sulfur ligands. The spherical cluster core is enclosed by a distorted icosahedron made up of the twelve phosphorus atoms. The sulfur substructure of **10** constitutes a cylinder-shaped polyhedron of near D_{5d} symmetry with a length of 17.14 Å. Underlining the supposition that **10** is formed through a form of dimerization−condensation from **9**, three inner sulfur atoms are present. Two of them − formally equivalent to the central sulfur atom in **9** − are also μ_4-bridging, resulting in an [SCu_4] fragment. However, one of the respective copper centers belongs to the cluster surface rather than being an inner metal atom, as a result of the structural differences between **9** and **10** when considering the center in **10**. Here, one observes the most unusual aspect of any of the copper sulfide clusters yet reported. The central sulfur ligand binds to six nearest copper atoms in a slightly corrugated chair-type manner. This arrangement, which is not found in any of the known copper sulfide compounds, displays very long Cu−S distances in the range of 2.633(4)−2.673(5) Å, which are about 0.3−0.5 Å longer than standard Cu−S bonds. Considering the ten next nearest copper atoms, 2.896(5)−3.814(5) Å out from the sulfur center, a near-spherical [SCu_{16}] arrangement is found for the cluster center. These structural observations are evidence for an interstitial S^{2-} anion rather than a covalently-bonded sulfur ligand. A summary of interatomic distances found in known copper sulfide systems for the different coordination numbers around copper is given in Table 2.

Considering the Cu−S distances listed in Table 2, one can recognize a first step in the direction of solid-state Cu−S phases in the structure of **10**.

By a comprehensive ab initio study of clusters [$Cu_{2n}S_n(PH_3)_m$] (n = 1−4, 6, 10; m = 0, 2, 4, 6, 8) at the MP2 level (program system TURBOMOLE), stabilization energies for the attachment of successive Cu_2S units to a given "naked" cluster (n = 1−4, 6, 10; m = 0; Figure 6), as well as the variation in the phosphane binding energies for clusters containing up to twelve copper atoms (n = 1−4, 6; m > 0; Figure 7), were calculated.[35]

For "naked" clusters, the stabilization energies increase continuously with the cluster size, which shows that the investigated molecules are thermodynamically unstable species in vacuo and that they have to be stabilized by ligands. Moreover, the increment in the stabilization energy per monomer unit decreases with increasing cluster size in the expected way, since it should theoretically converge at infinite cluster size, i.e. solid Cu_2S. Finally, the calculated Cu−P binding energy per Cu−P bond decreases rapidly from a value of ca. 140 kJ·mol^{-1} for [$Cu_2S(PH_3)_2$] − with a short relaxation when the Cu/P ratio is decreased (1 for n = 1−3, >1 for n = 4, 6) − to a value of ca. 56 kJ·mol^{-1} for the "Cu_{12}" species. Even if one assigns a higher Cu−P binding energy to the "real" tertiary phosphanes that bind to organic groups, it is evident that the phosphane ligands are bonded only very weakly to the copper sulfide core. Therefore, an additional stabilization by solvents or a crystal lattice is required.

3.2. Selenium-Bridged Copper Clusters

3.2.1. Syntheses

Scheme 3 summarizes the reactions yielding all PR_2R'-ligated, selenium-bridged copper clusters that have been isolated and structurally characterized to date, in order of increasing cluster size.

Unlike the sulfur-bridged compounds, the synthesis of selenium-bridged clusters can start from either copper acetate or copper chloride. This can be attributed to the lower standard formation enthalpy of Cu_2Se ($\Delta H_f° = -65.2$ kJ·mol^{-1})[49] when compared to its sulfur analogue Cu_2S ($\Delta H_f° = -81.2$ kJ·mol^{-1}).[50] Thus, the formation of Cu_2Se does not occur as rapidly as that of Cu_2S, although $Se(SiMe_3)_2$ is, in principle, more reactive than $S(SiMe_3)$. The cluster growth and protection of selenium-bridged clusters can therefore often be observed even at room temperature. However, with copper acetate as the starting material and by choosing low temperatures, one can obtain smaller clusters that could be considered as intermediates in the formation of the larger molecules. In addition to a great number of "stoichiometric" compounds that formally contain Cu^+ and Se^{2-}, some clusters have been characterized as having a Cu:Se ratio of less than two, indicating mixed-valence metal centers. All selenium ligands have a formal charge of −2 as one does not find any Se−Se binding inter-

Table 2. Interatomic distances of selected $Cu^{I}-S$ systems and metallic copper

System	Cu−Cu [Å]	Cu−S distances for the different coordination numbers (*CN*) [Å]			ref.
		CN = 2	*CN* = 3	*CN* = 4	
Cu−S clusters	2.511−2.985	2.111−2.291	2.103−2.673	–	[13−15,17,29]
$[Cu_{12}S_8]^{2-}$	2.774−2.950	2.156−2.179	–	–	[7]
ternary M−Cu^{I}−S phases	2.60−2.96	2.13−2.17	2.17−2.53	2.37−2.55	[48]
binary $Cu_{2-x}S$ phases	2.59−2.97	2.06	2.28−2.33	2.15−2.59	[38]
copper metal	2.56	–	–	–	[38a]

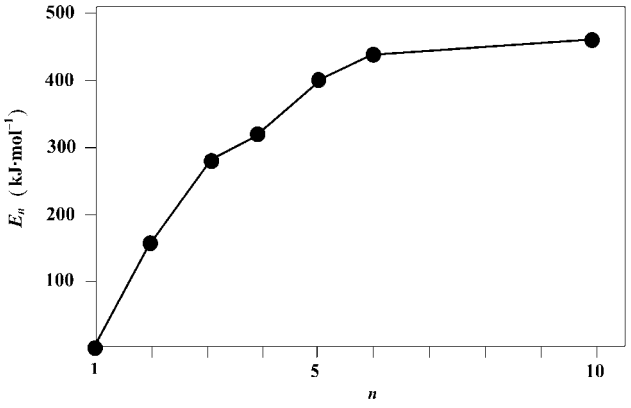

Figure 6. Variation in the stabilization energies per monomer unit in "naked" clusters $[Cu_{2n}S_n]$ (n = 1−4, 6, 10) with the given values taking into account the total energies of the most stable structural isomers computed at the MP2 level

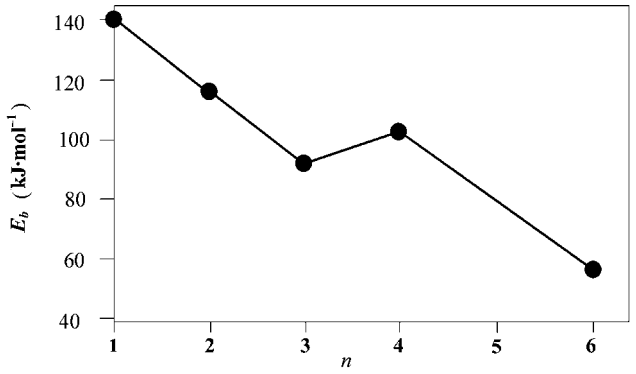

Figure 7. Variation in the Cu−P binding energies per Cu−P bond in phosphane-ligated clusters $[Cu_{2n}S_n(PH_3)_m]$ (n = 1−4, 6; m = 2, 4, 6, 8) with the given values taking into account the total energies of the most stable structural isomers computed at the MP2 level with respect to the total energy of PH_3 calculated by the same method

actions; therefore, one can assign Cu^{I} and Cu^{II} centers within the same cluster core in **14**, **17**, **27**, and **33**. The phosphane ligands again play a key role in determining the observed cluster sizes and shapes. The number of observed compositions is approximately four times that of the number of copper sulfide species, and the cluster growth proceeds to much higher nuclearity. Again, the lower tendency for precipitation of the binary phase can be invoked to account for this observation.

Another route to selenium-bridged copper clusters is by synthesis using $RSeSiMe_3$ (R = organic group) in the presence of either tertiary phosphanes or chelating ligands such as 1,2-bipyridyl, diphenylphosphanyl acid, or bidentate phosphanes dppR (R = organic spacer). The compounds prepared in this way are listed in Scheme 4 in order of increasing size.

Again, one finds clusters containing exclusively Cu^{I} centers, as well as compounds with mixed-valence metal centers. In contrast to the compounds presented in Schemes 2 and 3, one of the selenido/selenolato-bridged clusters (**52**; see below) apparently contains Cu^{0} as well as Cu^{I}. Apart from this peculiarity, the cluster size and conformation of the Se^{2-}/SeR^{-}-bridged compounds is not only influenced by the nature and steric demand of the phosphane used, but is also dependent on the spatial properties of the organic substituent on the selenium reactant. This determines both the Se^{2-}/SeR^{-} ratio as well as the arrangements of the Se^{2-} ligands positioned inside the cluster core and of the SeR^{-} ligands on the periphery of the molecules.

3.2.2. Structures and Stabilities

3.2.2.1. Se^{2-}-Bridged Copper Clusters

The subtle, nonlinear structural influence of the phosphane ligands allows the formation of different clusters of sometimes significantly different size and shape in the presence of the same phosphane. The isolation of a particular cluster compound is then determined by the choice of reaction conditions. Conversely, the use of different PR_2R' ligands can lead to clusters of the same $[Cu_{2n}Se_n]$ cores that may display differing numbers of terminal ligands and/or structural isomerism. These observations have already been illustrated and explained for the sulfur-bridged copper clusters, but they are more important for the Cu−Se species and a much greater structural variety is found. As with the copper sulfide compounds, one can distinguish between "small" and "middle-sized" clusters with regard to their shape and the coordination properties of the atoms involved. However, a third group, the "large" clusters, exists for the Cu−Se system. Whereas the transition from the first to the second type of molecular size is rather smooth, a clear break occurs when the number of copper atoms exceeds 59.

The only composition and structure that is equivalent for both copper sulfide and selenide clusters is $[Cu_{12}E_6(PR_2R')_8]$ (E = S, Se; PR_2R' = $PEtPh_2$, $PnPr_3$; respective cone angles: 141°, 132°). Compounds **11**[13] and **12**[29] are topologically identical to their sulfur analogues **3**

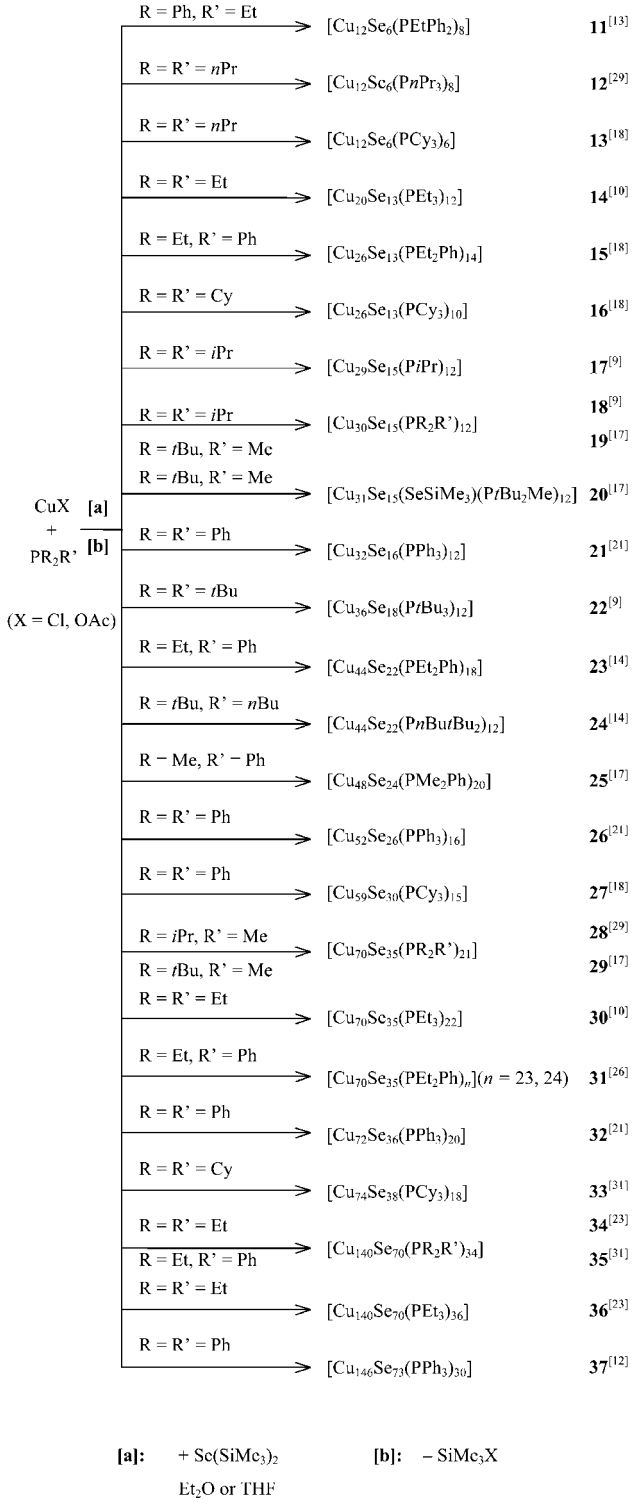

Scheme 3. Survey of the synthesis of selenium-bridged copper clusters protected by terminal phosphane ligands

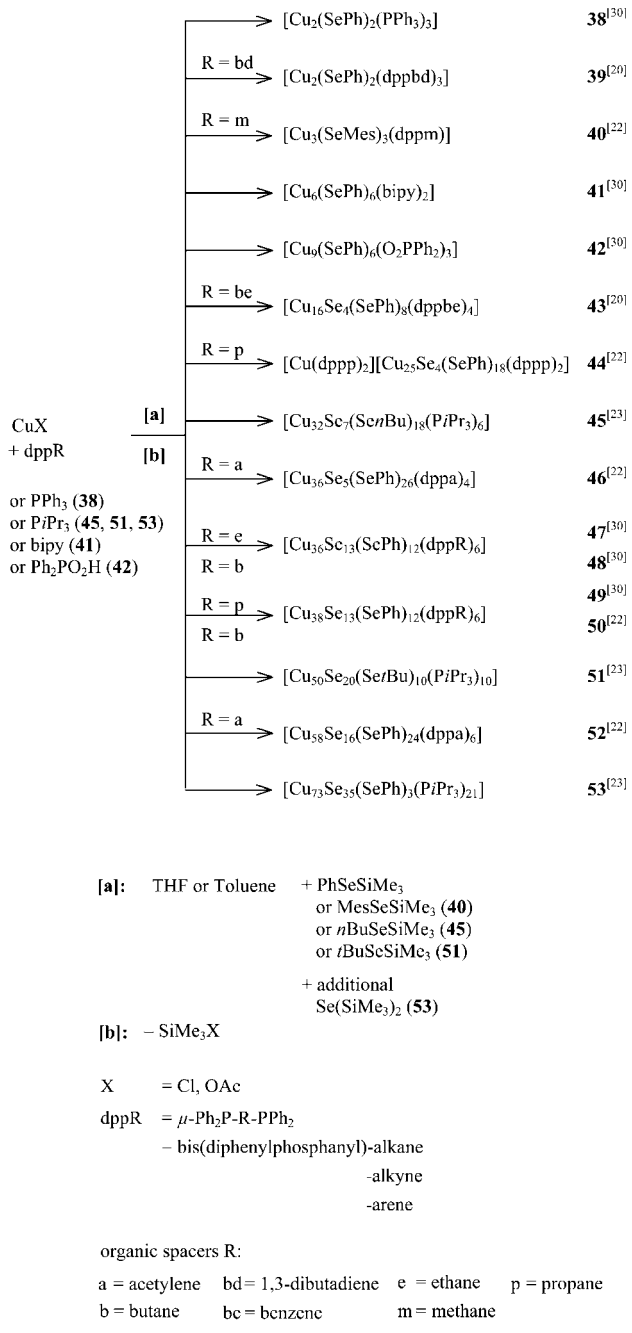

Scheme 4. Survey of the synthesis of selenido/selenolato-bridged copper clusters protected by monodentate or chelating bidentate ligands

and **4**. The use of a much bulkier phosphane ligand, PCy_3, does not lead to a condensation or dimerization of cluster cores as observed for **6**−**8**, which contain PR_2R' groups of medium or large steric bulk. In contrast to the copper sulfide clusters in the presence of PPh_3, $PnButBu_2$, or $PMeiPr_2$, a reduction to six terminal ligands is acceptable in the case of **13**[18] (Figure 8) and the resulting ligand shell can encapsulate the $Cu_{12}Se_6$ cluster core. The clearly larger cone angle of PCy_3 compared to PPh_3, $PnButBu_2$, or $PMeiPr_2$ (170° *vs.* 145°, 146°, or 165°) is sufficient to allow a distorted P_6 octahedron to protect the copper selenide framework. However, as might be expected, a third version of the distortion of the $[Cu_{12}E_6]$ core is observed in this case.

Considering the clusters presented thus far, there seems to be a strong preference for highly symmetrical substructures of all the components involved in the heavy atom framework. Capped or uncapped, sometimes condensed,

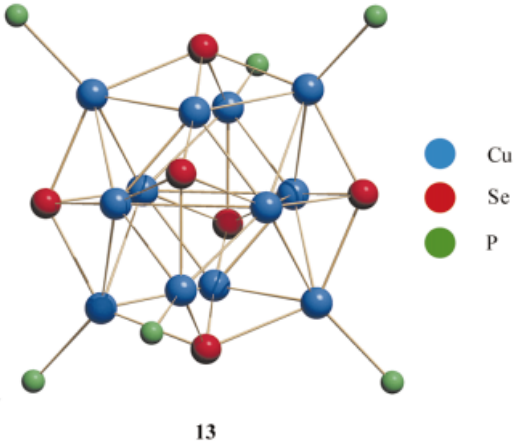

Figure 8. Molecular structure of $[Cu_{12}Se_6(PCy_3)_6]$ (**13**) (without organic groups)

octahedral, prismatic, cubic, dodecahedral, cubooctahedral, or icosahedral arrangements of either metal, chalcogen, or phosphorus atoms penetrate or enclose each other in all the structures. Among the compounds discussed, the "Cu_{12}" molecules possess the most symmetrical substructures. However, selenium ligands evidently prefer higher bridging modes. Therefore, the formation of "small" clusters with mostly μ_4-bridging selenium ligands is disfavored and these are consequently less common than larger ones. For the Cu−Se clusters, three further "middle-sized" compounds can be considered with regard to their symmetry properties as well as for a further illustration of the structural influence of the phosphanes. The cluster frameworks of **14**[10] and the $[Cu_{26}Se_{13}]$ isomers **15**[18] and **16**[18] can again be described as alternate packings of copper, selenium, and phosphorus polyhedra, respectively. However, regular polyhedra are only observed in the structures of **14** and **15**, whereas the $[Cu_{26}Se_{13}]$ core of **16**, being surrounded by only ten PCy_3 ligands instead of 14 PEt_2Ph groups, does not conform to a known polyhedral pattern. The molecular structures of **14**−**16** are shown in Figure 9.

To some extent, **14** and **15** are topologically related as both contain a centered icosahedron of selenium atoms. However, the penetrating polyhedra of copper atoms have different shapes according to the differing numbers of copper atoms and Cu−PR_2R' fragments (**14**: R = R′ = Et, **15**: R = Et, R′ = Ph) in the two clusters (Figure 10).

In **14**, a Cu_8 cube surrounds the inner selenium atom below Se_3 faces of the Se_{12} icosahedron. An outer Cu_{12} icosahedron follows, which is positioned above and rotated by 90° with respect to the Se_{12} shell. The eight copper centers inside the cluster thus form tetrahedral $[CuSe_4]$ groups and the twelve outer ones display an $[Se_3CuP]$ environment by binding to the similarly orientated P_{12} icosahedron formed by the PEt_3 ligands. In **15**, the inner selenium atom has twelve nearest copper neighbors that form an icosahedron, each edge being positioned below an Se−Se edge of the enclosing Se_{12} polyhedron and lying perpendicular to it, resulting in a coordinative occupation of one copper atom per Se_3 face. Slightly above the Se_{12} icosahedral surface, an

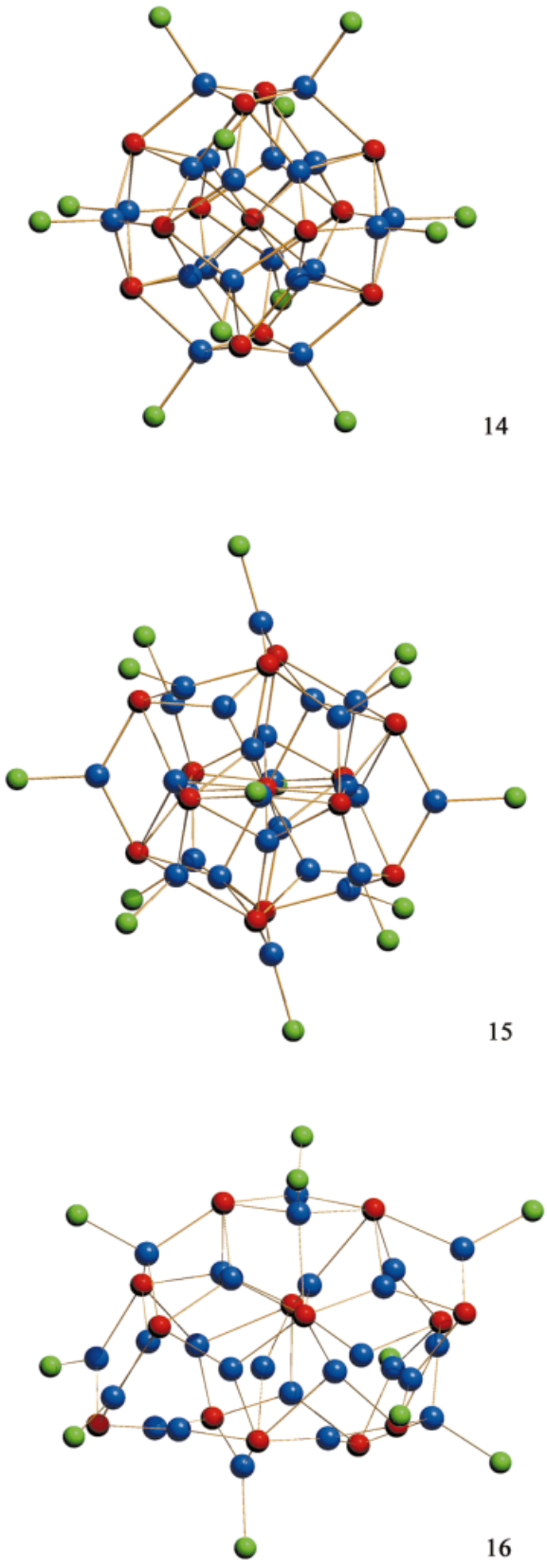

Figure 9. Molecular structures of $[Cu_{20}Se_{13}(PEt_3)_{12}]$ (**14**), $[Cu_{26}Se_{13}(PEt_2Ph)_{14}]$ (**15**), and $[Cu_{26}Se_{13}(PCy_3)_{10}]$ (**16**) (without organic groups)

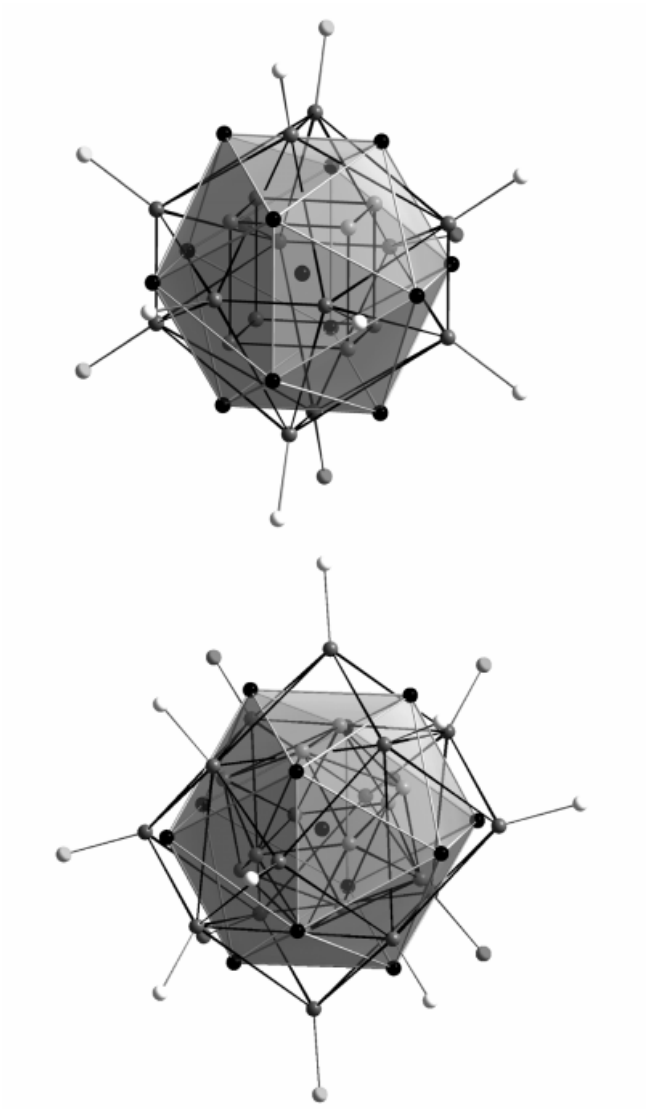

Figure 10. A comparison of the interpenetrating polyhedra in **14** (top) and **15** (bottom) that form the heavy atom cluster cores; the lines merely represent polyhedral edges and do not imply bonding interactions

arrangement of 14 $Cu-PEt_2Ph$ units can be described as a sixfold capped cube. The twelve inner copper atoms and the eight metal centers of the capped cube, which all reside near Se_3 faces, are approximately tetrahedrally coordinated by either four selenium ligands or three selenium ligands and one phosphorus ligand. This is characteristic of those clusters larger than those classified as "small". The six remaining $Cu-PEt_2Ph$ fragments are situated above six Se−Se edges and therefore represent tricoordinated $[Se_2CuP]$ units, as found in both "small" and "middle-sized" clusters. On comparing the Cu/Se ratios for **14** and **15**, the fundamental difference that can be invoked to account for the structural differences becomes apparent. Cluster **14** represents a mixed-valence compound formally incorporating six Cu^{II} and 14 Cu^{I} centers to neutralize the 26− charge of the Se_{13} substructure. However, the intermetallic distances in **14** [Cu(1)−Cu(1): 2.821(4), Cu(1)−Cu(2): 2.678(4) Å] do not indicate significant interatomic interactions despite the partial depletion of electrons. The only structural indication of different valence situations in **14** or **15** is that, apart from equal average Cu−P bond lengths (2.247 Å in **14** and **15**) and similar average intermetallic distances Cu−Cu (2.707 Å in **14**, 2.682 Å in **15**), one finds significantly shorter average Cu−Se bonds in the mixed-valence compound **14** (2.365 Å) than in **15** (2.457 Å). The molecular structure of **16** differs from those of **14** and **15** in that the selenium substructure consists of a very irregular Se_{13} deltahedron. Twelve of the copper centers and ten $Cu-PCy_3$ fragments bind to the Se_{13} polyhedron in such a way that they are again three- or four-coordinated. Unlike the situation in **14** or **15**, one additionally observes four copper atoms that are almost linearly coordinated by two selenium neighbors. This pattern is typical for "small" Cu−E clusters and again underlines the partial maintenance of these properties in the "middle-sized" compounds. The structure of **16** acutally resembles more the molecular structures of the next larger clusters **17**−**19** (Figure 11), being reduced by three or four copper atoms, two selenium, and two phosphane ligands.

Like the "Cu_{12}"−"Cu_{20}", the "Cu_{12}"−"Cu_{24}", or the "Cu_{28}"−"Cu_{50}" relationship discussed for copper sulfide clusters, the molecular structures of **14** and **15** can be seen to be closely related, at least in principle, even though the numbers and ratios of heavy atoms are very different. In contrast, a similar number of copper and selenium atoms *can* but does not always lead to a topological relationship (cf. **15/16**). Compounds **17**−**21**[9,17,21] contain 29, 30, 31, or 32 copper atoms and either 15 or 16 selenium ligands. Nevertheless, three completely different molecular frameworks are observed. The first structure type is adopted by **17**,[9] **18**,[9] and **19**.[17] As an example, the molecular structure of **17** is shown in Figure 11.

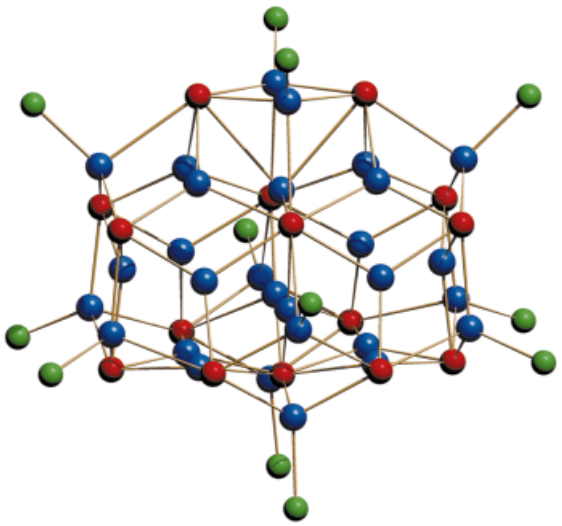

17

Figure 11. Molecular structure of $[Cu_{29}Se_{15}(PiPr)_{12}]$ (**17**) (without organic groups)

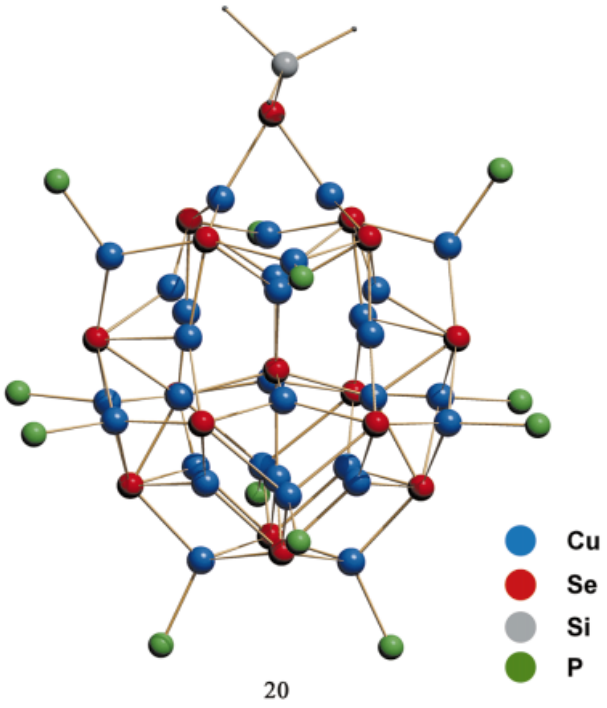

Figure 12. Molecular structure of $[Cu_{31}Se_{15}(SeSiMe_3)(PtBu_2Me)_{12}]$ (**20**) (without organic groups)

Although the number of copper atoms in **17** is one less than in **18** or **19**, indicating a mixed-valence situation in this system, all the clusters show equivalent Cu−Se−P cores. The additional copper atom in **18** or **19** is positioned in the cluster center. A reaction employing the same reactants and temperatures as for the synthesis of **19**, but using a 40% higher $PtBu_2Me$:CuOAc ratio, yields compound **20**[17] (see also Scheme 8). Although the cluster core of **20** (Figure 12) can also be described in terms of five parallel planes of copper and selenium atoms that are then surrounded by twelve phosphane ligands, analogous atomic arrangements or corresponding polyhedra in **19** or **20** are not found.

The $SeSiMe_3$ group, which is unique in the copper chalcogenide clusters, not only influences the molecular structure of **20**, but also indicates the obvious reason for the structural differences. Compound **20** can be viewed as a "frozen" intermediate en route to the formation of a larger cluster such as the "Cu_{70}" cluster **29**[17] (see below), since it still bears a leaving group. The latter uniquely acts as a protecting unit in addition to the phosphane ligands and consequently further cluster growth is slowed down to such an extent that compound **20** crystallizes instead. Thus, its formation is naturally independent of the cluster growth yielding **19**. A third structure type for this size of cluster is found for **21**,[21] as shown in Figure 13. The selenium atoms form a flattened polyhedron consisting of non-bonded Se_3 triangles. One observes four distinct copper environments: 24 of the copper atoms cap the selenium triangles, and of these 16 are bonded only to selenium ligands producing a distorted trigonal-planar coordination geometry slightly below the Se_3 faces. The other eight of these copper centers

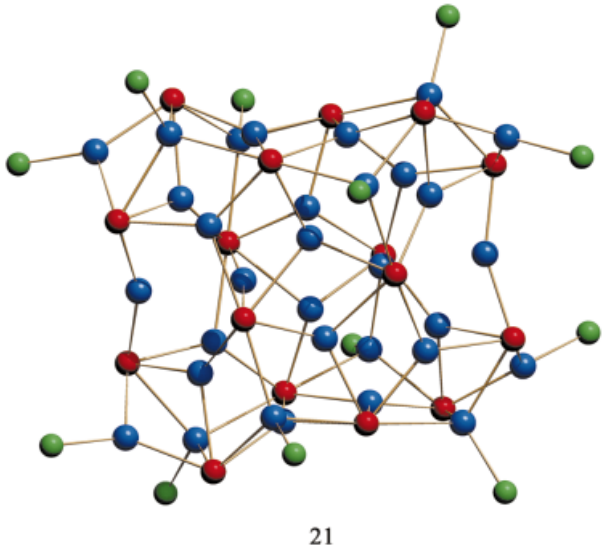

Figure 13. Molecular structure of $[Cu_{32}Se_{16}(PPh_3)_{12}]$ (**21**) (without organic groups)

are also coordinated by a phosphane ligand, giving a tetrahedral environment with the copper atoms situated on the exterior of the selenium substructure. Of the remaining copper atoms, four are coordinated in a quasi-linear fashion to two selenium ligands, and four are bonded in a distorted trigonal-planar manner to two selenium neighbors and one phosphorus atom from PPh_3. These coordination patterns, as well as bridging modes of μ_5 and μ_6 for the selenium ligands, are common for "middle-sized" Cu−E clusters. Compounds **16**, **17**, and **21** also represent exceptions for their cluster size in that they do not contain copper or selenium atoms inside an approximately spherical Cu−Se shell. All other "middle-sized" clusters containing 20 or more copper atoms (beginning with compound **14**) feature central copper atoms (**18**, **19**) or central selenium ligands (**14**, **15**, **20**).

The larger molecules **22**−**27**[9,14,17,18,21] all feature selenium atoms enclosed within an Se_n polyhedron (n = 18, 22, 24, 26, or 30). The number of inner selenium ligands increases with increasing cluster size from one central atom (**22**),[9] through two inner atoms (**23**−**25**),[14,17] to three selenium centers inside the cluster core (**26**, **27**).[18,21] The respective underlying selenium substructures are summarized and compared in Figure 14.

Even though these six compounds can be considered as spherical, "middle-sized" clusters, and all possess central units within a Cu−Se surface, two distinct basic shapes can be discerned. Compounds **22** and **26** (Figure 15) are based on a triangular structure, whereas **23**−**25** and **27** form ellipsoid-type cluster surfaces (Figures 16 and 17).

The molecular structure of **22** displays idealized D_3 symmetry, while the Cu−Se core of **26** shows near C_3 symmetry, although in neither case is this realized in the crystal (**22**: C_2 symmetry; **26**: C_1 symmetry). Along the idealized threefold axes, one finds one selenium ligand at the top and one at the bottom of the approximate flattened trigonal prism

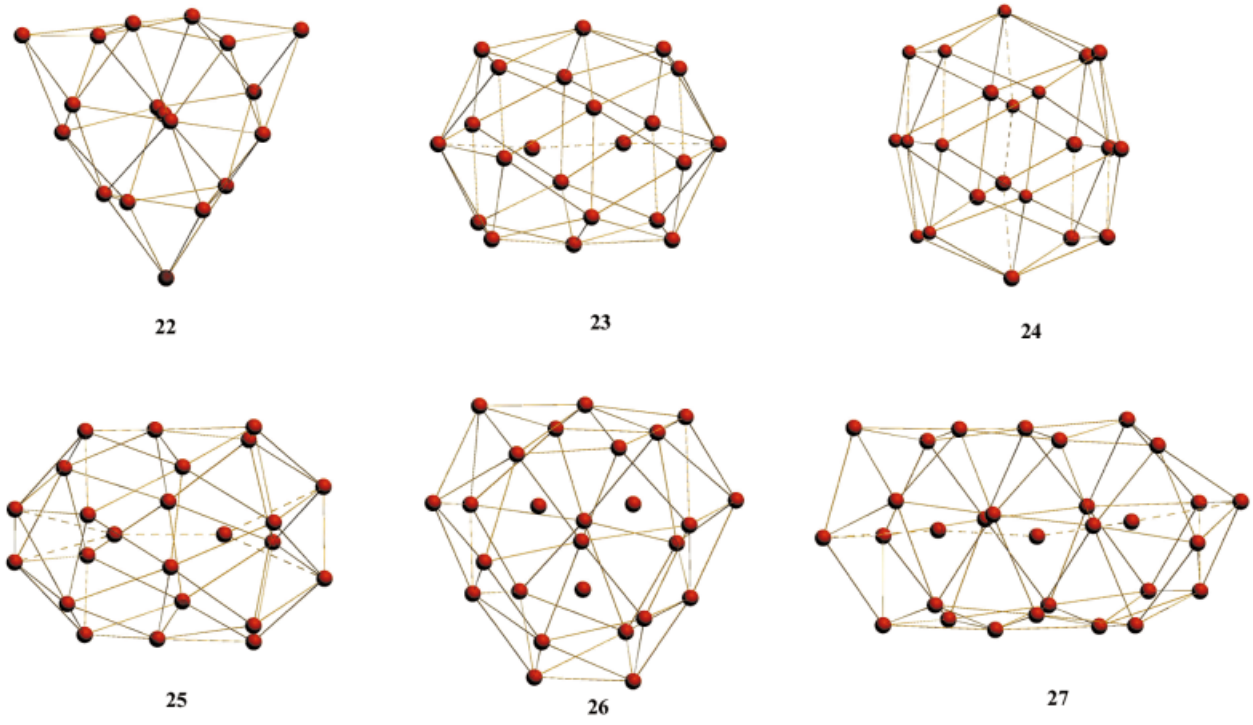

Figure 14. Selenium substructures in **22**−**27** (from top left to bottom right); the Se−Se lines do not represent bonding interactions, but merely help to visualize the geometries of the polyhedra

formed by the cluster atoms. In **22**, a third selenium ligand is positioned between these two at the cluster center. Conversely, in **26** a triangle of three inner selenium atoms lies at the center of the Cu−Se core, and two copper atoms are arranged along the near C_3 axis, between this Se_3 triangle and the two aforementioned selenium ligands. Considering first the central cores, the clusters are formed in the usual way by alternating bonds from copper to selenium atoms. For **22**, this leads to [Se_2Cu], [Se_3Cu], or [Se_2CuP] coordination environments around the copper centers and μ_3- to μ_6-bridging selenium ligands with Cu−Se distances of 2.347(4)−2.875(5) Å. The larger cluster core of **26** consequently features higher coordination numbers, including almost tetrahedral [Se_3CuP] arrangements besides di- or tricoordinated copper atoms as found in **22**, and the selenium atoms act as μ_4- to μ_8-bridges with a wide Cu−Se distance range of 2.19−2.91 Å. Twelve P*t*Bu_3 ligands enclose the copper selenide core of **22** in the following way. Six are bonded over rectangular faces when the cluster is viewed in a simplified manner as a trigonal prism. Six further P*t*Bu_3 units are situated over the respective triangular faces. In addition to nine PPh_3 ligands that are bonded over the rectangular faces of the "prismatic" Cu−Se core in **26**, seven phosphane groups surround the cluster core in a different manner on the two triangular faces in such a way that three are positioned on one side and four on the other.

By using different phosphane ligands and changing the CuOAc/PR_2R' molar ratios and final reaction temperatures, the structural isomers **23** and **24** can be obtained. The spatial demands of the phosphane ligands enabled ligand shells composed of either 18 PEt_2Ph or 12 P*n*Bu*t*Bu_2 groups to adequately protect a [$Cu_{44}Se_{22}$] core. In **23**, the phosphorus atoms form a quite regular polyhedron of alternating, eclipsed P_3, P_6, P_6, and P_3 rings perpendicular to the long axis of the cluster. The twelve phosphorus atoms at the periphery of the cluster core in **24** constitute a highly distorted icosahedron. As a result of the different numbers and arrangements of PR_2R' ligands, which modify the core geometry in the usual way by "pulling" the ligated copper atoms out of the Cu−Se core to some extent, some differences are observed when the copper selenide frameworks are considered in detail. This is clearly apparent when the respective Se_{22} substructures are compared (Figure 14). Both can be described as a staggered arrangement of three Se_6 rings, the middle one being larger than the outer rings. One additional selenium ligand caps each of the two terminal Se_6 faces of the face-sharing hexagonal anti-prisms. Apart from different distortions of these peripheral Se_{20} polyhedra (total lengths or widths of the Se_{22} substructures according to the orientations in Figure 14: 11.43 or 8.64 Å in **23**; 8.34 or 10.60 Å in **24**), the relative positions of the inner Se_2 units are perpendicular to each other. One can therefore consider units of twelve copper and two selenium atoms in each cluster core that have completely different orientations, a consequence of the significantly different situations on the cluster surface mentioned above. The isomerism observed with the "Cu_{44}" clusters again shows that certain [$Cu_{2n}E_n$] compositions represent "islands of stability" − within given limits of structural isomers − that are obtained experimentally whenever a suitable ligand shell

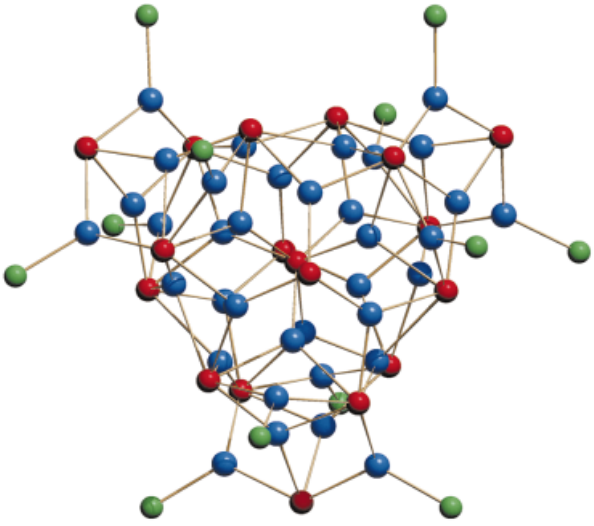

22

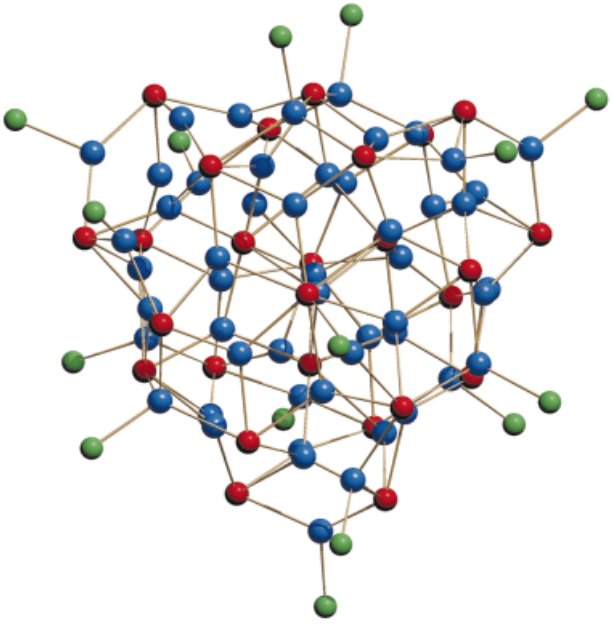

26

Figure 15. Molecular structures of $[Cu_{36}Se_{18}(PtBu_3)_{12}]$ (**22**) and $[Cu_{52}Se_{26}(PPh_3)_{16}]$ (**26**) (without organic groups)

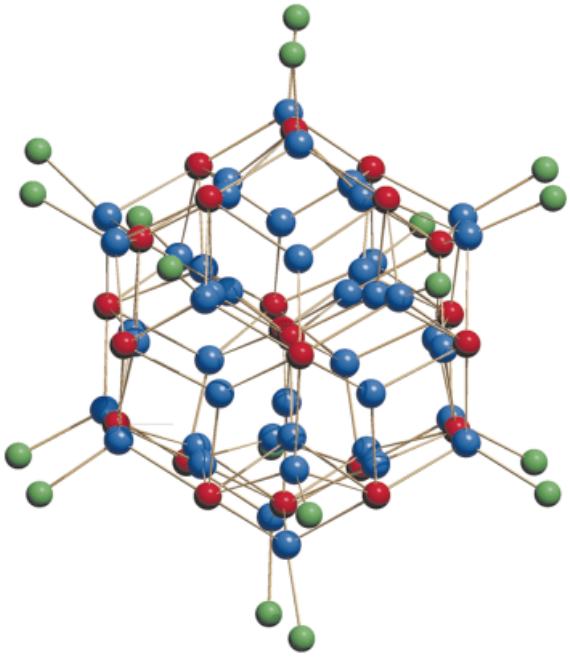

23

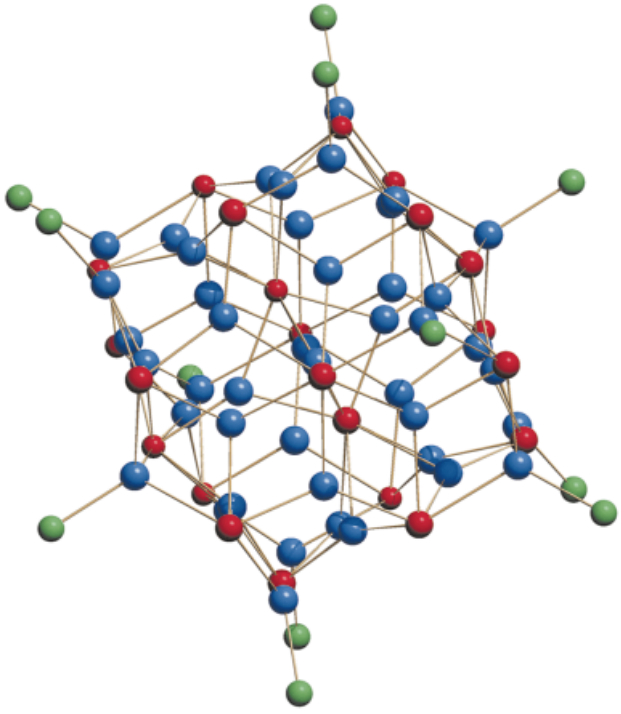

24

Figure 16. Molecular structures of $[Cu_{44}Se_{22}(PEt_2Ph)_{18}]$ (**23**) and $[Cu_{44}Se_{22}(PnButBu_2)_{12}]$ (**24**) (without organic groups)

can be realized by means of the available phosphane molecules.

Two further ellipsoid-like arrangements are found for clusters **25** and **27**, respectively. Apparently, it is not possible for a phosphane shell composed of PMe_2Ph ligands (cone angle: 127°) to surround a $[Cu_{44}Se_{22}]$ cluster. Instead, the smallest compound to be sufficiently stable and insoluble to allow its isolation is the slightly larger cluster **25**, although this is structurally related to the smaller species **23**. The ellipsoid-like Se_{24} substructure of **25** (Figure 14) can be derived from the Se_{22} arrangement in **23** by simple substitution of each of the single Se caps in the smaller

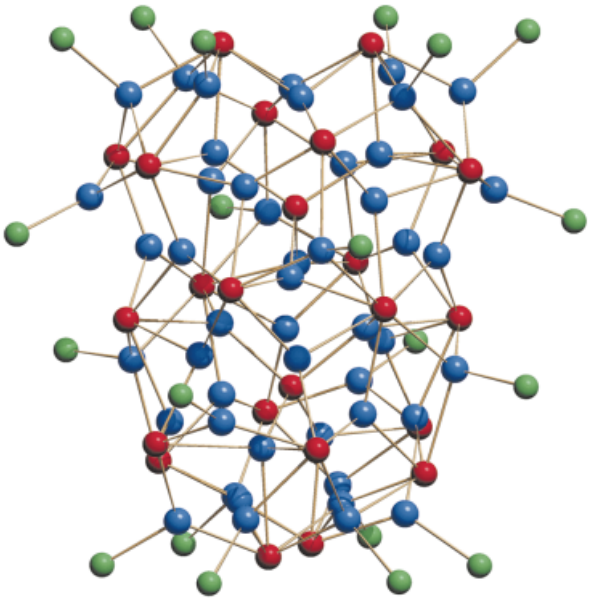

25

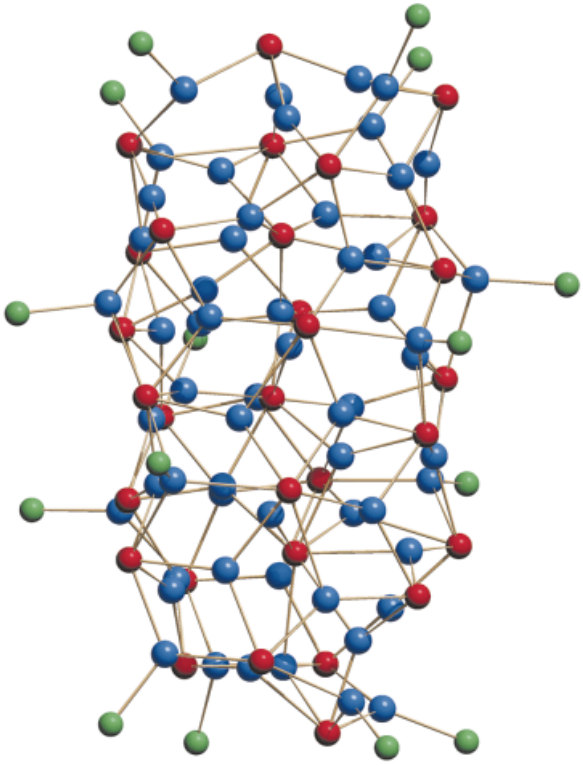

27

Figure 17. Molecular structures of $[Cu_{48}Se_{24}(PMe_2Ph)_{20}]$ (**25**) and $[Cu_{59}Se_{30}(PCy_3)_{15}]$ (**27**) (without organic groups)

polyhedron by two selenium ligands capping the outer Se_6 rings. Again, one finds all the coordination features typical for "middle-sized" Cu−Se clusters, even four copper atoms showing an almost tetrahedral environment of four selenium ligands. However, unlike all the smaller clusters that contain selenium atoms inside the cluster core, **25** features two tetrahedral $[SeCu_4]$ units − these being linked by a *trans*-edge junction through a compressed Cu_4 tetrahedron − with a uniquely low bridging mode (μ_4) for the two inner selenium ligands (cf. the bridging modes of the inner selenium ligands in **14**, **15**, **20**, **22**−**24**: μ_5 to μ_8, μ_{12}). Besides **14** and **17**, **27** is the third copper selenide cluster that has too few metal centers for an overall +1 oxidation state for the copper atoms. However, no single Cu^{2+} center can be assigned and the lack of one electron is likely to be delocalized over the whole cluster framework. As with **23**−**25**, the molecule is oblong in shape. It represents the largest spherical copper selenide cluster yet known, and thus it concludes the series of "middle-sized" Cu−Se clusters. The selenium atoms form a highly irregular Se_{27} polyhedron around three inner chalcogen centers (Figure 14), which can alternatively be viewed as an approximate arrangement of the selenium ligands into three layers. The molecular structure of **27** includes all possible coordination environments around copper atoms, i.e. $[Se_2Cu]$, $[Se_3Cu]$, $[Se_4Cu]$, $[Se_2CuP]$, and $[Se_3CuP]$. Selenium ligands are observed to act as μ_4-, μ_5-, μ_6-, or μ_7-bridges.

Summarizing the structural properties of the "small" Cu−Se clusters **11**−**13**, and the "middle-sized" ones **14**−**27**, the spherical shape and the absence of any topological relationship with the bulk material Cu_2Se are a central feature. Only the tendency towards higher coordination numbers at the copper centers, i.e. three and four, with increasing cluster size approaches the situation in the binary phase. However, the main difference between "small" and "middle-sized" clusters is the occurrence of inner atoms that first appear within a copper selenide core of 33 atoms (**14**). The coordination patterns in the "middle-sized" molecules typically show a mixture of higher and lower coordination numbers or bridging modes, whereas only lower coordination numbers are observed in "small" clusters.

Although only eleven more copper atoms are observed in compounds **28**−**31**[10,17,26,29] than in **27**, these represent the smallest examples of a new type of copper selenide clusters. The so-called "large" Cu−Se clusters are characterized by significantly different cluster shapes, structural principles, and relationships to the bulk material than the smaller species. Clusters **28**−**37** display *A*-*B*-*A*-type packed layers of selenium atoms that form large triangles. At first sight, this might appear to be reminiscent of the "triangular" structures of **22** or **26**. However, a closer look clearly reveals the differences between these two clusters and the layer-type structures of the "large" clusters. Compounds **28**−**37** are all based on three *hcp* selenium layers, of which the middle one is the largest. Figure 18 shows the selenium networks of the "large" clusters **28**[29] (as an example of a $Cu_{70}Se_{35}$ core), **32**[21] ($Cu_{72}Se_{36}$ core), **33**[31] ($Cu_{74}Se_{38}$ core), **34**[23] ($Cu_{140}Se_{70}$ core), and **37**[12] ($Cu_{146}Se_{73}$ core). It is worth

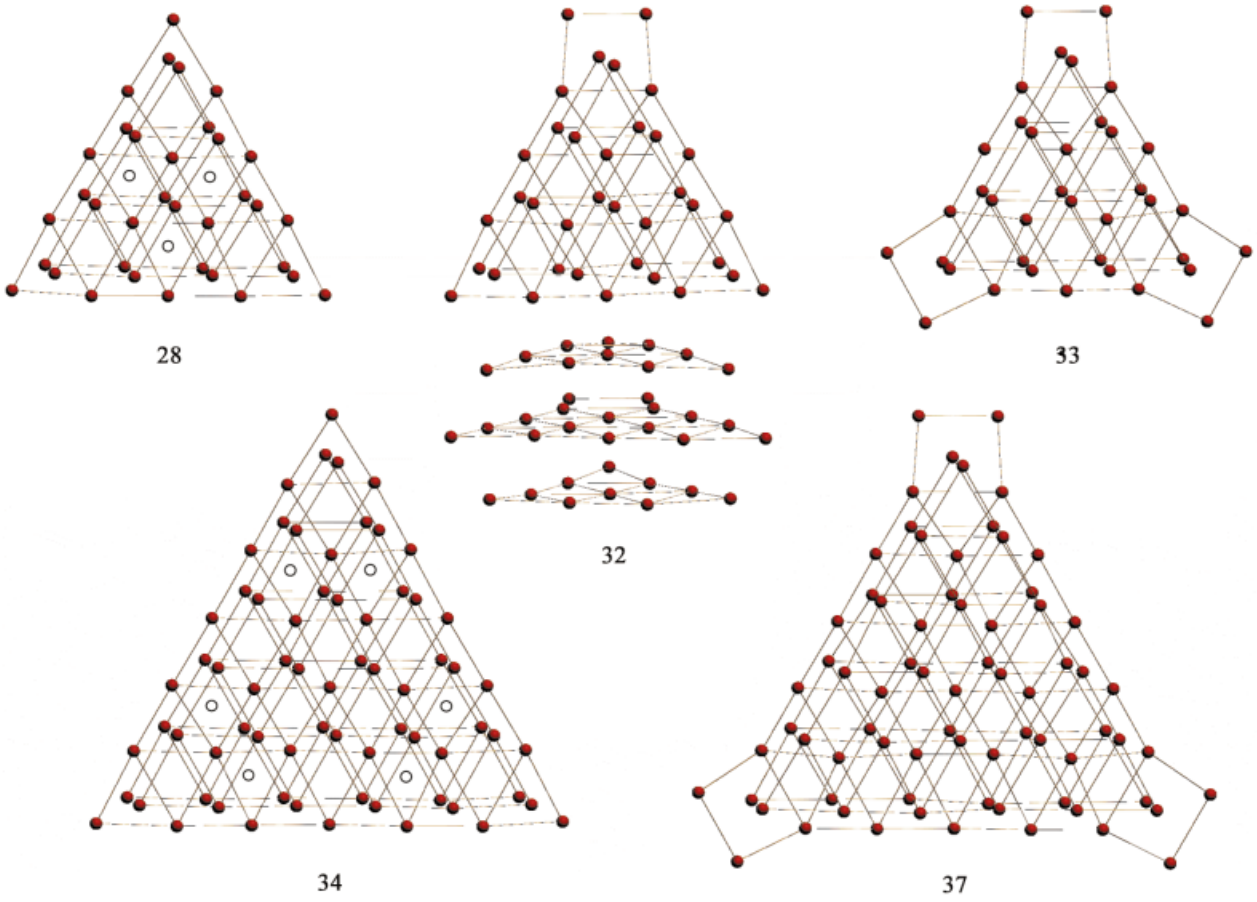

Figure 18. Selenium substructures in **28**, **32**, **33**, **34**, and **37** (from top left to bottom right) that contain 35, 36, 38, 70, or 73 selenium atoms; the drawn Se−Se contacts do not represent binding interactions, but merely serve to visualize the *A-B-A* packing of selenium atoms in three layers; this is additionally demonstrated by the supplementary view of the Se_{36} substructure of **32** (top middle); open circles mark disorder positions of copper atoms (see text)

mentioning that this structural pattern seems to be exceptionally favored for huge copper selenide clusters since it is observed over a size range from "Cu_{70}" to "Cu_{146}", i.e. over a more than twofold increase in the nuclearity.

Clusters **28**−**31** contain Se_{10}, Se_{15}, and Se_{10} layers that form perfect triangles. Thus, the next largest selenium substructure should be formed by an arrangement of triangular Se_{15}, Se_{21}, and Se_{15} layers incorporating one more row of selenium atoms each. However, the corresponding "[$Cu_{102}Se_{51}$]" cluster core is not yet known. Instead, one observes the formation of intermediate clusters incorporating selenium layers similar to those in **28**−**31**, but with the middle one deviating from a perfectly triangular shape. In **32**, one corner of the middle layer is modified with respect to the corresponding layer of the "Cu_{70}" clusters in that two selenium atoms replace one former corner atom. Similarly, all three corners are modified in this way to result in the $Se_{10}-Se_{18}-Se_{10}$ selenium framework of **33**; this compound is another "Cu-deficient" cluster featuring fewer copper centers than Cu_{2n} with respect to Se_n. The third "ideal" cluster composition has been observed in compounds **34**−**36**. The underlying selenium layers contain 21, 28, and 21 atoms, respectively. By replacing all corner selenium centers of the middle triangle by two chalcogen atoms, one obtains the Se_{73} substructure that is observed in **37**. For this third possible size, successive modification of one or two triangle corners of the middle layer has not yet been observed, whereas for the first size (35 selenium atoms), a modification of one or three corners has been found.

The reason for the missing "Cu_{102}" cluster might be related to the primary steps of the cluster growing mechanism. Selenium networks consisting of three triangular *hcp* layers based on $0.5\cdot[n\cdot(n+1)]$ selenium atoms (n = number of straight rows in the triangular network) in *A-B-A* order permit three possible orientations of the central threefold axis of the network {layers with a central Se atom are those containing $0.5\cdot[n\cdot(n+1)]$ atoms, where $n = (3m+1)$, i.e. Se_1, Se_{10}, Se_{28}, etc.; layers where $n = 3m$ or $n = (3m+2)$ have a central hole: Se_3, Se_6, Se_{15}, Se_{21}, Se_{36}, Se_{45}, etc.}: one either finds a hole (representing the unoccupied *C* position), one selenium atom in the middle layer (located in a *B* position), or two selenium atoms belonging to the two outer layers (located in *A* positions). Since all the "large" Cu−Se clusters characterized to date have only been consistent with the last two possibilities, the presence of a central Cu_xSe_y axis ($Se_A-Cu-Cu-Se_A$ in **28**−**33**; $Cu-Se_B-Cu$ in **34**−**37**) would seem to be necessary for the formation of a stable cluster core. Assuming that the cluster growth starts

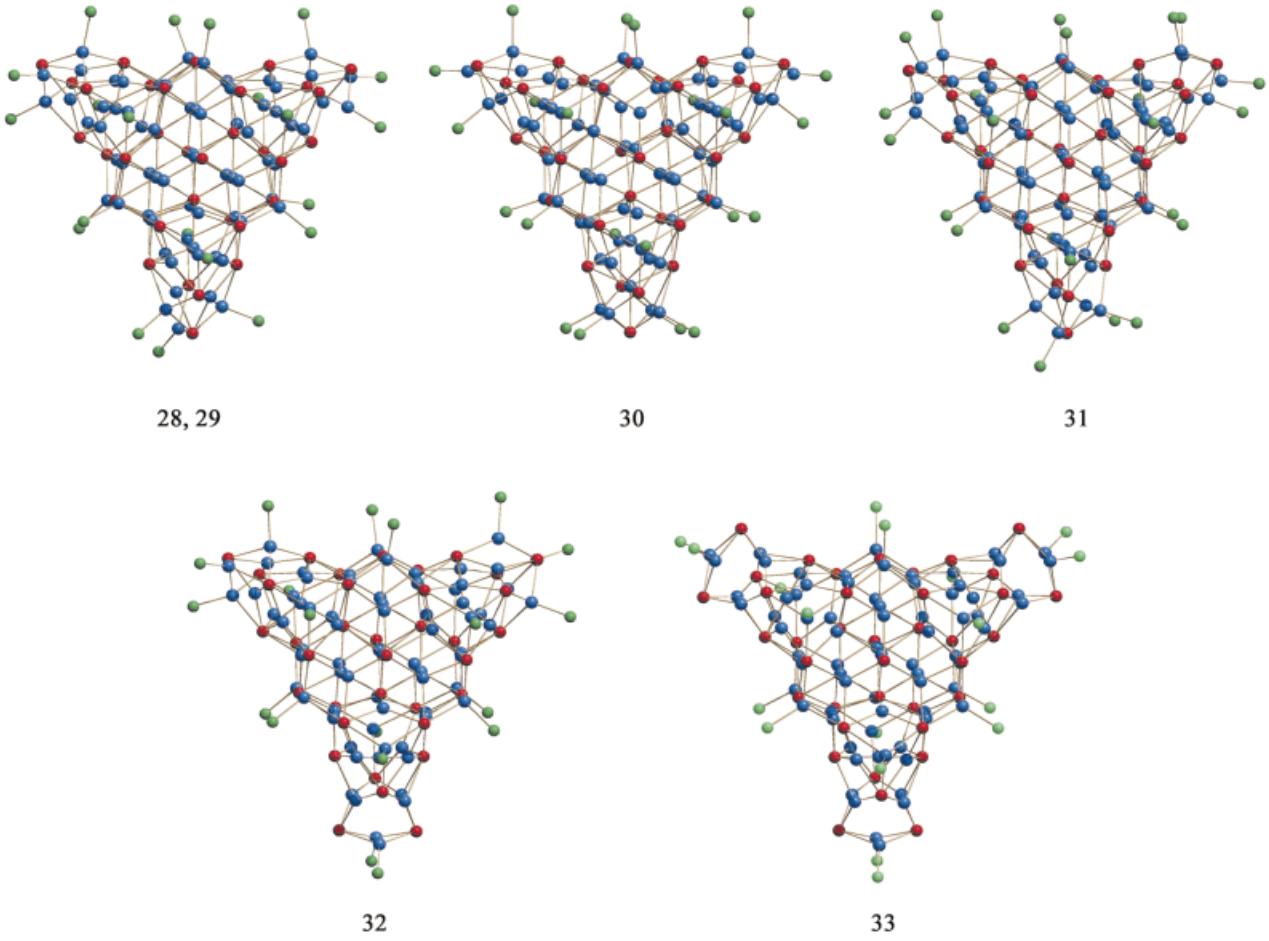

Figure 19. Molecular structures of $[Cu_{70}Se_{35}(PR_2R'_{21}]$ (R = *i*Pr, *t*Bu; R′ = Me) (**28**, **29**), $[Cu_{70}Se_{35}(PEt_3)_{22}]$ (**30**), $[Cu_{70}Se_{35}(PEt_2Ph)_n]$ (n = 23, 24) (**31**), $[Cu_{72}Se_{36}(PPh_3)_{20}]$ (**32**), and $[Cu_{74}Se_{38}(PCy_3)_{18}]$ (**33**) (without organic groups); two copper atoms that are positioned around the central Se−Cu−Cu−Se axis are statistically distributed with occupancies of 0.67 over three positions in **28**, **29**, and **31**

from the center of the molecule, the need for such a $[Cu_2Se]$ or a $[Cu_2Se_2]$ fragment situated along the C_3 axis appears understandable for a non-spherical cluster. Therefore, only those molecules that contain either one (middle; cf. **34**−**37**) or two (outer; cf. **28**−**33**) selenium layers with a central selenium atom instead of a central triangular hole are formed and observed experimentally. Both the Se_{15} and the Se_{21} layers that would conceivably form a "Cu_{102}" molecule do not contain central selenium atoms, thus suggesting why the $[Cu_{102}Se_{51}]$ core has not been observed.

In Figure 19, the cluster cores of the clusters containing 70 (**28**−**31**), 72 (**32**), and 74 (**33**) copper atoms are compared.

The "Cu_{70}" core is quite tolerant with regard to its ligand shell. An increase in the spatial demand of the PR_2R' molecules is not strictly coupled with a decreasing number of terminal ligands. However, one still finds a rough correlation, since 21 of the bulkier phosphane ligands PMe*i*Pr$_2$ (cone angle: 146°) and P*t*Bu$_2$Me (cone angle: 161°) are arranged around the Cu−Se core in **28** and **29**, whereas 22, and 23 or 24, terminal ligands are observed for the smaller phosphanes PEt_3 (cone angle: 132°; **30**) or PEt_2Ph (cone angle: 136°; **31**), respectively. Clusters **28**, **29**,[17] and **31**[26] differ marginally in their molecular structures. The only observable difference between **28** and **29** is a slightly less complete ligand shell achieved by the less sterically demanding PMe*i*Pr$_2$ groups. Cluster **31** displays a disorder problem with the PEt_2Ph groups, such that it cannot be determined with complete certainty whether the total number of phosphane ligands amounts to 23 or 24. Accordingly, for the formation of the cluster, another two (or three) additional phosphane molecules − compared to **28** or **29** − are situated at the triangle corners in such a way that two (or three) corners possess four instead of three Cu−PEt_2Ph groups, while one (or no) corner still bears three groups. The intermediate number of phosphane ligands, 22, is accompanied by a more distinct structural modification in **30**. Again, this affects the corner region. In contrast to all the corner arrangements of copper and selenium atoms in the other "Cu_{70}" clusters, none of which can be described in terms of regular patterns, in **30**[10] only two corners have an irregular structure. The third one shows a highly symmetrical $[Cu_9Se_3(PEt_3)_4]$ configuration featuring a centered cube of copper atoms that is capped on three faces by μ_4-selenium ligands and bears a square of four phosphane groups on the four outer atoms. This peculiarity of one cluster corner in

30 is one of two reasons for the absence of pseudo-threefold molecular symmetry. A C_3 symmetry of the $[Cu_{70}Se_{35}]$ core of **28**, **29**, or **31** is additionally approached − apart from one "wrong" Cu−PR_2R' position in **28** and **29** − by the statistical disorder of two copper atoms. The latter are distributed over three positions − each with site occupancies of 0.67 − forming a triangle around and perpendicular to the Se−Cu−Cu−Se pseudo-threefold axis running through the center of the molecule. In Figure 18, the three disorder sites are marked with open circles. The disorder of the PEt_2Ph ligands in **31** also leads to a pseudo-C_3 axis if 24 phosphane groups are assigned to the ligand shell. In contrast, close inspection of the cluster center in **30** reveals an unoccupied copper atom position. The two other metal atom sites are fully occupied, leading to a lower − yet crystallographically realized − C_2 symmetry.

The molecular structure of **32** can be derived from that of **28** or **29** in a simple manner if one first fully occupies all the copper atom positions around the Se−Cu−Cu−Se axis as mentioned above, and then formally substitutes one corner selenium atom by an $[Se_2(CuPPh_3)_2]$ unit after removal of three PPh_3 ligands at that corner. This leads to a modification of the middle selenium layer, as discussed earlier. Additionally, the number of phosphane groups that enclose the respective corner is reduced to two, since two of the three copper atoms that are coordinated by PR_2R' ligands in the analogous corner in **28** or **29** remain "naked" in **32**. Modification of all three cluster corners in this way, again together with full occupation of the Cu_3 group around the cluster center, generates the structure of the mixed-valence cluster framework in **33**. With idealized C_{3h} symmetry for the cluster framework, the symmetry of the molecule does not exceed C_2 in the crystal due to slight distortions and the positions of the organic groups bonded to the phosphorus atoms.

The largest copper selenide clusters yet known contain 140 or 146 copper atoms and 70 or 73 selenium ligands, respectively. The molecular structures of **34**, **36**,[23] and **37** are shown in Figure 20.

The different number of PR_2R' groups observed in **34** or **35**,[31] on the one hand, and in **36** on the other, affects the molecular structures in a different manner as seen for the "Cu_{70}" species **30** and **31**. Considering the corners again, **34**, with 34 terminal PEt_3 ligands, resembles an enlarged analogue of **30**. As in the smaller compound, two corners are arranged irregularly, whereas the third shows the regular, centered-cubic pattern. On increasing the number of PEt_3 groups to 36, as in **36**, all three corners now show this ordered arrangement of copper, selenium, and phosphorus atoms. This corner unit, which is only found for the PEt_3-ligated "large" Cu−Se clusters, underlines the structural relationship between **30**, **34**, and **36**, and again highlights the steric influence of a particular PR_2R' ligand. All other phosphane ligands that surround "large" copper selenide clusters feature larger cone angles, which could be the reason for the adoption of a more staggered arrangement if four Cu−PR_2R' units are present at a corner. Consequently, in **35**, all three corners show arrangements like that in the smaller analogue **31**. Disorder of copper atoms that increases the apparent idealized molecular symmetry is again present in the "Cu_{140}" clusters. A twofold disorder of one copper atom, between positions on the pseudo-C_3 axis (above and below the central selenium atom), results in an apparent "$Cu_{0.5}$"−Se−"$Cu_{0.5}$" central axis. In addition, four copper atoms are disordered over six equivalent sites, each with occupancies of 0.67. As for the "Cu_{70}" clusters, these sites lie within the plane of the middle selenium layer. However, in contrast to the smaller clusters **28**, **29**, and **31**, where the disorder sites form part of the $[Cu_3Se_3]$ hexagon at the center of the clusters, the six disorder sites in **34**−**36** are more distant from the cluster centers, as marked with open circles in Figure 18.

The formal replacement of each of the three corner selenium atoms and twelve PR_2R' molecules in **36** by three $[Se_2Cu(PR_2R')_2]$ units, as well as full occupation of all the copper sites present in the "Cu_{140}" clusters, exactly yields the composition and D_{3d} symmetric molecular structure of **37**. Thus, the structural relationship between **36** and **37** is analogous to that between the "Cu_{70}" and the "Cu_{72}" and "Cu_{74}" clusters.

All the "large" Cu−Se clusters show an *A-B-A* packing of hexagonal layers of selenium atoms. The metal centers occupy either trigonal or tetrahedral holes, or are situated outside the selenium layers in trigonal or tetrahedral coordination environments. Thus, the layer-type clusters clearly show a closer relationship to solid-state structures than do the spherical ones. However, for the $Cu_{2-x}Se$ phases, hexagonal structures are unknown and only cubic modifications are found. Interestingly, for the Cu_2S (chalcosine) high-temperature phase,[38] a hexagonal lattice with mainly trigonally-surrounded copper atoms, with some tetrahedrally and linearly coordinated ones, does exist. In contrast, the cubic $Cu_{2-x}Se$ crystal structures[39] can be derived from an antifluorite lattice[51] by positioning the selenium atoms at defined lattice sites, and positioning six to eight copper atoms per unit cell − according to the phase composition − in trigonal, tetrahedral, or octahedral holes. In α-Cu_2Se, the metal centers are positioned in an ordered manner within the selenium lattice, whereas in β-Cu_2Se they are statistically disordered over the observed sites. Even though the reported structural properties of copper selenide binary phases are not uniform, there is a clear agreement regarding the dominant coordination number of four for the copper atoms and the absence of any linearly-coordinated metal centers. Due to the hexagonal modification and the preferred coordination number of three for the copper atoms, the layer-type Cu−Se clusters approach the bulk material situation only in principle. Table 3 summarizes the interatomic distances in several copper(I) selenide compounds with respect to different coordination numbers around the metal atoms (cf. Table 2 for Cu−S systems).

Regarding the copper selenide clusters reviewed here, it is clear that a given phosphane ligand does not just generate clusters within a given size range, with another PR_2R' ligand resulting in the next largest clusters, and so on. Instead, it is evident that even very different types of phos-

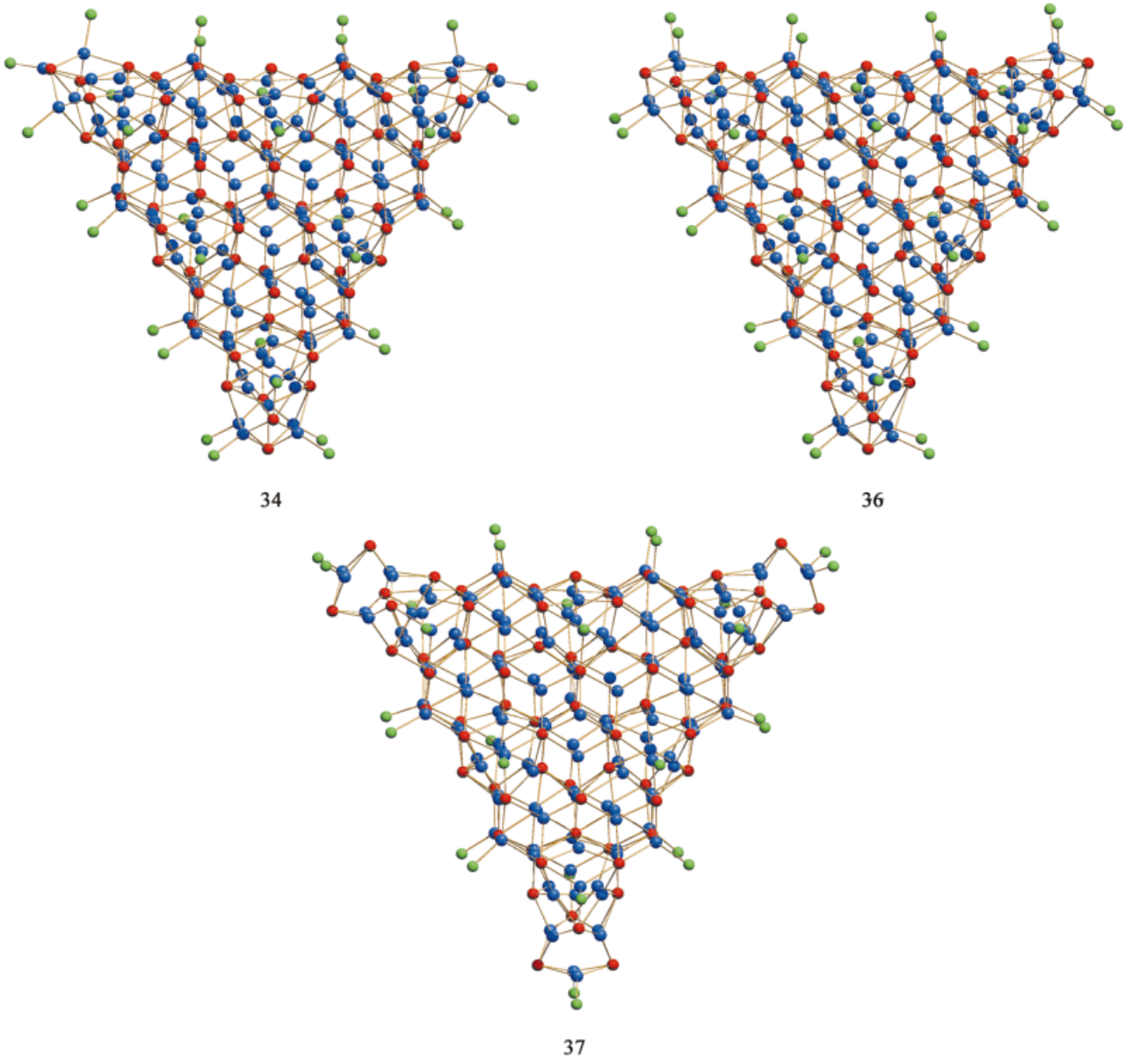

Figure 20. Molecular structures of $[Cu_{140}Se_{70}(PEt_3)_{34}]$ (**34**), $[Cu_{140}Se_{70}(PEt_3)_{36}]$ (**36**), and $[Cu_{146}Se_{73}(PPh_3)_{30}]$ (**37**) (without organic groups); in **34** and **36**, the two central copper atoms each have occupancies of 0.5, to result in one atom overall, which is statistically distributed over two sites; six further copper atoms are assigned occupancies of 0.67, resulting in four instead of six metal atoms in the overall formula

Table 3. Interatomic distances of selected Cu^I−Se systems

System	Cu−Cu [Å]	Cu−S distances for the different coordination numbers (*CN*) [Å]			Ref.
		CN = 2	*CN* = 3	*CN* = 4	
Cu−Se clusters	2.427−3.047	2.169−2.295	2.317−2.897	2.291−2.986	[9,10,12−14,17,18,21]
Cu^I−(Se_n) complexes	2.77 (av.)	−	2.37 (av.)	−	[52]
α-$KCuSe_4$	2.64−3.00	−	2.35−2.50		[53]
Binary $Cu_{2-x}Se$ phases	2.35−2.92	2.06	2.28−2.33	2.15−2.59	[39]

phanes, of different steric bulk, can lead to the formation and crystallization of similar, isomeric, or even identical Cu−Se cores if the ligand shells comply with certain requirements of regular geometry and thus protective properties. Inspection of Scheme 3 reveals that several clusters, varying significantly in size, may be formed in the presence of the same phosphane, although under different reaction conditions, so long as various suitable ligand shells can be

realized. In order to illustrate the size dependence of the cluster core on the use of different copper salts, reaction stoichiometries, solvents, and reaction temperatures, selected cluster formation reactions are shown in Schemes 5, 6, 7, and 8 with precise specifications of the respective conditions. Each scheme deals with one phosphane type.

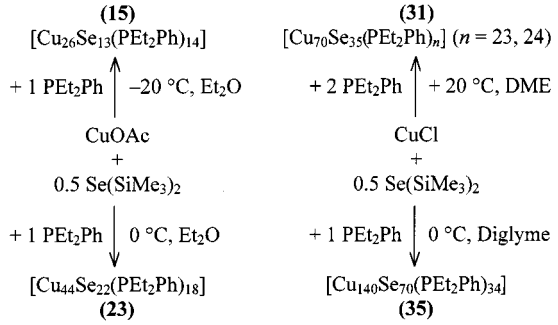

Scheme 5. Synthesis of various copper selenide clusters in the presence of PEt_2Ph under different reaction conditions

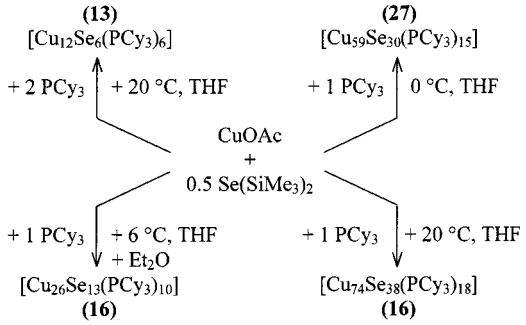

Scheme 6. Synthesis of various copper selenide clusters in the presence of PCy_3 under different reaction conditions

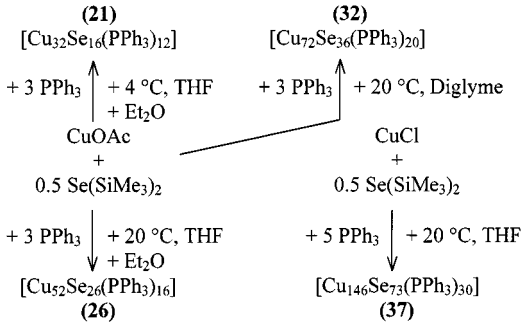

Scheme 7. Synthesis of various copper selenide clusters in the presence of PPh_3 under different reaction conditions

As for the copper sulfide clusters, comprehensive theoretical investigations within the MP2 approximation (program system TURBOMOLE) were carried out for the $[Cu_{2n}Se_n]$ clusters.[34] Again, stabilization energies per monomeric unit for a "naked" cluster growth from $n = 1$ through $n = 2-4$, 6 to $n = 10$ were calculated, along with phosphane binding energies for mono-, di-, tri-, tetra-, and hexameric species. The results are presented in Figures 21 and 22, respectively. The corresponding graphs for the Cu−S clusters, shown in Figures 6 and 7, respectively, are given once more for comparison purposes.

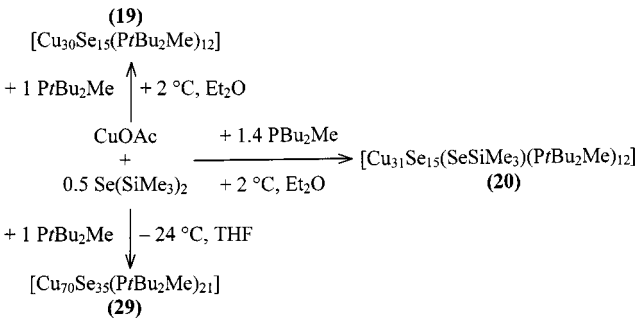

Scheme 8. Synthesis of various copper selenide clusters in the presence of $PtBu_2Me$ under different reaction conditions

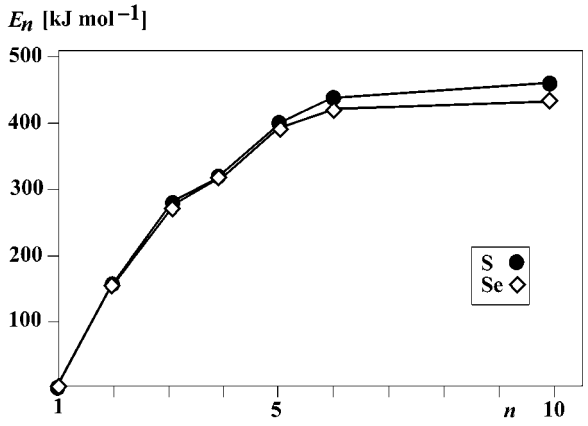

Figure 21. Variation of the stabilization energies per monomer unit in "naked" clusters $[Cu_{2n}E_n]$ (E = S, Se; $n = 1-4$, 6, 10) with the given values taking into account the total energies of the most stable structural isomers computed at the MP2 level

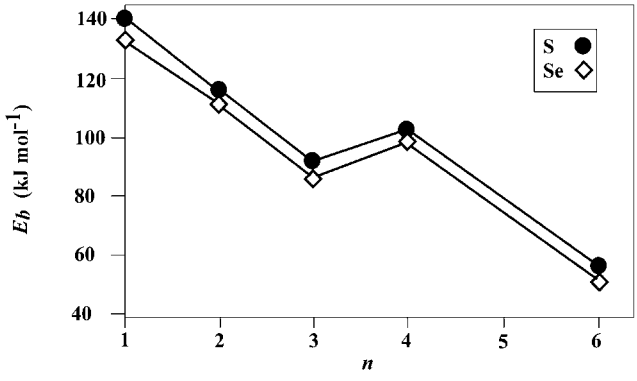

Figure 22. Variation of the Cu−P binding energies per Cu−P bond in phosphane-ligated clusters $[Cu_{2n}E_n(PH_3)_m]$ (E = S, Se; $n = 1-4$, 6; $m = 2$, 4, 6, 8); the given values taking into account the total energies of the most stable structural isomers computed at the MP2 level with respect to the total energy of PH_3 calculated by the same method

The variations in both energies are similar for the quantum chemically investigated sulfur- and selenium-bridged copper clusters. Thus, the kinetic rather than the thermodynamic stabilities of the species, and the very low

Cu−P binding energy, are the same as for the Cu−S compounds. Additionally, a comparison of the energetic properties of sulfur- vs. selenium-bridged copper clusters leads to two results. First, after nearly identical stabilization energies (maximum differences: ±5 kJ·mol^{-1}, < 2%) up to $n = 4$, a slightly higher stabilization for the Cu−S species is seen from $n = 6$ onwards. This correlates with a larger absolute value for the formation enthalpy of solid Cu_2S ($\Delta H_f° = -81.2$ kJ·mol^{-1}) than for solid Cu_2Se ($\Delta H_f° = -65.2$ kJ·mol^{-1}). However, the differences between the stabilization energies per monomeric unit for the calculated, rather small clusters do not exceed 5%. Thus, it is understandable why laser ablation spectra of copper chalcogenides do not vary much for the different chalcogens. Secondly, the Cu−P bond energies are generally 4−7 kJ·mol^{-1} (4−9%) higher for the sulfur-bridged compounds. This correlates with the discrepancy between the experiments reported by Dance et al.,[32] which show similar behavior for different chalcogens − in agreement with the calculations on "naked" species − and the experimental observations of significant differences in the syntheses and structures of phosphane-coordinated sulfur- and selenium-bridged copper clusters. The larger Cu−P binding energies computed for Cu−S clusters, relative to those computed for their Cu−Se analogues, help to explain the different ranges of observed products in the following way. Assuming that on going from the Cu−Se to the Cu−S systems the activation energy E_a for the Cu−P bond cleavage increases by a similar value as the Cu−P binding energy itself, a decrease in the respective reaction rate constant k can be calculated by means of the Arrhenius equation[54] [Equation (1)].

$$k = A \cdot e^{-E_a/RT} \quad (1)$$

At a typical cluster formation temperature of $T = 250$ K, an increase in the activation energy E_a of about 5 kJ·mol^{-1} causes a reduction in the rate constant k by one order of magnitude. Thus, the cluster growth that is initiated by the loss of a primary terminal phosphane ligand shell will occur at a lower rate for sulfur-bridged clusters. Consequently, unlike the selenium-bridged copper clusters, the Cu−S species show a much lower tendency to aggregate beyond "Cu_{12}".

3.2.2.2. Se^{2-}/SeR^--Bridged Copper Clusters

The use of alkylated or arylated derivatives $RSeSiMe_3$ (R = organic group) results in aggregation according to another mechanism, and leads to the formation of selenido/selenolato-bridged copper clusters. The given synthetic route using $RSeSiMe_3$ (Schemes 1 and 4) has not produced any selenolato-free species. This observation is at variance with those made for similar reactions with tellurolato reactants $RTeSiMe_3$ (see below). The experimentally isolated and characterized compounds listed in Scheme 4 display significantly different structures with respect to the purely E^{2-}-bridged molecules (E = S, Se). This applies even for reactions in the presence of tertiary phosphanes PPh_3 or P*i*Pr$_3$ used for the syntheses of the copper selenide clusters. The expanded ligand properties of SeR^-, which can act as both a bridging and a terminal ligand, lead to the crystallization of low nuclearity complexes with two, three, six, or nine metal centers (**38**−**42**),[20,22,30] if Se−C bond cleavage is suppressed. Larger cluster compounds can be isolated whenever Se^{2-} particles are produced during the reaction to facilitate the formation of inner selenium bridges. However, those molecules containing both selenide and selenolato ligands show structural patterns that are also common for Cu−Se clusters as far as the inner core is concerned. Figure 23 depicts compounds **38**−**42**, which only contain selenolato ligands and not selenide.

The binuclear complexes **38**[30] and **39**[20] formally show analogous molecular formulae but differ structurally according to the requirements of the different ligating components that are present. These requirements are of structural relevance for all Se^{2-}/SeR^--bridged copper clusters, as outlined in the following. Firstly, bidentate phosphanes dppR (R = organic spacer) bridge two copper centers at the periphery of the polynuclear complex or cluster molecule and therefore act simultaneously as both protecting groups and linking molecules. Secondly, selenolato ligands SeR^- have the capability to bridge between two *or* three metal centers. Additionally, they *can* be terminally bonded, as in **39**, when the Cu−Cu distance (9.01 Å) is too large for a monoatomic μ_2-bridge. Thirdly, tertiary phosphanes PR_2R' act exclusively as terminal ligands. Therefore, the copper atoms in **38** are bridged by $SePh^-$ fragments at a Cu−Cu distance of 2.846(1) Å. The molecular structure of **40**[22] also conforms to these constraints, again with the ubiquitous key factor of optimal protection of the heavy atom framework by organic groups. Compounds **41**[30] and **42**[30] are the only examples that could be isolated employing the bidentate amine ligand bipyridyl (**41**) or diphenylphosphanyl acid Ph_2PO_2H (**42**). Compound **41** seems to represent a "snapshot" molecule during cluster growth, since two $[Cu(bipy)]^+$ fragments are unsymmetrically attached to a regular cluster center. The latter is formed by a distorted Cu_4 tetrahedron [Cu−Cu: 2.650(4)−2.824(4) Å], the six edges of which are each μ_2-bridged by $SePh^-$ ligands. However, four of the phenyl selenolato groups act as μ_3-bridges in the molecule, since two bind to each of the additional $Cu(bipy)^+$ units. Having achieved charge neutrality, the sufficiently protected compound precipitated in this low nuclearity state. Much higher molecular symmetry − even crystallographic symmetry − is found for **42**. Two six-membered $Cu_3(SePh)_3$ rings are linked by three "naked" copper centers leading to a μ_3-bridging function of the $SePh^-$ groups. Additionally, the rings are clamped by three $Ph_2PO_2^-$ ligands, which bind to the six copper atoms in the two six-membered rings. Twelve phenyl groups perfectly wrap the uncharged cluster and therefore allow the termination of atomic aggregation and crystallization in THF.

As was found for the copper chalcogenide clusters **1**−**37**, the nature of the phosphane ligands plays a key role in determining the size and structures of the observed product molecules, even though they are no longer the sole protective groups at the cluster peripheries. Great success in the synthesis of copper selenide/selenolate clusters was achieved by the use of bidentate phosphanes. The variation of or-

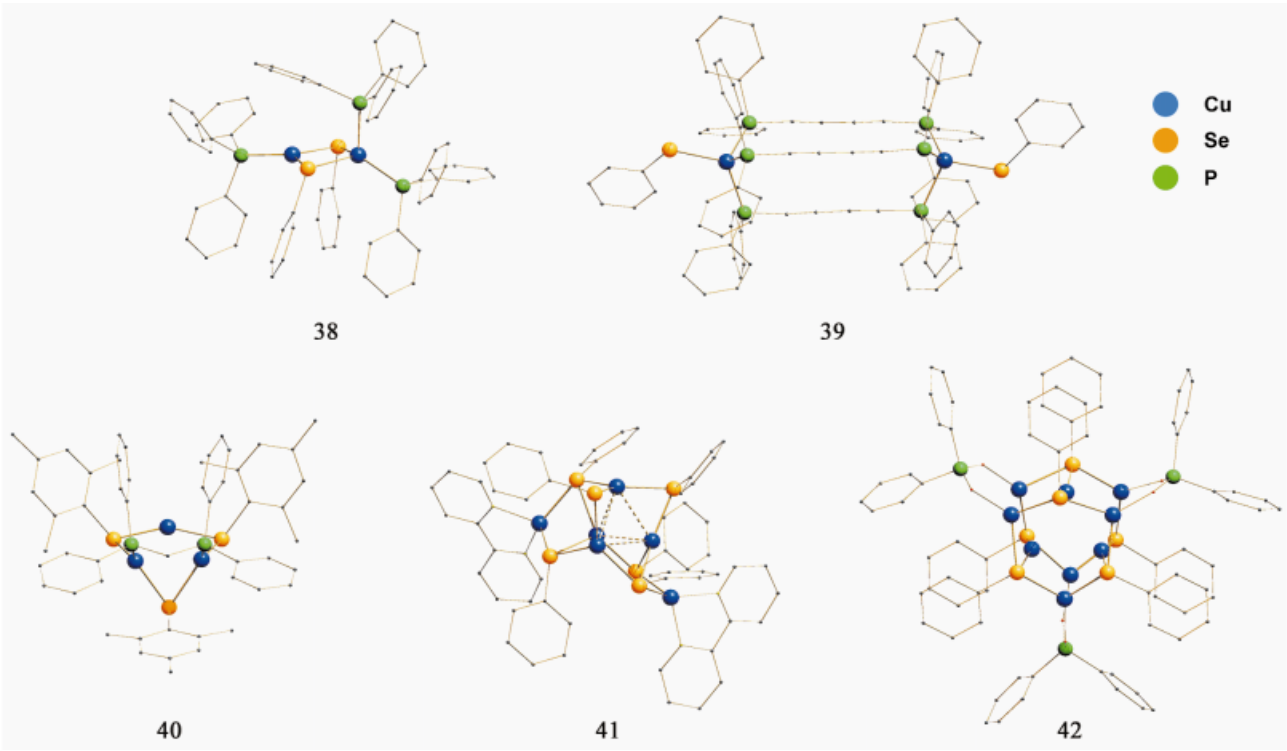

Figure 23. Molecular structures of $[Cu_2(SePh)_2(PPh_3)_3]$ (**38**), $[Cu_2(SePh)_2(dppbd)_3]$ (**39**), $[Cu_3(SeMes)_3(dppm)]$ (**40**), $[Cu_6(SePh)_6(bipy)_2]$ (**41**), and $[Cu_9(SePh)_6(O_2PPh_2)_3]$ (**42**) (without hydrogen atoms)

ganic spacers between the two ligating $[Ph_2P]$ fragments replaces the former variation of organic substituents R of PR_2R' in the selenolate-free clusters. Again, a given dppR ligand does not inflexibly restrict the synthesis to the formation of one single cluster product. Other reaction conditions discriminate between several potential compounds that can all be conveniently protected by the phosphane employed. Thus, with ethane, propane, butane, acetylene, or benzene spacers, one obtains clusters with 16, 25, 36, 38, or 58 copper centers (**43**,[20] **44**,[22] **46**−**50**,[22,30] **52**[22]), respectively. The only tertiary phosphane PR_3 to have been successfully used for the formation of higher nuclearity $Se^{2-}/SePh^-$-bridged copper clusters is P*i*Pr$_3$. With this ligand, the synthesis of molecules featuring 32, 50, or even 73 metal centers (**45**, **51**, and **53**)[23] was observed, depending on the reaction conditions. Figure 24 shows the molecular structures of **43** and the anion in **44**, which represents the only ionic copper selenide cluster compound isolated to date.

Both clusters are oblong in shape. The selenium substructure of **43** can, however, be viewed as an incipient hexagonal packing of selenium atoms. The middle "layer" consists of six atoms arranged in a zigzag fashion, while the two enclosing "layers" each contain three selenium centers occupying the quasi *A* position with respect to the quasi *B* position of the atoms in between. Four of the chalcogen bridges do not bind to phenyl groups and act as μ_4- or μ_6-bridging ligands. The $SePh^-$ ligands bind to two or three copper neighbors each, and at the same time contribute to the protection of the Cu−Se core by means of their organic substituents. Six copper atoms are linearly coordinated by two

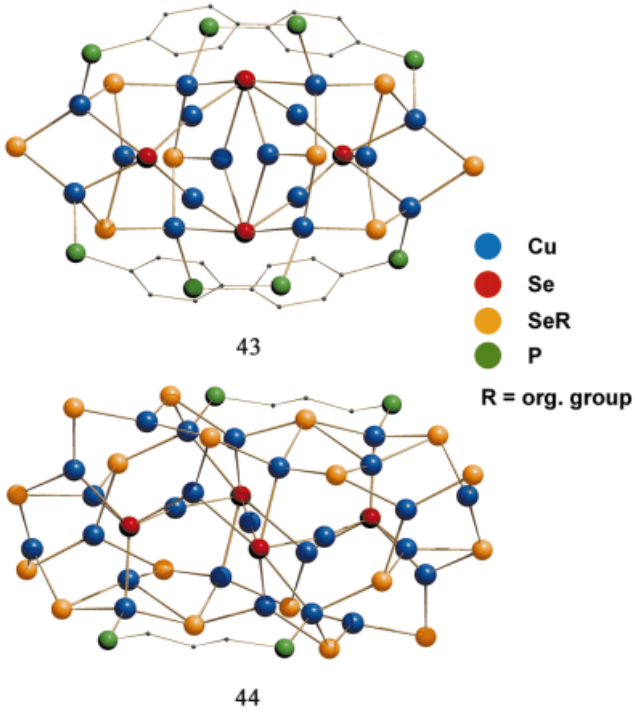

Figure 24. Molecular structures of $[Cu_{16}Se_4(SePh)_8(dppbe)_4]$ (**43**) and the anion in $[Cu(dppp)_2][Cu_{25}Se_4(SePh)_{18}(dppp)_2]$ (**44**) (without terminal phenyl groups)

selenium ligands, two show an almost trigonal-planar $[Se_3Cu]$ coordination, whereas the remaining eight metal centers occupy the centers of slightly distorted $[Se_3P]$ tetra-

hedra. Unlike in **43**, the chalcogen framework of **44** is composed of an ellipsoid-type deltahedron of four Se^{2-} ligands and 18 selenium atoms of the $SePh^-$ groups. Again, the bridging mode of the chalcogen centers is higher for the "naked" ligands (μ_5 or μ_7) than for the $SePh^-$ fragments (μ_2 to μ_4 with regard to the Cu−Se bonds). Eighteen copper atoms are positioned at the cluster periphery and belong to almost planar [Se_3Cu] or distorted tetrahedral [Se_3CuP] units. The observation that less linear [Se_2Cu] arrangements are present (four in **43**, three in **44**) underlines the trend to higher coordination numbers at the metal center with increasing molecular size, as reported for the copper selenide clusters without selenolato ligands. The cluster core is large enough to accommodate seven inner copper atoms that are either two-, three-, or four-coordinated by selenium neighbors. Comparing the compositions of **43** and the anion in **44**, one perceives an increasing preference for ligation by $SePh^-$ ligands rather than by phosphane donors. This may be explained by the dual character of the $SePh^-$ groups, which primarily form fairly stable Cu−Se cluster bonds, but also bear protective organic substituents. Thus, the ratio of selenolato selenium atoms to phosphorus atoms increases from 1:1 in **43** to 4.5:1 in **44**.

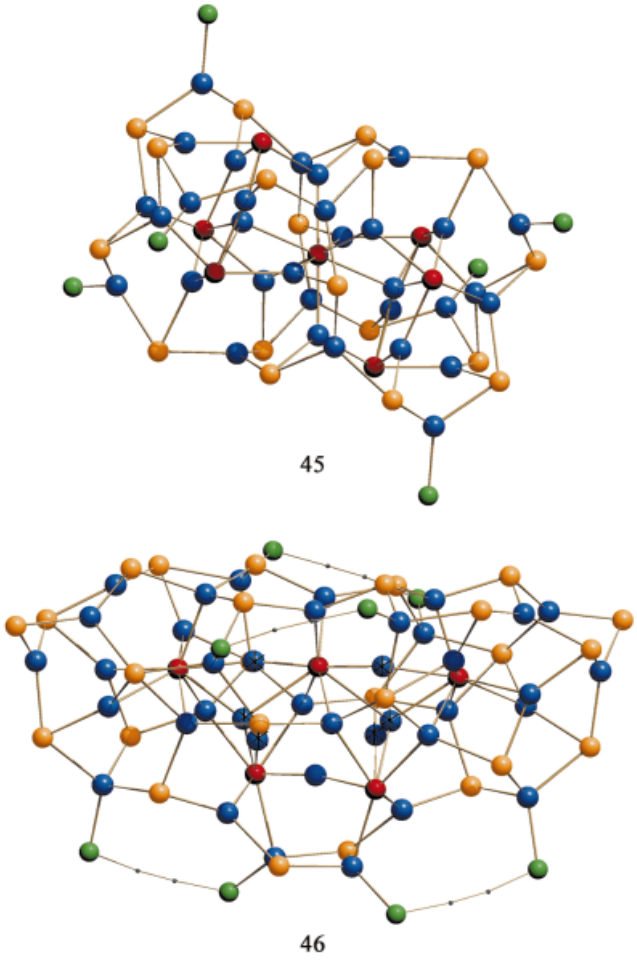

Figure 25. Molecular structures of $[Cu_{32}Se_7(SenBu)_{18}(PiPr_3)_6]$ (**45**) and $[Cu_{36}Se_5(SePh)_{26}(dppa)_4]$ (**46**) (without *n*-butyl, isopropyl, or phenyl groups); three copper atoms (marked with an asterisk) in the cluster center of **46** are distributed over six sites with occupancies of 0.5

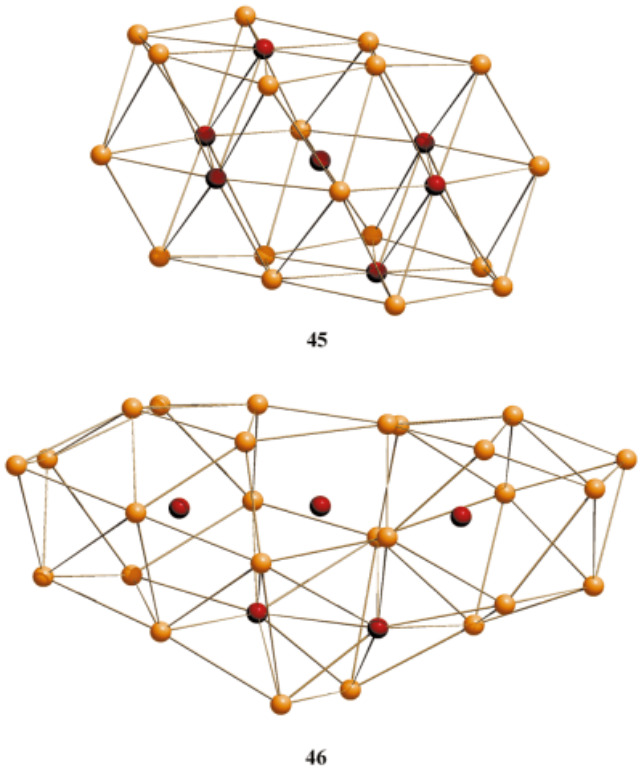

Figure 26. Selenium substructures in **45** (top) and **46** (bottom); the Se−Se lines do not represent bonding interactions, but merely help to visualize the *A-B-C* packing of selenium atoms in three layers in **45** or explain the geometry of the polyhedron in **46**

The molecular structures of the cluster compounds **45** and **46** are shown in Figure 25, while Figure 26 compares the selenium substructures in these two clusters.

As in the comparison between **43** and **44**, we again have a smaller cluster for which the structure is based on a regular packing of selenium atoms in hexagonal layers (**45**) and a larger, rather spherically shaped compound that features a polyhedral selenium framework (**46**). However, the selenium layers in the $SenBu^-$-bridged species **45** are packed in an *A-B-C* fashion similar to the Cu_2Se solid-state structure, which is unparalleled for all copper chalcogenide clusters characterized to date. This similarity between the atomic arrangement of a cluster molecule and the non-molecular Cu_2Se suggests that a nanosized fragment of a bulk structure may indeed be stabilized by coating the surface with suitable groups. This tendency has also been observed in three silver selenide/selenolate clusters, $[Ag_{112}Se_{32}(SenBu)_{48}(PtBu_3)_{12}]$, $[Ag_{114}Se_{34}(SenBu)_{46}(PtBu_3)_{14}]$, and $[Ag_{172}Se_{40}(SenBu)_{92}(dppp)_4]$.[55] Compound **45** is the only copper selenide/selenolate compound that contains $SenBu^-$ groups like those found in these silver clusters. It is not yet proven, but is nevertheless conceivable, that the packing of the selenium atoms is influenced by the nature of the organic group attached to the selenolato ligand. The chalcogen layers in **45** are centered by a large planar rhombus of nine selenium atoms. Five of them are "naked" Se^{2-} ligands in

the cluster network, while the four vertex atoms belong to Se*n*Bu$^-$ groups. Above and below this middle layer, one finds two similar but truncated rhombuses consisting of only eight selenium atoms, the "central" ones not being bonded to organic substituents. However, the size dependency of the structural properties seems to be different from that of the selenolato-free copper clusters. Thus, layer-type structures are observed even for smaller molecules like **43** or **45**, as well as for larger spherical ones. Additionally, a return to lower average coordination numbers in larger clusters may arise, as observed in **45**. The location of the copper atoms in **45** can be described with reference to the selenium grid. The six phosphane-bound copper centers bind to two selenium atoms of Se*n*Bu$^-$ ligands and are situated on the cluster periphery. Six copper atoms are located approximately within the selenium layers and have trigonal-planar coordination geometries with normal Cu−Se bond lengths of 2.406(2)−2.483(2) Å. The other 20 metal centers are positioned between the layers of selenium atoms. Two of these show ideal tetrahedral environments, while the others are shifted away from the centers of tetrahedral holes. As a result, each of these displays only three normal Cu−Se bonds, with the fourth Cu−Se distance being relatively long (3.18−3.35 Å). The tendency to occupy tetrahedral holes − even unsymmetrically − is again consistent with the structural properties of bulk Cu_2Se. In **46**, five inner Se^{2-} ligands are enclosed by a shell of 26 $SePh^-$ fragments. The bridging modes of the Se^{2-} ligands amount to μ_7 or μ_8, whereas the selenium atoms of the $SePh^-$ groups act only as μ_2- to μ_4-bridges between adjacent copper atoms. The copper centers show coordination numbers of two, three, or four, within $[Se_2Cu]$, $[Se_3Cu]$, and $[Se_4Cu]$ or $[Se_3CuP]$ units, respectively. Depending on their position inside the cluster or at the surface, the selenium neighbors of the metal atoms are exclusively Se^{2-}, or both Se^{2-} and $SePh^-$ ligands. As for compounds **43** or **44**, the number of terminal selenolato groups is greater than the number of ligating phosphorus atoms (SeR/P ratios: 3:1 in **45**, 3.25:1 in **46**).

Four very similar Cu/Se/SePh clusters are formed in the presence of either dppe, dppp, or dppb (**47**−**50**). The syntheses of the isomeric, mixed-valence compounds **47** and **48**, containing 36 copper centers, were carried out in THF. The isomeric "Cu_{38}" clusters **49** and **50**, which formally contain exclusively Cu^+, were crystallized from toluene. Besides the different solvents, the reactions producing the dppb-ligated compounds **48** and **50** differed in the CuCl:dppb ratios (3.1:1 for **48**, 5:1 for **50**). In Figure 27, the molecular structures of **47** and **49** are given as examples.

Cluster **47** crystallizes in the trigonal space group $R\bar{3}$, whereas **48**−**50** crystallize in triclinic $P\bar{1}$. Despite the different crystallographic symmetries, all four compounds display very similar structural properties. A closer look at the atomic arrangements may explain the preference for this prototypical cluster framework in terms of the highly symmetrical substructures. A central selenium atom positioned at the inversion centers of the clusters is surrounded by a distorted icosahedron of twelve copper atoms. The latter is itself enclosed by another distorted Se_{12} icosahedron. An

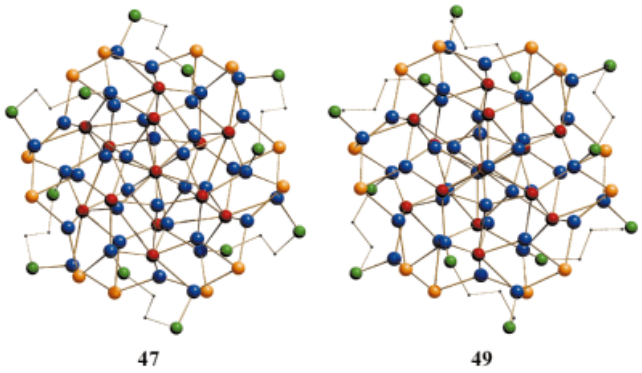

Figure 27. Molecular structures of $[Cu_{36}Se_{13}(SePh)_{12}(dppe)_6]$ (**47**) and $[Cu_{38}Se_{13}(SePh)_{12}(dppp)_6]$ (**49**) (without phenyl groups)

alternate packing of Cu_{12} and Se_{12} icosahedra has already been discussed for the Cu−Se clusters **14** and **15** (Figures 9 and 10). In these compounds, one polyhedron is positioned with its edges perpendicular to the edges of the polyhedron beneath. Unlike that pattern, the Se_{12} and Cu_{12} icosahedra in **47**−**50** are arranged such that one of the idealized fivefold axes of one polyhedron is parallel to one of the idealized threefold axes of the other and vice versa. The central $[Se_{13}Cu_{12}]$ unit of **47** is shown as an example in Figure 28.

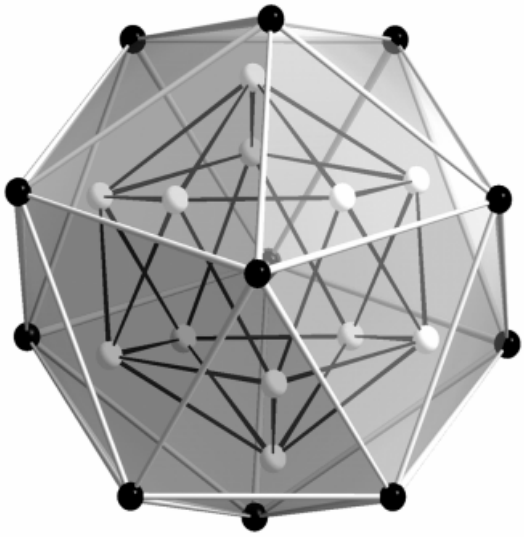

Figure 28. The central $[Se_{13}Cu_{12}]$ unit in **47**; the drawn lines only represent polyhedral edges and do not imply bonding interactions

In this way, six edges and six faces of the Cu_{12} icosahedron are bridged by the selenide ligands that form the Se_{12} polyhedron. The cluster core is then extended to the periphery by coordination of the Se_{12} substructure by another 24 copper atoms, twelve of which are ligated by the six dppR ligands. All 24 of these copper atoms are also bridged by twelve μ_3-$SePh^-$ groups, which are positioned at the cluster surface between the phosphane molecules. Except for the μ_{12}-bridging central selenium atom, the selenide ligands act as μ_6-bridges (six in both **47** and **48**, all twelve in **49** and **50**) or μ_5-bridges (six in both **47** and **48**) between copper centers. The different numbers of copper neighbors

per selenium atom in **47** or **48** on the one hand, and in **49** or **50** on the other, is caused by two copper atoms being formally absent in the molecular structures of **47** or **48**, resulting in the mixed-valence situation, but present in **49** and **50**. The respective copper atoms each coordinate to one of the Se_{12} icosahedral faces and form a straight Cu−Se−Cu axis, with the central selenium atom in the middle. At the same time, this $[Cu_2Se]$ arrangement represents an idealized threefold axis that is not realized crystallographically in **49** or **50**. The metal centers are surrounded in a distorted trigonal-planar or tetrahedral fashion. All Cu−Se distances in the mixed-valence clusters lie within the range of the Cu−Se bond lengths in all four clusters [2.301(4)−2.888(3) Å] and thus give no evidence for any localization of the Cu^{2+} centers. However, the range of the Cu−Cu contacts in **47** or **48** [2.511(3)−2.943(4) Å] is rather narrower than that found for **49** or **50** [2.305(4)−3.040(3) Å]. The spherical, somewhat oblate molecules show a maximum total diameter of 23.9−25.7 Å.

The use of different selenolato sources and different optimized reaction conditions leads to three different copper selenide/selenolate clusters with terminal $PiPr_3$ ligands, i.e. **45** (Figures 25 and 26), **51**, and **53**. The latter is synthesized in an unusual manner by the use of both $PhSeSiMe_3$ and $Se(SiMe_3)_2$ in the same reaction and is discussed below. Scheme 9 summarizes the syntheses of the $PiPr_3$-ligated clusters, specifying the reaction conditions in detail. Figure 29 shows the molecular structure of compound **51**.

Looking at Figure 29, one gets the impression that "normal" cluster growth occurred in the presence of a tertiary phosphane, and with Se−C bond cleavage, to result in the formation of a copper selenide cluster represented by the $[Cu_{40}Se_{20}]$ central unit of **51**. Only the lateral attachment of two symmetry-equivalent $[Cu_5(SetBu)_5(PiPr_3)_2]$ fragments reminds us of the presence of the selenolato reactant. This is in contrast to the equally $PiPr_3$-ligated structure of **45**, which shows only seven Se^{2-} ligands along with 18 $SetBu^-$ groups. No definite correlation between the clearly different courses of cluster formation and the respective reaction conditions can be delineated based on such a limited sample size, but it is very likely that the Cu:P ratio of the reactants and the temperature play important roles. The copper atoms in **51** bind to Se^{2-}, $SePh^-$, and $PiPr_3$ ligands in different ratios to achieve coordination numbers of two (albeit with a bent coordination geometry indicating a weak third interaction), three, or four. The selenium atoms bearing *tert*-butyl groups act as μ_3-bridges between copper atoms, whereas the Se^{2-} ligands bridge between five, six, or seven copper neighbors. The molecules are protected in the usual way by the $PiPr_3$ ligands and the organic substituents of the $SetBu^-$ groups.

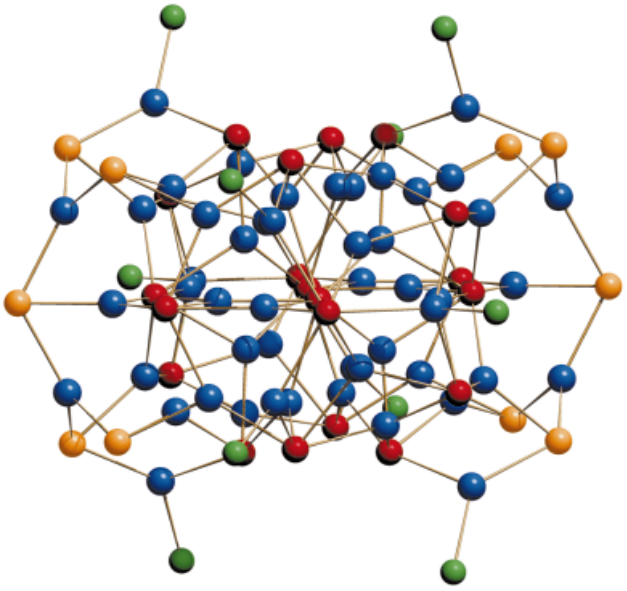

Figure 29. Molecular structure of $[Cu_{50}Se_{20}(SetBu)_{10}(PiPr_3)_{10}]$ (**51**) (without organic groups)

The molecular structure of another dppR-ligated copper cluster (R = a = acetylene) with both selenido and selenolato ligands, **52**, again possesses a high symmetry. This time, the molecular symmetry is underlined by a very high crystallographic symmetry. The compound crystallizes in the cubic space group $F\bar{4}3c$ and thus represents the second known copper chalcogenide cluster besides **14** (space group $Fm\bar{3}$) with a cubic crystal lattice. The molecular structure of **52** is illustrated in Figure 30.

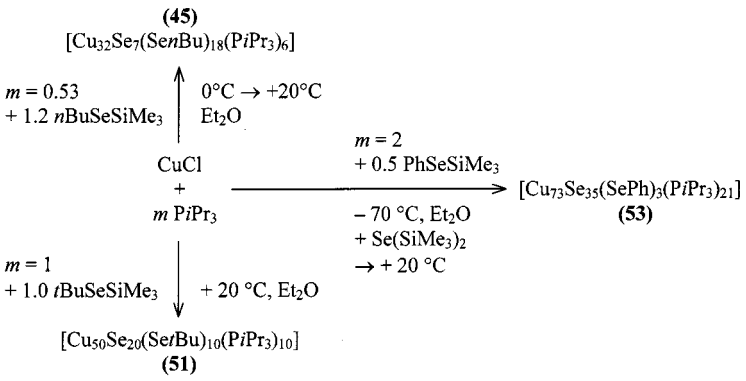

Scheme 9. Synthesis of various selenido/selenolato-bridged copper clusters in the presence of $PiPr_3$ under different reaction conditions

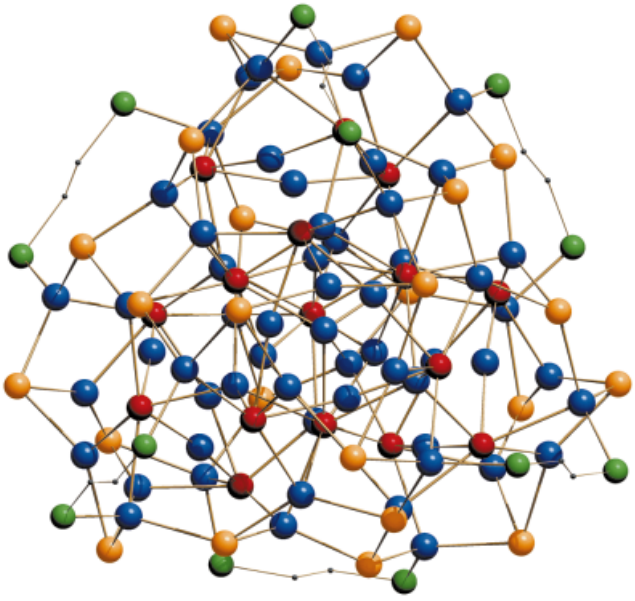

52

Figure 30. Molecular structure of $[Cu_{58}Se_{16}(SePh)_{24}(dppa)_6]$ (**52**) (without phenyl groups)

As observed for compounds **47**−**50**, the cluster core is oblate in shape, but in contrast to **47**−**50** it is not based on icosahedral fragments. Instead, a central Cu_4 tetrahedron shares its corners with four further Cu_4 units, which, in turn, share their *trans* faces with a Cu_6 octahedron. The remaining 30 copper atoms are situated between these polyhedra or are connected at the exterior of the polyhedral arrangement. The copper substructure of **52** is shown in Figure 31.

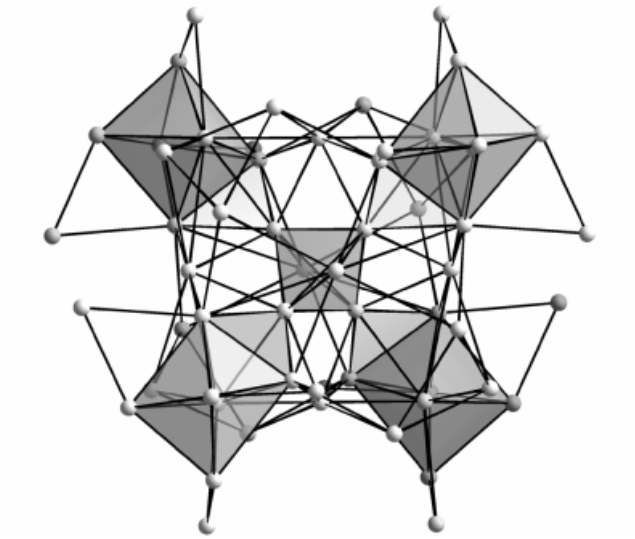

Figure 31. The copper substructure in **52**; the connected Cu_4 tetrahedra and Cu_6 octahedra are highlighted by gray shading; Cu−Cu distances are drawn up to 3.012(4) Å

Even though the Cu_{58} substructure has to be assigned a formal charge 56+ (assuming Se^{2-} and $SePh^-$ ligands as well as electroneutrality in the sum), which implies an extraordinary mixed-valence Cu^+/Cu^0 compound, one does not find any indication of exceptional Cu−Cu binding interactions. The Cu−Cu distances lie within the usual range of 2.540(3)−3.012(4) Å. Thus, the cluster core is held together by bridging selenido or selenolato ligands in the usual way. The former act as μ_5- or μ_6-bridges, while the latter form μ_3-bridges between adjacent copper atoms. Despite the large cluster size, metal centers with near-linear, trigonal-planar, and tetrahedral coordination are observed. Therefore, it is again apparent that the size-dependencies of the structural principles discussed for chalcogenolato-free copper sulfide or copper selenide clusters are generally invalid in the Cu/Se/SeR cluster systems. Six dppa ligands and 24 phenyl groups of the $SePh^-$ fragments protect the cluster molecule. Hence, **52** continues the series of compounds that show a significant preference for protection by the SeR^- groups rather than by the phosphane ligands. The clusters **43** and **47**−**51** represent exceptions from this series as their SeR/P ratios all amount to 1:1.

The largest cluster that displays both Se^{2-} as well as SeR^- ligands in the cluster framework is **53**. Its molecular structure is shown in Figure 32.

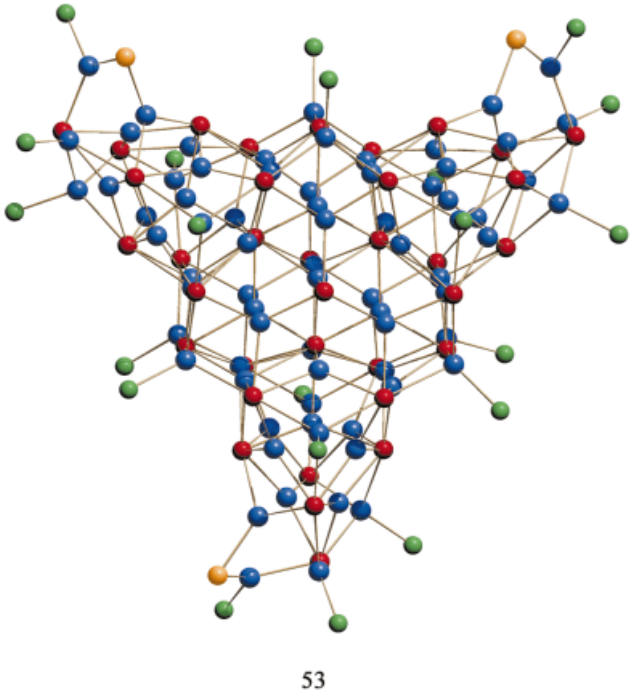

53

Figure 32. Molecular structure of $[Cu_{73}Se_{35}(SePh)_3(PiPr_3)_{21}]$ (**53**) (without organic groups)

This cluster displays a $[Cu_{70}Se_{35}]$ core, which is identical to that observed in **28** and **29** (Figures 18 and 19). Only three additional Cu−SePh fragments positioned at the corners of the triangular molecule distinguish **53** from the slightly smaller "Cu_{70}" clusters. The fact that one observes a typical copper selenide cluster structure with only a few

selenolato groups present is surprising, since $PhSeSiMe_3$ was the first selenium source to be added during the synthesis. This again illustrates the distinct preference for the "Cu_{70}" molecular structure, which is formed whenever the reaction conditions (Scheme 9) and the solubility situation enable the cluster growth to proceed until this large cluster compound crystallizes.

3.2.3. Optical Spectra and Thermal Behavior

The discrete molecular cluster species reviewed thus far are ideal subjects for studying the molecular quantum size effect,[3] which is one of the most absorbing questions connected with research in the field of cluster chemistry. In this regard, one must investigate the electronic properties of the cluster species, and first of all the relationship between cluster size and the HOMO−LUMO gap. Theoretical investigations have provided preliminary answers to this question.[34,37] The first dipole- and spin-allowed singlet or triplet excitations of selected "naked" copper selenide clusters $[Cu_{2n}Se_n]$ (up to $n = 15$) were calculated at the CIS level[56] (CIS = configuration interaction considering single excitations) for structures previously optimized for the same symmetry employing the CCSD(T) method[57] [CCSD(T) = coupled cluster approximation up to single and double excitation with additional consideration of third excitations by means of perturbation theory] ($n = 1, 2$) or the MP2 method ($n > 2$). Triplet excitations were investigated in order to take into account the fact that relativistic effects (spin-orbit coupling)[58] are significant in Cu−Se compounds. The results are presented in Figure 33.

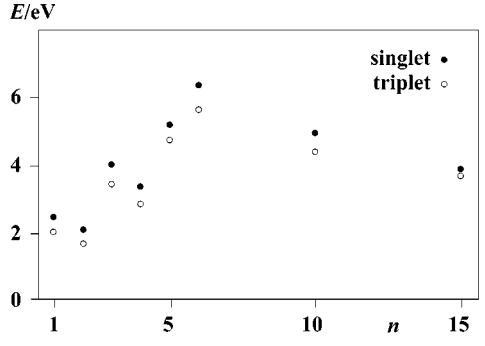

Figure 33. First dipole- and spin-allowed singlet or triplet excitations of selected "naked" copper selenide clusters $[Cu_{2n}Se_n]$ (up to $n = 15$), calculated at the CIS level (CIS = configuration interaction with single excitations) for structures previously optimized for the same symmetry employing the CCSD(T) method [CCSD(T) = coupled cluster up to single and double excitation with additional consideration of third excitations by means of perturbation theory] ($n = 1, 2$) or the MP2 method ($n > 2$)

The changes in the energy values for singlet or triplet excitations with increasing cluster size show similar trends, with the triplet excitation energies being 0.2−0.7 eV lower than the singlet ones. The excitation energies increase with a slight oscillation to a value of around 6 eV for the hexamer ($n = 3$), decreasing thereafter down to a value of ca. 3.8 eV for the $[Cu_{30}Se_{15}]$ species. The initial increase in the excitation energy values can be explained firstly by a stabilization of selenium *p*-orbitals by admixture of *s*-, *p*-, or *d*-contributions from the copper atoms, and secondly by an increasing degree of completion of the selenium shell around the copper substructure. The latter reduces the space for electrons in excited states with *s*-character. Thus, for $[Cu_{12}Se_6]$, significant *p*-type contributions are observed for the calculated transitions. The two exceptions ($n = 2, 4$) to this trend feature less compact molecular structures, which lead to lower excitation energies. Once the covering of selenium atoms on the copper framework has been completed, the overall size of the cluster molecules becomes more important. This confirms the assumption of separating the Se-*p* and Cu-*s* states to form valence and conducting bands. For clusters of ever increasing size, and ultimately bulk Cu_2Se, the first excitation energy should approach a value of ca. 1 eV.[59,60] According to the quantum chemical investigations, "naked" "middle-sized" copper selenide clusters should be colorless insulators that gradually adopt semiconductor properties with increasing cluster size. Calculations on small PH_3- or PMe_3-ligated copper selenide clusters indicate an increase in the first excitation energies compared to the corresponding "naked" clusters. Estimating a degree of error of about 1.5 eV, the respective transitions could indeed lead to the absorption of violet light, in agreement with the observed red color of the small copper selenide clusters.

The crystals obtained in the cluster formation reactions are colored. The intensity of the color increases on going from sulfur- to selenium- to tellurium-bridged compounds (see below), as expected for an increase in covalent or (semi)metallic binding properties. Small copper sulfide or selenide clusters form light-red, orange, or purple crystals. With increasing cluster size, the color becomes dark-red, reddish-black, and finally black with a metallic sheen. The optical spectra of some copper selenide cluster compounds were studied by means of solid-state UV/Vis spectroscopy. The single-crystalline samples were powdered and sus-

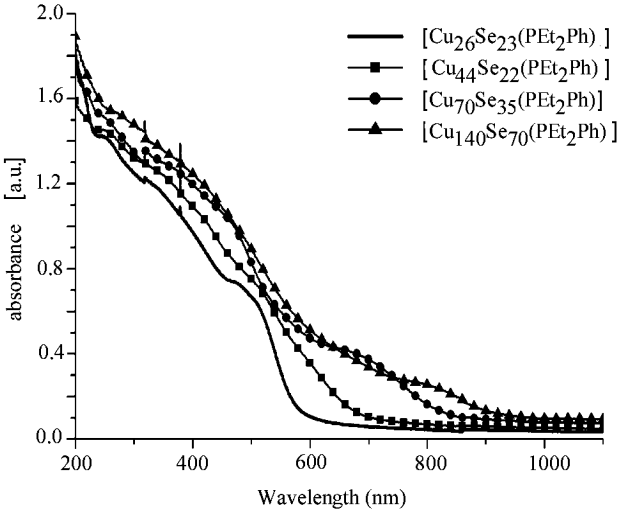

Figure 34. Solid-state UV/Vis absorption spectra of PEt_2Ph-ligated compounds **15**, **23**, **31**, and **35** that contain 26, 44, 70, and 140 copper atoms; for the measurements, powdered single-crystalline samples in mineral oil were placed between two quartz plates

pended in mineral oil between two quartz plates. Figure 34 shows the absorption spectra of the PEt_2Ph-ligated compounds **15**, **23**, **31**, and **35**, which contain 26, 44, 70, and 140 copper atoms, respectively. The influence of the phosphane ligands should be broadly the same for all four clusters, hence the increments in the position of the absorption band can be attributed solely to the increasing size and structural changes of the Cu−Se framework.

A shift of the absorption band to higher wavelengths with increasing cluster size is observed. In principle, this is consistent with a decrease in the HOMO−LUMO gap in the same direction. Although the experimental value for the band gap in Cu_2Se (1.1 eV, i.e. 1127 nm, from optical measurements;[59] 0.37 eV, i.e. 3350 nm, from electrochemical measurements[61]) is not reached, the trend can be explained in terms of the quantum size effect. An approximation of the HOMOs and LUMOs with increasing nuclearity is clearly observed. The broadness of the bands in the cluster spectra may be a result of the measurements being made at room temperature and/or a charge-transfer contribution to the observed transitions.

It has been known for several years that Cu−P bond cleavage occurs upon heating the copper selenide clusters, forming Cu_2Se as a black powder. In addition, XPS experiments (XPS = X-ray photoelectron spectroscopy) have shown that partial removal of the terminal ligands under the experimental conditions (room temperature, high vacuum) leads to an aggregation of the remaining clusters to larger, still ligated particles with a very narrow size distribution.[33] This agrees with the results of the quantum chemical investigations, which indicated the clusters to be metastable species with respect to the binary chalcogenide Cu_2E, and pointed to very low calculated Cu−P binding energies (see above). Thermogravimetric analysis of **31** (Figure 35) showed that all the phosphane ligands are removed in a single-step process within 20 minutes. The temperature required for this process is dependent on the experimental pressure.

Carrying out the experiment at normal pressure in a nitrogen flow, the ligands are all lost at 226 °C. On reducing the pressure down to $2\cdot10^{-6}$ mbar, this temperature decreases to 145 °C. However, on calculating the mass difference, one observes a loss of 33.6% rather than the 35.6% that should have been lost theoretically. This observation, as well as a residue of 1.2% carbon in the resulting copper selenide powders, indicates a slight amount of decomposition of the PR_2R' ligands. Following the process by means of powder diffraction, the intense reflections of the crystalline cluster in the range $2\Theta = 2-10°$ disappear during the thermogravimetric experiments, and are replaced by lower intensity reflections in the 2Θ range 10−55°. Sharp reflections from crystalline α-Cu_2Se are finally observed after annealing the powder at 600 °C. The Scherrer equation[62] [Equation (2)] gives a relationship between the medial peak width β and the particle size *D*.

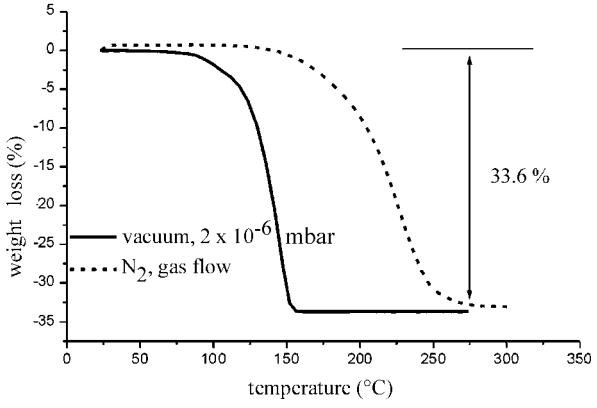

Figure 35. Results of a thermogravimetric analysis of **31** under different pressures

$$D = (K\cdot\lambda\cdot57.3)/(\beta\cdot\cos\theta) \quad (2)$$

where *D* is the average particle size perpendicular to the reflecting plane, *K* is the atomic form factor (here 1.0), λ is the wavelength of the X-ray radiation (here Cu-K_α: λ = 1.5418 Å), β is the peak width measured at half maximum intensity, and θ is the diffraction angle.

After calibration of the peak width at half maximum intensity for the diffractometer using LaB_6, an average particle size of $D = 117$ Å could be calculated for Cu_2Se powders generated by heating **31** to 150 °C at $2\cdot10^{-6}$ mbar for 20 min. This value for *D* is 7.8 times the size of the $[Cu_{70}Se_{31}]$ core of **31** (15 Å). The results give a further indication of a partial, controlled collapse of the cluster particle lattice.

3.3. Tellurium-Bridged Copper Clusters

In this section we focus on the description of the syntheses and structures of ligand-stabilized copper telluride cluster molecules. Solid-state copper tellurides as well as ternary alkali metal copper telluride compounds, which consist of *n*-dimensionally linked copper telluride clusters, are beyond the scope of this review. Their syntheses have become more frequent, although there are still only a limited number of examples, e.g. KCuTe,[63] NaCuTe,[48a] KCu_3Te_2,[64] $NaCu_3Te_2$,[65] $K_2Cu_5Te_5$,[66] and $K_4Cu_8Te_{11}$,[67] all of which have been prepared by means of melt reactions. The recently synthesized compound $K_3Cu_{11}Te_{16}$ [68] is the first example of a ternary alkali metal copper telluride crystallized from supercritical 1,2-diaminoethane.

3.3.1. Synthesis

According to the reaction pathways shown in Scheme 10, the syntheses of ligand-stabilized copper telluride clusters have mainly been achieved in one of three different ways.[11,16,19,20,24,25,31,69]

The reaction of copper(I) acetate with $Te(SiMe_3)_2$ at low temperatures (−50 to −20 °C) yields small cluster compounds with stoichiometric compositions. At higher reaction temperatures, up to 25 °C, larger clusters can be isolated that are mostly of the mixed-valence type. Similar mixed-valence compounds have also been isolated from reactions of copper(I) chloride with $Te(SiMe_3)_2$ at lower tem-

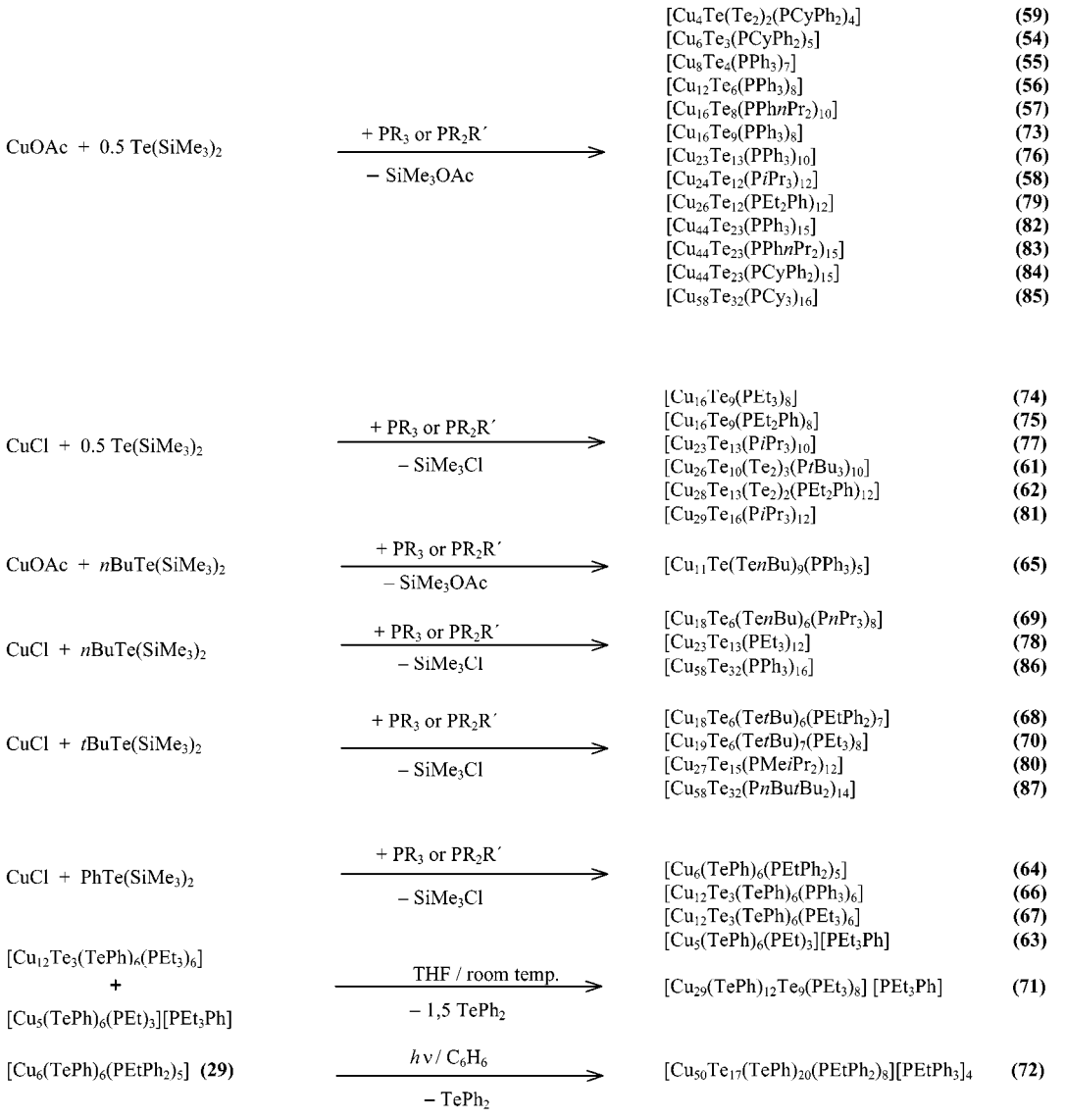

Scheme 10. Survey of the reaction pathways for the synthesis of ligand-stabilized tellurido or tellurido/tellurolato-bridged copper clusters

peratures (down to −70 °C). By treating copper(I) chloride or copper(I) acetate with tellurolate compounds $RTeSiMe_3$ (R = *t*Bu, *n*Bu, Ph), one obtains clusters containing both RTe^- and Te^{2-} ligands as a result of the facile cleavage of the Te−C bond. In some cases, we isolated clusters featuring Te−Te bridges. Examples of syntheses of larger copper telluride clusters starting from cluster precursors are the light-induced formation of $[Cu_{50}Te_{17}(TePh)_{20}(PEtPh_2)_8][PEtPh_3]_4$ (**72**) from $[Cu_6(TePh)_6(PEtPh_2)_5]$ (**64**) in benzene,[19] and the co-condensation of $[Cu_{12}Te_3(TePh)_6(PEt_3)_6]$ (**67**) with $[Cu_5(TePh)_6(PEt)_3][PEt_3Ph]$ (**63**) to form $[Cu_{29}(TePh)_{12}Te_9(PEt_3)_8]$ $[PEt_3Ph]$ (**71**).[69]

Table 4 summarizes all the Cu−Te cluster compounds that have been synthesized and structurally characterized by single-crystal X-ray diffraction analysis to date. The species can be subdivided into four main groups, three of which consist of compounds of stoichiometric compositions $[Cu_{2n}Te_{n-x}(TeR)_{2x}(PR_2R')_m]$ that differ in the nature of their tellurium ligands, while the fourth represents the group of mixed-valence clusters.

3.3.2. Structures

The structures of the tellurium-bridged copper clusters (Figures 39−42; see below) differ from those of the copper sulfide or selenide clusters, with the exception of some smaller ones. This can be understood against the background of the larger atomic and ionic radii of the tellurium atoms compared to the lighter chalcogen atoms, allowing higher coordination numbers and therefore new binding geometries, which lead to different structures. In addition, one finds a greater tendency to form mixed-valence clusters. This is in line with the existence of many stable binary compounds with compositions $Cu_{2-x}Te$[40] and with the situ-

Table 4. Classification of copper telluride clusters into stoichiometric or mixed-valence systems according to the types of tellurium ligands

Stoichiometric						Mixed-valence	
with only Te^{2-} ligands		with additional Te−Te bridges		with additional TeR^- ligands			
$[Cu_6Te_3(PCyPh_2)_5]$	**(54)**[31]	$[Cu_4Te(Te_2)_2(PCyPh_2)_4]$	**(59)**[31]	$[Cu_5(TePh)_6(PEt)_3][PEt_3Ph]$	**(63)**[69]	$[Cu_{16}Te_9(PPh_3)_8]$	**(73)**[24]
						$[Cu_{16}Te_9(PEt_3)_8]$	**(74)**[11]
						$[Cu_{16}Te_9(PEt_2Ph)_8]$	**(75)**[11]
$[Cu_8Te_4(PPh_3)_7]$	**(55)**[24]	$[Cu_4(Te_2)_2(PiPr_3)_4]$	**(60)**[11]	$[Cu_6(TePh)_6(PEtPh_2)_5]$	**(64)**[19]	$[Cu_{23}Te_{13}(PPh_3)_{10}]$	**(76)**[24]
						$[Cu_{23}Te_{13}(PiPr_3)_{10}]$	**(77)**[11]
						$[Cu_{23}Te_{13}(PEt_3)_{12}]$	**(78)**[16]
$[Cu_{12}Te_6(PPh_3)_8]$	**(56)**[24]	$[Cu_{26}Te_{10}(Te_2)_3(PtBu_3)_{10}]$	**(61)**[11]	$[Cu_{11}Te(TenBu)_9(PPh_3)_5]$	**(65)**[16]	$[Cu_{26}Te_{12}(PEt_2Ph)_{12}]$	**(79)**[24]
$[Cu_{16}Te_8(PPhnPr_2)_{10}]$	**(57)**[24]	$[Cu_{28}Te_{13}(Te_2)_2(PEt_2Ph)_{12}]$	**(62)**[11]	$[Cu_{12}Te_3(TePh)_6(PPh_3)_6]$	**(66)**[19]	$[Cu_{27}Te_{15}(PMeiPr_2)_{12}]$	**(80)**[25]
				$[Cu_{12}Te_3(TePh)_6(PEt_3)_6]$	**(67)**[69]		
$[Cu_{24}Te_{12}(PiPr_3)_{12}]$	**(58)**[24]			$[Cu_{18}Te_6(TetBu)_6(PEtPh_2)_7]$	**(68)**[25]	$[Cu_{29}Te_{16}(PiPr_3)_{12}]$	**(81)**[11]
				$[Cu_{18}Te_6(TenBu)_6(PnPr_3)_8]$	**(69)**[16]		
				$[Cu_{19}Te_6(TetBu)_7(PEt_3)_8]$	**(70)**[25]	$[Cu_{44}Te_{23}(PPh_3)_{15}]$	**(82)**[24]
						$[Cu_{44}Te_{23}(PPhnPr_2)_{15}]$	**(83)**[24]
						$[Cu_{44}Te_{23}(PCyPh_2)_{15}]$	**(84)**[24]
				$[Cu_{29}(TePh)_{12}Te_9(PEt_3)_8]$-$[PEt_3Ph]$	**(71)**[69]	$[Cu_{58}Te_{32}(PCy_3)_{16}]$	**(85)**[31]
						$[Cu_{58}Te_{32}(PPh_3)_{16}]$	**(86)**[16]
						$[Cu_{58}Te_{32}(PnButBu_2)_{14}]$	**(87)**[25]
				$[Cu_{50}Te_{17}(TePh)_{20}(PEtPh_2)_8]$-$[PEtPh_3]_4$	**(72)**[19]		

ation found in the ternary alkali copper telluride compound $K_2Cu_5Te_5$.[66]

In the case of copper telluride clusters, we have not yet reached the turning point in size where the whole core structures display bulk structure characteristics, as seen for the copper selenide species. Nevertheless, the tellurium frameworks in the largest cluster compounds, **85**−**87**, display hexagonal structure properties. Powder diffraction patterns of Cu_2Te could also be indexed on the basis of a hexagonal cell of tellurium atoms, although the structural details for bulk Cu_2Te have not yet been completely established.[40b]

In all the copper tellurium cluster molecules, the tellurium atoms form polyhedra with triangular faces. In the larger ones, some of the tellurium atoms are located inside the polyhedra. For smaller cluster molecules, the tellurium polyhedra can usually be derived from classical polyhedra (Figure 36). Those of the larger ones often show unusual cage structures. The distances between the tellurium atoms are usually nonbonding, except for the Te−Te units in **59**−**62** (Table 5).

The copper atoms reside in the holes and on the surface of the polyhedra and are coordinated by either two, three, or four tellurium atoms, with some being additionally coordinated by one further phosphane ligand (Figure 37).

The Cu−Te distance ranges that are regarded as bonding contacts are listed in Table 6 for all the clusters under discussion. Even though coordination numbers (*CN*) for Te^{2-} ligands range from 4 to 12 and those for TeR^- are usually smaller (*CN* = 2, 3, 4), there is no significant difference in the average Cu−Te distances for the Te^{2-} and TeR^- ligands.

Those tellurium atoms that are located in the center of the cluster molecules tend to bond to a large number of copper atoms. In some compounds, the copper atoms themselves form polyhedra, which can be described as Frank−Kasper polyhedra.[70] In these cases, the clusters consist of interpenetrating Frank−Kasper polyhedra, which are well-known from a number of intermetallic phases (e.g. Laves phases) (Figure 38).

However, the observed Cu−Cu distances (Table 7) give no indication of strong metal−metal, i.e. d^{10}−d^{10} interactions. Theoretical investigations pointed to the same conclusion.[34b,71] The shortest Cu−Cu contacts were observed in the molecular structures of **62** (2.383 Å) and **78** (2.382 Å), but these involve copper atoms exhibiting elongated thermal ellipsoids.

In the following section, all cluster structures will be briefly described and discussed according to the division into four groups indicated in Table 4.

3.3.2.1. Stoichiometric Clusters Containing Only Te^{2-} Ligands

The molecular structures of the stoichiometric copper telluride clusters **54**−**58** are shown in Figure 39.

In **54**, three tellurium atoms form a triangle, in the center of which a copper atom is coordinated in a slightly distorted triangular fashion. Four $[CuPPh_2Cy]$ units are doubly-bridging two of the edges. The third edge is bridged by a copper atom, which is coordinated by two phosphane ligands.

The tellurium atoms in **55** form a tetrahedron, the six edges of which are bridged by $[CuPPh_3]$ groups. An additional μ_3-$[CuPPh_3]$ fragment is bonded to a Te_3 face, and one naked copper atom is located in the center of the Te_4 tetrahedron.

Cluster **56** features a Te_6 octahedron. Six $[CuPPh_3]$ groups act as μ_2-bridges above six of the octahedral edges. Two further $[CuPPh_3]$ groups are coordinated by three tellurium atoms, giving a tetrahedral environment about the

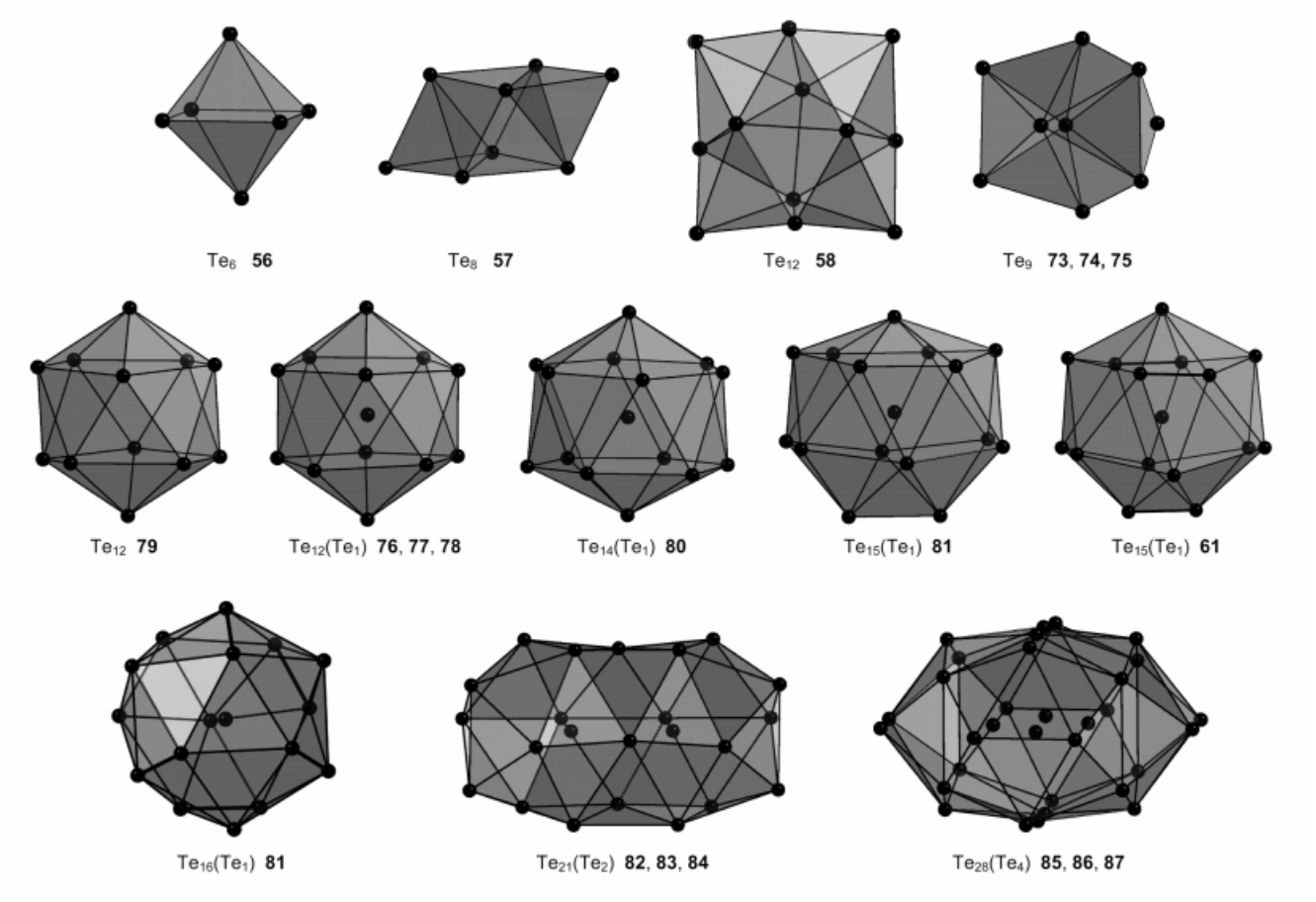

Figure 36. Tellurium polyhedra in copper telluride clusters (values for Te−Te distances in Table 5); connections to the central tellurium atoms are omitted for clarity; direct Te−Te bonds in **61** are drawn in bold

Table 5. Te−Te distances [Å] in copper telluride cluster molecules

with only Te^{2-} ligands		Stoichiometric with additional Te−Te bridges			Mixed-valence with additional TeR^- ligands			
	nonbonding		within Te−Te bridges	nonbonding		nonbonding		nonbonding
54	4.323−4.645	**59**	2.811; 2.799	4.375−4.382	**63**	3.831−4.807	**73**	4.165−4.687
							74	4.134−4.677
							75	4.140−4.652
55	4.556−4.662	**60**	2.791	4.234	**64**	4.022−4.713	**76**	4.083−4.663
							77	3.937−4.722
							78	4.246−4.577
56	4.486−4.764	**61**	2.878; 2.891; 2.895	4.180−4.883	**65**	4.009−4818	**79**	4.302−4.599
57	4.210−4.796	**62**	2.893; 2.897; 3.150; 3.183; 3.360; 3.531;	4.260−4.649	**66**	3.892−4.596	**80**	4.019−4.787
					67	4.053−4.653		
58	4.126−4.697				**68**	3.947−4.737	**81**	3.922−4.801
					69	3.822−4.795		
					70	3.907−4.765	**82**	3.967−4.752
							83	3.967−4.746
							84	3.924−4.768
					71	3.634−4.927	**85**	3.658−4.939
							86	3.733−4.944
							87	3.825−4.800
					72	3.583−4.868		

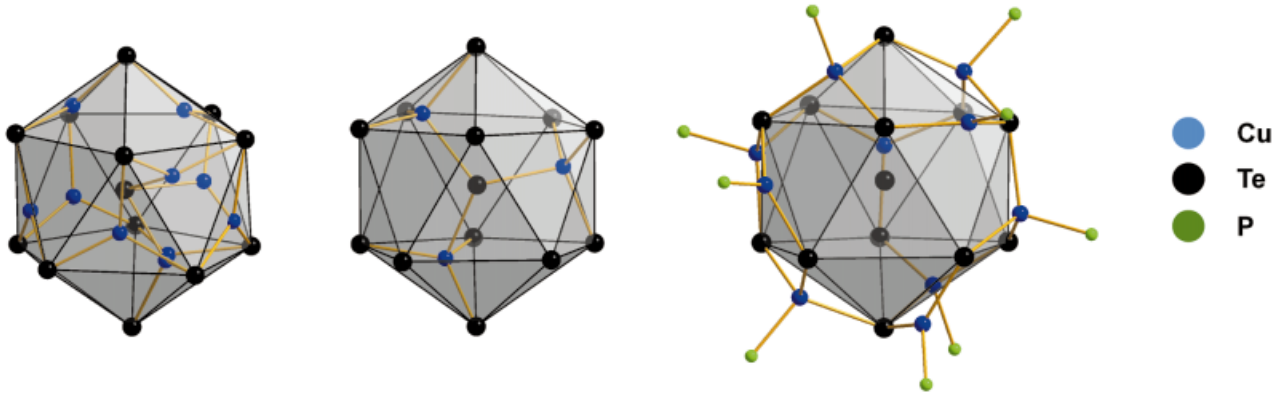

Figure 37. Different coordination modes of copper atoms in copper telluride clusters shown using the structure of **76** as an example; left-hand picture: μ_3-copper atoms only coordinated by tellurium atoms situated within the tellurium polyhedron; middle picture: μ_4-copper atoms only coordinated by tellurium atoms; right-hand picture: μ_3- and μ_4-copper atoms located at the surface of the tellurium polyhedra coordinated by tellurium atoms and one phosphane ligand

Table 6. Cu−Te contacts [Å] in copper telluride cluster molecules

with only Te^{2-} ligands		Stoichiometric with additional Te−Te bridges		with additional TeR^- ligands			Mixed-valence	
					Cu−TeR	$Cu-Te(-Cu)_n$		
54	2.518−2.782	**59**	2.525−2.769	**63**		2.490−2.660	**73**	2.511−2.790
							74	2.526−2.856
							75	2.540−2.791
55	2.532−2.925	**60**	2.574−2.856	**64**		2.511−2.854	**76**	2.530−3.128
							77	2.533−3.327
							78	2.468−2.961
56	2.552−3.187	**61**	2.521−3.337	**65**	2.600−2.897	2.553−3.104	**79**	2.585−2.818
57	2.549−2.794	**62**	2.420−3.310	**66**	2.623−2.743	2.607−2.665	**80**	2.538−3.183
				67	2.606−2.769	2.627−2.666		
58	2.525−2.904			**68**	2.578−2.924	2.519−2.767	**81**	2.567−2.757
				69	2.565−2.889	2.468−2.742		
				70	2.569−3.066	2.504−2.758	**82**	2.589−2.979
							83	2.588−3.033
							84	2.576−3.007
				71	2.576−3.140	2.552−2.855	**85**	2.403−3.115
							86	2.514−3.100
							87	2.515−3.078
				72	2.522−2.926	2.537−2.922		

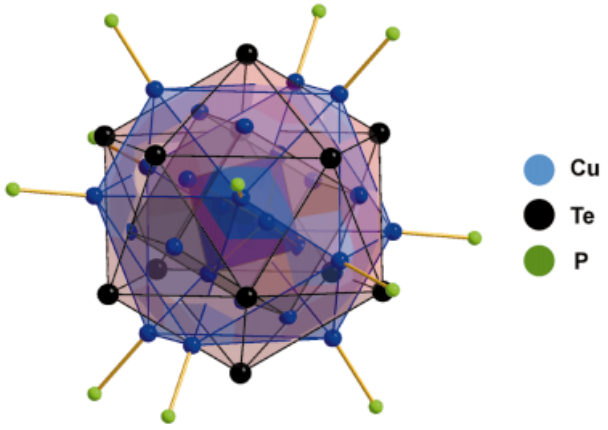

Figure 38. Interpenetrating copper and tellurium polyhedra in **79**

copper atoms. The other four copper atoms are each coordinated by three tellurium atoms. Thus, **56** represents a novel isomer of the $[Cu_{12}E_6(PR_3)_8]$ clusters (see above), which was not observed for E = S, Se.

An octahedron of tellurium atoms is also found in **57**. However, two further tellurium atoms additionally cap two opposite triangular faces. Eight [CuPPh*n*Pr$_2$] groups are bonded along the edges of this polyhedron. Of the other eight copper centers, two are tetrahedrally coordinated by one phosphane and a Te_3 face. The six remaining metal atoms are bonded in a distorted trigonal-planar mode by three tellurium atoms, and are located inside the cluster cavity.

The Te_{12} substructure of **58** cannot be described as a classical deltahedron, but rather shows an arrangement of two highly distorted face-sharing tetragonal antiprisms. Four [CuP*i*Pr$_3$] groups bridge one Te−Te non-bonding edge

Table 7. Cu−Cu contacts [Å] in copper telluride cluster molecules

with Te^{2-} ligands		Stoichiometric with Te−Te bridges		with RTe^- ligands		Mixed-valence	
54	2.510−2.625	**59**	2.797	**63**	2.587−2.613	**73**	2.478−2.730
						74	2.481−2.729
						75	2.475−2.742
55	2.510−2.625	**60**	2.609−2.641	**64**	2.568−2.747	**76**	2.490−2.714
						77	2.507−2.775
						78	2.382−2.725
56	2.479−2.724	**61**	2.581−2.793	**65**	2.469−2.800	**79**	2.566−2.747
57	2.529−2.795	**62**	2.383−2.797	**66**	2.552−2.727	**80**	2.539−2.721
				67	2.563−2.698		
58	2.523−2.764			**68**	2.459−2.774	**81**	2.563−2.763
				69	2.483−2.946		
				70	2.466−2.764	**82**	2.466−2.734
						83	2.476−2.788
						84	2.453−2.789
				71	2.479−2.786	**85**	2.426−2.800
						86	2.448−2.801
						87	2.433−2.796
				72	2.462−2.799		

each, and eight [CuP*i*Pr$_3$] units act as μ_3-bridges above Te_3 faces. The other twelve copper atoms are each surrounded by three tellurium atoms and are slightly shifted away from the Te_3 planes towards the center of the molecule.

3.3.2.2. Stoichiometric Clusters Containing Te−Te Bridges

Some reactions of copper(I) chloride or copper(I) acetate lead to the formation of copper telluride clusters that contain Te−Te bridges (**59**−**62**; Figure 40).

In **59**, three tellurium atoms form an approximate isosceles triangle with a Te−Te bond along the short edge (Te−Te: 2.791 Å). The two longer edges of the triangle are bridged by one [CuPPh$_2$Cy] unit each. The two other copper atoms are located above and below the triangular face and are additionally coordinated by phosphane ligands.

The four copper atoms in **60** form a "butterfly" structure bridged by two ditelluride ligands (Te−Te: 2.800−2.812 Å). Each copper atom is additionally coordinated by a phosphane ligand.

Clusters **61** and **62** are spherical molecules based on tellurium polyhedra, parts of which are strongly distorted due to the presence of Te−Te bonds. Both compounds display Frank−Kasper polyhedra containing 15 (**61**) or 16 (**62**) tellurium atoms centered by one additional tellurium ligand. The tellurium polyhedron of **61** is similar to that observed in **20**, although it differs in the presence of three Te−Te bonds (2.936−3.011 Å). The copper atoms are bonded to the tellurium atoms in a different arrangement to that in **20**. Eight [CuP*t*Bu$_3$] units are situated above Te_3 faces of the polyhedron, while two such units are edge-bridging. Eleven further copper atoms are coordinated by three tellurium atoms, eight of which are localized below Te_3 faces, while the other three bind between the central tellurium atom and the tellurium atoms of the polyhedron. The remaining copper atoms are localized in the center of the molecule and are each tetrahedrally surrounded by four tellurium atoms.

In **62**, two of the copper centers display relatively high thermal parameters, from which it can be concluded that their positions are only partly occupied. A deficiency of electrons at the tellurium atoms resulting from the partial occupation of copper sites could either be formally delocalized in the valence band or localized as a ditelluride group following a structural deformation similar to a Peierls deformation.[72] Considering the tellurium polyhedra, the molecular structure of **62** shows two short Te−Te bonds (2.848 and 2.876 Å) and four Te−Te distances in the range 3.150−3.351 Å. The latter tellurium atoms have thermal ellipsoids that are elongated in the direction of the formal Te−Te bond. As the Te−Te bonds and copper centers seem to be disordered to a certain extent in **62**, the given formula represents the idealized composition of a stoichiometric cluster compound with three Te−Te bonds. The situation in **62** can therefore be viewed as being somewhat similar to that in CuS, a well-known mixed-valence compound that can be described as $(Cu^+)_2Cu^{2+}(S_2)^{2-}S^{2-}$ or as $(Cu^+)_3(S_2)^{2-}S^-$.[73]

3.3.2.3. Stoichiometric Clusters Containing Tellurido and Tellurolato Ligands

In a different approach towards the synthesis of copper telluride cluster compounds, we used alkyl- and aryl(trimethylsilyl)tellurium compounds RTeSiMe$_3$ (R = organic group). Due to the facile cleavage of the carbon−tellurium bond, one obtains clusters featuring either exclusively TeR^- ligands, a mixture of TeR^- and Te^{2-} ligands, or solely Te^{2-} ligands. The tellurium atoms of the tellurolato ligands bridge at most two or three copper atoms, whereas "naked" Te^{2-} ligands can coordinate to up to seven copper atoms. The polyhedra of tellurium atoms usually possess unusual structures, even in the smaller clusters. In the larger clusters, one already observes the characteristics of layer-type ar-

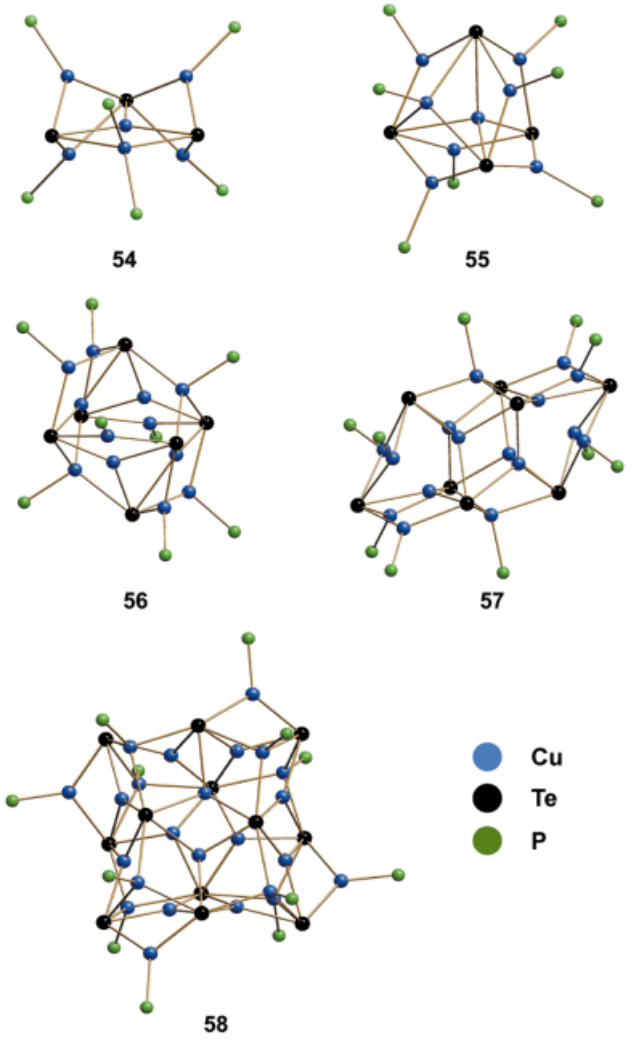

Figure 39. Molecular structures of stoichiometric copper telluride clusters $[Cu_6Te_3(PCyPh_2)_5]$ (**54**), $[Cu_8Te_4(PPh_3)_7]$ (**55**), $[Cu_{12}Te_6(PPh_3)_8]$ (**56**), $[Cu_{16}Te_8(PPhnPr_2)_{10}]$ (**57**), and $[Cu_{24}Te_{12}(PiPr_3)_{12}]$ (**58**); C and H atoms are omitted for clarity

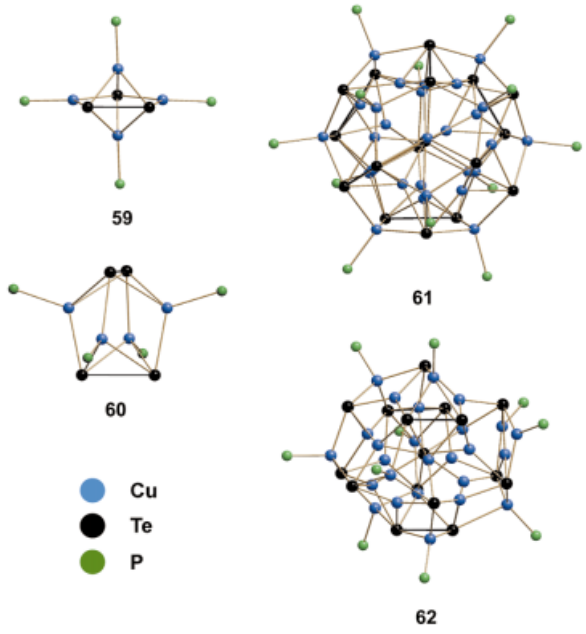

Figure 40. Molecular structures of stoichiometric copper telluride clusters $[Cu_4Te(Te_2)_2(PCyPh_2)_4]$ (**59**), $[Cu_4(Te_2)_2(PiPr)_4]$ (**60**), $[Cu_{26}Te_{10}(Te_2)_3(PtBu_3)_{10}]$ (**61**), and $[Cu_{28}Te_{13}(Te_2)_2(PEt_2Ph)_{12}]$ (**62**) containing Te−Te bridges; C and H atoms are omitted for clarity

rangements of tellurium atoms. As in the cluster compounds discussed earlier, the copper atoms are coordinated in linear, trigonal, or tetrahedral geometries by tellurium atoms. Metal centers coordinated by two or three chalcogens may also be ligated by a phosphane ligand. The molecular structures of the copper telluride/tellurolate clusters **63**−**66** and **68**−**72** are shown in Figure 41.

The ionic cluster compound **63** contains six $TePh^-$ ligands, the tellurium atoms of which define an octahedron. In contrast to **64** (see below), all the tellurolato ligands act as μ_2-bridges. There are two distinct coordination geometries around the copper centers. Two of the metal centers are located inside the cluster below Te_3 faces. The others are coordinated by three tellurium atoms above Te_3 faces, and are also ligated by one phosphane ligand each.

The structure of **64** is also based on a non-bonded octahedral array of tellurolato ligands. With the exception of one tellurium atom, which forms two Cu−Te bonds, all of these are bridging three copper sites. Four of the copper atoms adopt tetrahedral geometries, either with three tellurium atoms and one phosphorus ligand or through two Cu−Te and two Cu−P bonds. The other two copper atoms lie in opposite deltahedral Te_3 faces of the Te_6 octahedron. Compound **64** is therefore related to the recently published homoleptic hexanuclear copper selenolate complex $[Cu_6\{Se(2,4,6\text{-}iPr_3C_6H_2)\}_6]$.[8]

In **65**, the nine tellurium atoms of the tellurolato ligands form three-quarters of a cubooctahedron, which is capped on the hexagonal face by the Te^{2-} ligand. Seven $TenBu^-$ groups act as μ_3-bridges between copper atoms, while the other two bind to four copper atoms. The "naked" tellurium atom at the base of the cluster coordinates to seven copper atoms. Five of the eleven metal atoms are ligated by triphenylphosphane ligands, four of which are tetrahedrally coordinated due to three additional Cu−Te bonds. One $[CuPPh_3]$ unit bridges only two tellurium atoms, resulting in an almost trigonal-planar coordination environment. Three of the six interstitial copper atoms exhibit tetrahedral coordination geometries, while the other three show three bonding contacts to tellurium atoms and have nearly trigonal-planar coordination geometries.

Clusters **66** and **67** are identical except for the organic groups R of the PR_3 ligands. Both contain two tellurolato layers of three $TePh^-$ groups each and one central tellurido layer of three Te^{2-} ligands. The resulting Te_9 polyhedron can alternatively be viewed as two face-sharing Te_6 octahedra. Six of the twelve copper atoms are coordinated in a distorted trigonal fashion by three tellurium atoms, resulting in shorter contacts to the Te^{2-} ligands than to the $TePh^-$. The other six copper atoms are tetrahedrally surrounded by three tellurium atoms and one phosphane li-

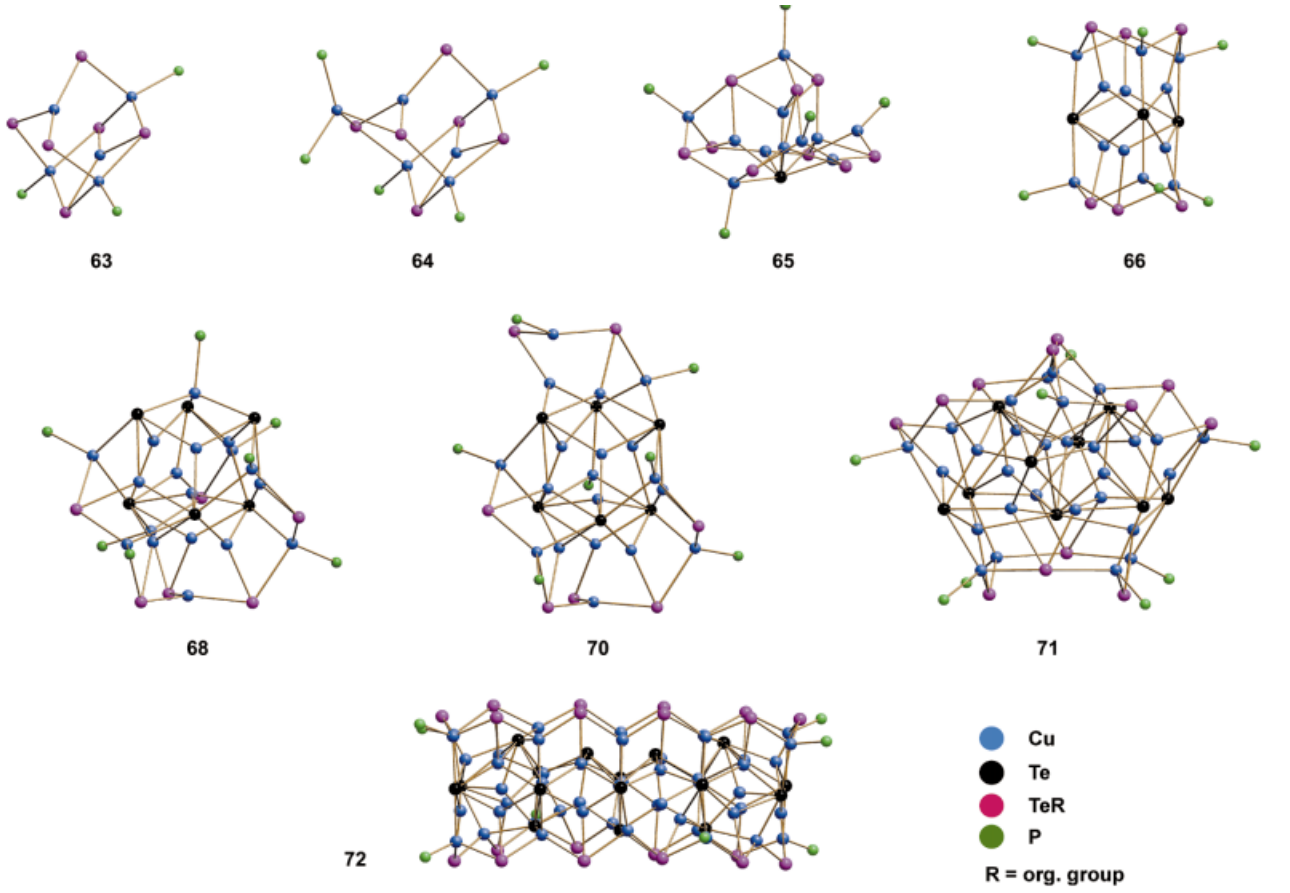

Figure 41. Molecular structures of stoichiometric copper telluride/tellurolate clusters $[Cu_5(TePh)_6(PEt)_3][PEt_3Ph]$ (**63**), $[Cu_6(TePh)_6(PEtPh_2)_5]$ (**64**), $[Cu_{11}Te(Te\mathit{n}Bu)_9(PPh_3)_5]$ (**65**), $[Cu_{12}Te_3(TePh)_6(PPh_3)_6]$ (**66**), $[Cu_{18}Te_6(Te\mathit{t}Bu)_6(PEtPh_2)_7]$ (**68**), $[Cu_{19}Te_6(Te\mathit{t}Bu)_7(PEt_3)_8]$ (**70**), $[Cu_{29}(TePh)_{12}Te_9(PEt_3)_8][PEt_3Ph]$ (**71**), and $[Cu_{50}Te_{17}(TePh)_{20}(PEtPh_2)_8][PEtPh_3]_4$ (**72**) containing TeR^- ligands; C and H atoms are omitted for clarity

gand. Compounds **66** and **67** might be viewed as condensation products of two $(TePh)_6$ frameworks like those found in **64**.

The molecular structures of **68** and **69** differ only by an extra phosphane ligand bonded to the former, in line with the smaller cone angle of $P\mathit{n}Pr_3$ relative to that of $PEtPh_2$. The layering of the tellurium atoms is clearly evident, and the twelve atoms adopt a distorted hexagonal packing. The three layers consist of a "top" layer of three "naked" Te^{2-} ligands, a second layer of three $Te\mathit{n}Bu^-$ and three Te^{2-} ligands, with the former lying at the corners of the triangular array, and a third basal triangle consisting of another three $Te\mathit{n}Bu^-$ groups. Eight of the copper atoms cap open Te_3 triangular faces, with a fourth bonding interaction to a phosphane ligand. Of the interstitial copper atoms, seven display only three bonding contacts to the neighboring tellurium atoms, while three metal atoms are tetrahedrally surrounded by tellurium atoms.

Compared to **68** and **69**, **70** contains one additional [Cu-Te*t*Bu] group. However, the structures are partly comparable. Again, a layering of the tellurium atoms can be observed, which is related to that in **68** and **69** as follows. There are now four formal layers of tellurium atoms, with one $Te\mathit{t}Bu^-$ group less in the former middle layer, and two additional $Te\mathit{t}Bu^-$ groups at the "top" of the molecule forming the fourth layer. One of the seven $Te\mathit{t}Bu^-$ ligands acts only as a doubly-bridging ligand, whereas the other six form μ_3-bridges between copper atoms. The six Te^{2-} ligands and 16 of the copper centers are situated in similar positions as in **68** or **69**. Three further copper atoms are located between the "top" Te−Te unit and the adjacent "naked" Te_3 layer. The similarities and differences between the structures of **68**, **69**, and **70** demonstrate the complicated influence of the phosphane ligands, which have different cone angles, and of the tellurolate ligands, which have different degrees of flexibility in their organic substituents. These systems may stem from a common intermediate, but due to the different steric demands of the ligands they develop in different ways.

The synthesis of the ionic cluster compound, **71**, is the only example to date of a co-condensation reaction of two smaller clusters to form a larger one. However, the structure of **71** cannot be considered as being built-up from recognizable structural fragments of the precursor compound. The tellurium atoms form an unusual polyhedron consisting of twelve $TePh^-$ ligands and nine Te^{2-} ligands. Two of the tellurolato ligands act as μ_4-bridges, while the other ten act as μ_3-bridging atoms between the copper centers. The tel-

luride ligands each coordinate six, seven, eight, or ten copper atoms with Cu−Te distances between 2.58 and 3.14 Å. Eight of the copper atoms coordinated by phosphane ligands cap Te_3 faces at the cluster surface, while four further copper atoms without phosphane ligands coordinate to Te_3 faces from the inside of the cluster core. The remaining 17 copper atoms are surrounded in a tetrahedral manner in the center of the molecule. Interestingly, a structurally related silver tellurium compound, $[Ag_{30}(TePh)_{12}Te_9(PEt_3)_{12}]$,[69] can be prepared by the direct reaction of AgCl with $Te(SiMe_3)_2$/$PhTeSiMe_3$, which is in contrast to the synthesis of **71**. This cluster represents the only known example of a copper-telluride-tellurolate cluster that shows a distinct structural relationship with its silver analogue.

Upon standing in daylight, solutions of **64** in benzene gradually darken to a brown color. Over the course of several days, brown platelets of the ionic, mixed tellurido/tellurolato cluster **72** crystallize from these solutions. In contrast, when solutions of **64** in benzene are protected from light, they show no sign of darkening, even after several weeks at room temperature. The detection of a $^{125}Te\{^1H\}$ NMR signal at $\delta = 688$ reveals the formation of $TePh_2$ in the solution, giving good evidence for the mechanism of formation of the "naked" tellurido ligands. The most striking feature of the cluster core is the manner in which the tellurium ligands are arranged: the molecule consists of "top" and "bottom" layers of μ_3-$TePh^-$ ligands with a central tellurido (Te^{2-}) layer. Sandwiched between these are the 50 copper atoms along with the remaining seven tellurido ligands. The 20 phenyltellurolato ligands are each bonded to three copper atoms and, in conjunction with the eight coordinated PEt_2Ph ligands, serve to effectively stabilize the inner copper telluride core. The telluride ligands of the middle Te_{10} layer act as μ_6- and μ_7-bridges between the copper sites. The seven remaining Te^{2-} centers function as μ_6-, μ_7-, or μ_8-ligands. Eight of the copper atoms are bonded to Te_3 faces at the surface of the cluster molecule and to one phosphane ligand. The 42 copper atoms in the center of the molecule are either trigonally (18) or tetrahedrally (24) coordinated by their tellurium neighbors.

3.3.2.4. Mixed-Valence Clusters

Counting the electrons for **73**−**85** on the assumption of Te^{2-} and Cu^+ leads to an overall electron excess for **79** and to electron deficiencies for the other compounds. These compounds can therefore be thought of as being of mixed-valence type. The molecular structures of **73**, **76**, **79**−**82**, and **85** are depicted in Figure 42.

The smallest mixed-valence cluster molecules, **73**−**75**, feature 16 copper atoms arranged around a Te_9 polyhedron. However, the tellurium substructure cannot be derived from the skeleton of **57** by simply adding one tellurium atom, as one might have assumed. Two of the copper atoms that are coordinated by a phosphane ligand bridge Te−Te nonbonding edges. The other six $[CuPR_2R']$ units bridge three tellurium atoms, the copper atoms thus being tetrahedrally coordinated. The remaining eight copper atoms are coordinated by three tellurium atoms in a distorted trigonal-planar manner. Assuming that the tellurium atoms have a formal charge of 2−, one can formally assign 14 Cu^+ centers and two Cu^{2+} centers. However, the co-existence of Cu^{2+} and Te^{2-} is unlikely for thermodynamic reasons because of an electron-transfer process from the reducing Te^{2-} ligand to the oxidizing Cu^{2+} center. An assignment of

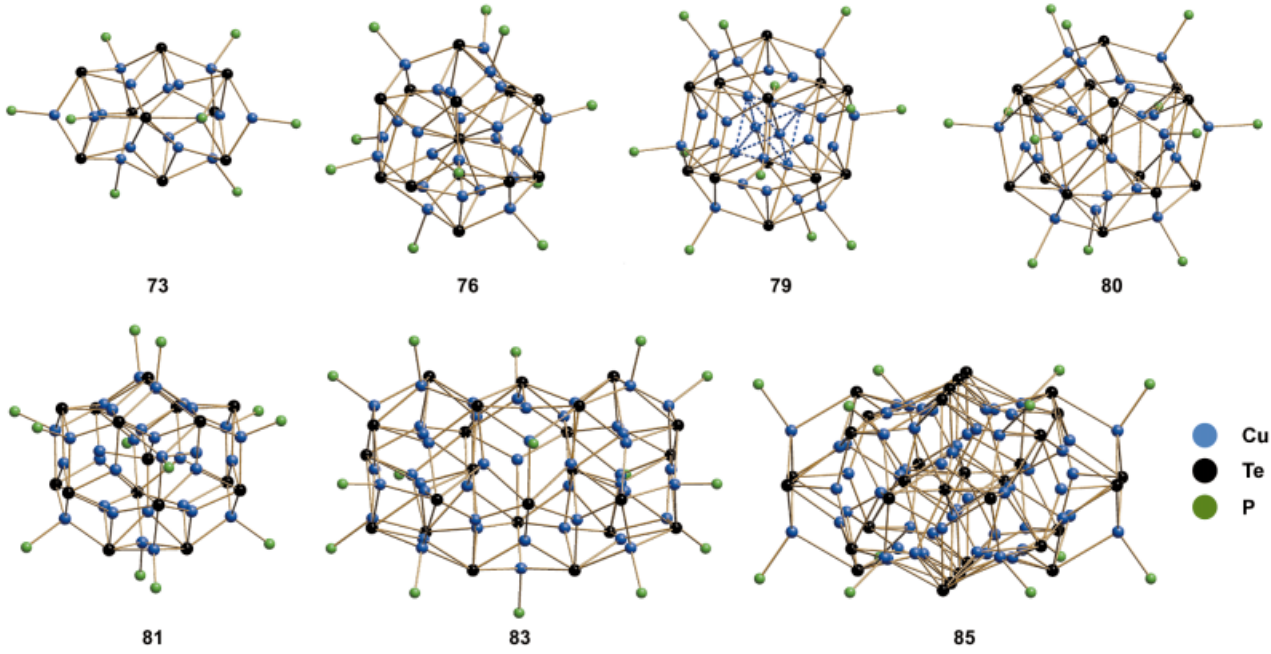

Figure 42. Molecular structures of mixed-valence copper telluride clusters $[Cu_{16}Te_9(PPh_3)_8]$ (**73**), $[Cu_{23}Te_{13}(PPh_3)_{10}]$ (**76**), $[Cu_{26}Te_{12}(PEt_2Ph)_{12}]$ (**79**), $[Cu_{27}Te_{15}(PMe\textit{i}Pr_2)_{12}]$ (**80**), $[Cu_{29}Te_{16}(P\textit{i}Pr_3)_{12}]$ (**81**), $[Cu_{44}Te_{23}(PPh_3)_{15}]$ (**82**), and $[Cu_{58}Te_{32}(PCy_3)_{16}]$ (**85**); C and H atoms are omitted for clarity

16 Cu^+, seven Te^{2-}, and two Te^- is not supported by structural means. The compounds should therefore rather be described in terms of a "pure" Cu^+ substructure ligated by tellurium centers with an average charge of −1.78. This electron deficiency can be delocalized in the valence band of the compound, as has recently been shown by calculations on the electron-rich compound **79** (see below).[74]

Thirteen tellurium atoms form a distorted, centered icosahedron in the closely-related compounds **76**−**78**. In **76** and **77**, ten of the 20 Te_3 faces are bridged by copper-phosphane units, whereas ten more copper atoms are situated below the remaining faces, either trigonally coordinated or tetrahedrally surrounded due to an additional Cu−Te bond to the central tellurium atom. Compound **78** needs twelve phosphane ligands for a sufficient shielding of the cluster core. This can be ascribed to the smaller steric demand of the phosphane PEt_3 (Table 1) compared to PPh_3. As a result, in **78**, twelve of the copper atoms are coordinated above Te_3 faces and eight below. The three remaining copper atoms in all three compounds are positioned inside the respective icosahedra. They each have three tellurium neighbors, two of which belong to the Te_{12} shell, while the third is the central tellurium ligand. Formal counting of charges leads to an electron excess of three and, assigning a charge of 1+ to every copper atom as discussed above, an average charge of −1.77 is obtained for the 13 tellurium ligands.

An icosahedron of tellurium atoms is also found in **79** but, in contrast to those observed in **76**−**78**, it does not contain a central atom. The arrangement of the copper atoms above the Te_3 faces is similar to that found in **78**. This might have been anticipated, given the Tolman angle for both phosphanes. Twelve $[CuPEt_2Ph]$ units are bonded above Te_3 faces and eight copper atoms cap the other Te_3 faces from the interior. In contrast to the situation in **76**−**78**, in **79** six rather than three copper atoms are located in the center of the cluster molecule, forming an octahedron with intermetallic distances between 2.592 and 2.607 Å. These distances lie within the range of Cu−Cu distances measured in the other copper telluride clusters under investigation. Therefore, it cannot be concluded from these distances whether d^{10}−d^{10} interactions are present within the Cu_6 octahedron. However, it is remarkable that two of the copper atoms must be formally uncharged Cu^0 atoms, alongside 24 Cu^+ centers, if one assigns a formal charge of 2− to all the tellurium ligands. Calculations of the electronic band structure reveal that a localization of the oxidation states does not occur and that the excess electron density cannot be assigned to d^{10}−d^{10} interactions.[74] The "additional" electron pair, which arises if one assigns exclusively Cu^+ and Te^{2-} centers, is better described as an MO embedded in the valence band of tellurium 5p orbitals and copper 4s orbitals.

The cluster molecules **80** and **81** are constructed in an analogous way. Both compounds consist of tellurium polyhedra which, however, form Frank−Kasper polyhedra: **80** contains a Te_{14} polyhedron, while **81** is based on a Te_{15} polyhedron. Both chalcogen substructures enclose an additional tellurium ligand at the center. Similar to the situations in **76**−**79**, all Te_3 faces are μ_3-capped by copper atoms. The Te_{14} polyhedron displays 24 such faces and the Te_{15} substructure forms 26 Te_3 triangles. Copper atoms that are additionally coordinated by a phosphane ligand are situated above the Te_3 faces, while the other copper atoms lie below, as observed previously. In both **80** and **81**, twelve copper atoms that are coordinated by a phosphane ligand are tetrahedrally coordinated above the cluster surface. One then finds 17 (**81**) or 15 (**80**) copper atoms below the Te_3 faces in the two cluster structures. Similarly to the situation in **76**−**78**, three metal centers are situated inside the polyhedral cages. Assuming that only Cu^+ centers and Te^{2-} ligands are present, three electrons are formally missing in each compound. Therefore, **80** and **81** are also compounds of mixed-valence type, each featuring three formal Cu^{2+} centers. However, from the structural data it is again impossible to divide the atomic positions into those that are occupied by Cu^{2+} and those that are Cu^+ sites.

The largest copper telluride cluster molecules synthesized to date are also mixed-valence compounds. Compounds **82**−**87** display ellipsoidal tellurium deltahedra with an increasing number of inner tellurium atoms, ranging from two inner tellurium atoms in **82**−**84**, to four such tellurium atoms in the centers of the molecular structures of **85**−**87**. As usual, the copper atoms that are coordinated by phosphane ligands are coordinated above the Te_3 triangles on the cluster surface. The other copper atoms are either coordinated by three or, especially in the cluster center, by four tellurium ligands. The structures of **85**−**87** already suggest the formation of distorted layers of tellurium atoms showing incipient characteristics of bulk Cu_2Te.[40] However, the turning point has not yet been reached for copper telluride cluster compounds. If one continues the reported tendency for ever bigger molecules being required for the observation of bulk structure properties on going from Cu−S to Cu−Se clusters, the cluster size that might begin to show Cu_2Te structural characteristics should in fact be considerably larger than a "Cu_{58}" species, and probably even larger than a "Cu_{70}" analogue of the turning point to "large" clusters found for the copper selenide system.

3.3.3. Optical Spectra in the Solid State

The colors of the microcrystalline powders of the various copper telluride clusters already reveal differences in the electronic properties of the compounds. Larger clusters are significantly darker in color than the smaller ones. For a more detailed investigation, UV/Vis spectra of the stoichiometric clusters **55** and **57**, as well as of the mixed-valence compounds **73**, **76**, **79**, and **83** were measured in the solid state.[24] Absorption spectra of the crystalline samples were measured in transmission mode from suspensions in Nujol between two quartz plates. As representative examples, the spectra of **57**, **73**, and **83** are shown in Figure 43.

In line with its red color, **57** exhibits charge-transfer bands between 600 and 200 nm, together with bands that can be assigned to transitions related to the ligands. The UV/Vis spectrum of **73** also shows similar bands between

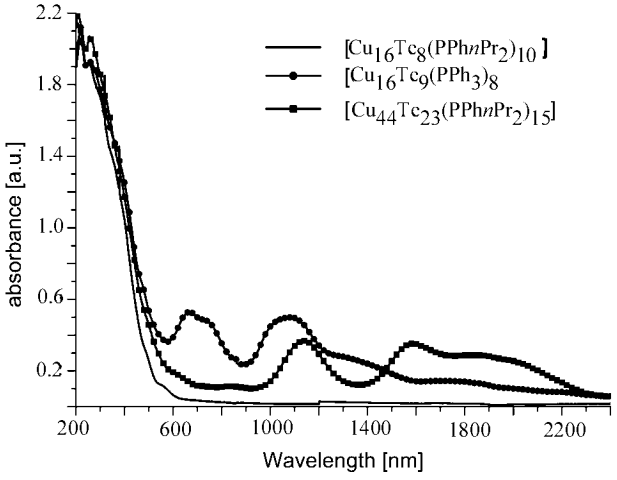

Figure 43. The UV/Vis solid-state absorption spectra (Nujol mulls) of copper telluride clusters $[Cu_{16}Te_8(PPh_nPr_2)_{10}]$ (**57**), $[Cu_{16}Te_9(PPh_3)_8]$ (**73**), and $[Cu_{44}Te_{23}(PPh_nPr_2)_{15}]$ (**83**)

600 and 200 nm, but additionally displays broad and weaker peaks at higher wavelengths, specifically at 670, 750, 1050, and 1350 nm. As outlined above, **73** can be described as a mixed-valence compound with an overall electron deficiency that is delocalized in the valence band. In general, compounds containing metal atoms in formally different oxidation states exhibit interesting spectroscopic behavior. Depending on the degree of delocalization of the charges over the molecular framework, one may detect additional bands in the near-infrared region. According to the classification of Robin and Day,[75] which describes the different degrees of electron delocalization between the metal atoms, the copper telluride clusters under investigation should belong to class IIIa (metal clusters). In this class, metal centers with different valencies cannot be distinguished and total delocalization of the charge is achieved. The larger cluster **83** also formally contains an electron deficiency of two and thus shows broad peaks that are shifted even further to longer wavelengths than in the case of **73**. Since the energy of the mixed-valence transition is strongly correlated with the degree of delocalization, an even better charge delocalization − i.e. a smaller transition energy − is observed for **83**, as might have been expected for such a large cluster. In **79**, the assignment of formal charges results in two Cu^0 atoms and 24 Cu^+ centers, which implies a formal electron excess of two. In principle, this should also cause mixed-valence bands. However, the absorption spectrum of **79** only shows a red shift of the onset of the charge-transfer bands with respect to **57** from 600 to 800 nm. It cannot yet be established whether this is a general behavior of the two different types of mixed-valence copper telluride clusters possessing either an electron deficiency or an electron excess.

4. Conclusion and Outlook

Reactions of copper salts such as copper(I) acetate and copper(I) chloride with silylated chalcogen compounds $E(SiMe_3)_2$ or $RE(SiMe_3)$ (E = S, Se, Te; R = organic group) in the presence of tertiary phosphane ligands lead to the formation of ligand-stabilized copper chalcogenide or copper chalcogenide/chalcogenolate cluster molecules of different sizes. The synthesis of the cluster molecules is influenced in a complex manner by the reactants, ligands, and solvents used, and by the reaction temperature.

All copper sulfide clusters characterized to date show spherical molecular structures that give an insight into the structural principles of $[Cu_2E]_n$ aggregates. Rules that lead to maximum stability have been delineated by comparing the observed structures, and by quantum-chemically investigating a series with up to 20 copper atoms. They are strictly adhered to by small clusters, and remain widely valid for the larger Cu−S cluster compounds.

In the case of the copper selenide clusters, the molecular structures of smaller or middle-sized clusters of up to 59 copper atoms exhibit spherical cluster shapes and also follow the structural principles elucidated for the copper sulfide species. These cluster structures differ significantly from those of the larger molecules that possess hexagonal lattices of selenium atoms. Hence, the cluster formation of the smaller copper chalcogenide clusters seems to follow spontaneous aggregation processes leading to molecular species, whereas the crystallization of the larger ones represents instead the incipient formation of ordered solid-state structures. Although the final structure determination of the low-temperature α-Cu_2Se phase is still a point of discussion, the best refinement of the data is achieved by assuming a cubic lattice of selenium atoms with copper atoms occupying the tetrahedral and trigonal holes.[76] Therefore, it is possible that the cluster molecules display fragments of a new structure type of an as yet unknown Cu_2Se polymorph.

In contrast to the clusters containing sulfur or selenium ligands, copper telluride systems show a significant tendency to form non-stoichiometric clusters, with either an electron deficiency or an electron excess. This is not only evident from the overall charge, but is also shown by the occurrence of intervalence bands in the optical spectra of these compounds. Structural considerations as well as calculations on the electronic band structure reveal that a localization of the different formal oxidation states is not possible. Even though compound **79** contains a central Cu_6 octahedron with sufficiently short Cu−Cu distances, the charge excess cannot be assigned to $d^{10}-d^{10}$ interactions. The "additional" electron pair that arises from the formal assignment of charges Cu^+ and Te^{2-} is instead delocalized in an MO embedded in the tellurium(5*d*)−copper(4*s*) valence band. The distinct differences from the Cu_2S or Cu_2Se mixed-valence cluster systems can generally be attributed to the small differences between the ionization potentials (IP), electron affinities (EA), and electronegativities (EN) of copper and tellurium, which do not allow a discrete separation into Cu^+ and Te^{2-} centers [IP(Cu): 745.4, IP(Te): 869.2; EA(Cu): 118.5, EA(Te):190.2; EN(Cu, Pauling): 1.9, EN(Te): 2.1].

In the future, we aim to further investigate the thermal properties of these materials and to use them as precursor

compounds for the synthesis of nanostructured Cu_2E (E = S, Se, Te) phases. This will include the preparation of thin films of these materials, which may have applications in solar cell technology, as well as the synthesis of $Cu_{2-x}E$ compounds of precise, known compositions that may show interesting magnetic and electrical properties.

Acknowledgments

This work has been supported by the Deutsche Forschungsgemeinschaft (SFB 195), the State of Baden-Württemberg, the Fonds der Chemischen Industrie, and the Forschungszentrum Karlsruhe GmbH. We wish to acknowledge the financial support throughout this long period of time. The authors also gratefully acknowledge the help of Dr. Chris Anson in correcting the English.

[1] V. A. Fedorin, *Semiconductors* **1993**, *27*, 354−357.
[2] [2a] B. A. Mansour, S. E. Demian, H. A. Zayed, *J. Mater. Sci.* **1992**, *3*, 249−252; [2b] Z. Vučić, O. Milat, V. Horvatić, Z. Ogorelek, *Phys. Rev.* **1981**, *B24*, 5398−5401.
[3] [3a] G. Nimtz, P. Marquard, H. Gleiter, *J. Cryst. Growth* **1988**, *86*, 66−79; [3b] J. Koutecky, P. Fantucci, *Chem. Rev.* **1986**, *86*, 539−587; [3c] M. D. Morse, *Chem. Rev.* **1986**, *86*, 1049−1071; [3d] M. M. Kappes, *Chem. Rev.* **1988**, *88*, 369−389; [3e] H. Weller, *Angew. Chem.* **1993**, *105*, 43−50; *Angew. Chem. Int. Ed. Engl.* **1993**, *32*, 88−95.
[4] [4a] H. Weller, *Angew. Chem.* **1998**, *110*, 1748−1749; *Angew. Chem. Int. Ed.* **1998**, *37*, 1658−1659; [4b] A. P. Alivisatos, *Science* **1996**, *271*, 933−937; [4c] H. Weller, *Angew. Chem.* **1996**, *108*, 1159−1161; *Angew. Chem. Int. Ed. Engl.* **1996**, *35*, 1079−1081; [4d] *Clusters and Colloids* (Ed.: G. Schmid), VCH, Weinheim, **1995**.
[5] [5a] J. P. Fackler, Jr., D. Coucouvanis, *J. Am. Chem. Soc.* **1966**, *88*, 3913−3920; [5b] L. E. McCandlish, E. C. Bissell, D. Coucouvanis, J. P. Fackler, K. Knox, *J. Am. Chem. Soc.* **1968**, *90*, 7357−7359.
[6] I. G. Dance, *Aust. J. Chem.* **1978**, *31*, 2195−2206.
[7] P. Betz, B. Krebs, G. Henkel, *Angew. Chem.* **1984**, *96*, 293−294; *Angew. Chem. Int. Ed. Engl.* **1984**, *23*, 311−312.
[8] D. Ohlmann, H. Pritzkow, H. Grützmacher, M. Anthamatten, P. Glaser, *J. Chem. Soc., Chem. Commun.* **1995**, 1011−1012.
[9] D. Fenske, H. Krautscheid, S. Balter, *Angew. Chem.* **1990**, *102*, 799−801; *Angew. Chem. Int. Ed. Engl.* **1990**, *29*, 796−798.
[10] D. Fenske, H. Krautscheid, *Angew. Chem.* **1990**, *102*, 1513−1516; *Angew. Chem. Int. Ed. Engl.* **1990**, *29*, 1452−1454.
[11] D. Fenske, J. C. Steck, *Angew. Chem.* **1993**, *105*, 254−257; *Angew. Chem. Int. Ed. Engl.* **1993**, *32*, 238−242.
[12] H. Krautscheid, D. Fenske, G. Baum, M. Semmelmann, *Angew. Chem.* **1993**, *105*, 1364−1367; *Angew. Chem. Int. Ed. Engl.* **1993**, *32*, 1303−1305.
[13] S. Dehnen, A. Schäfer, D. Fenske, R. Ahlrichs, *Angew. Chem.* **1994**, *106*, 786−790; *Angew. Chem. Int. Ed. Engl.* **1994**, *33*, 764−768.
[14] S. Dehnen, D. Fenske, *Angew. Chem.* **1994**, *106*, 2369−2372; *Angew. Chem. Int. Ed. Engl.* **1994**, *33*, 2287−2289.
[15] S. Dehnen, D. Fenske, A. C. Deveson, *J. Clust. Sci.* **1996**, *7(3)*, 351−369.
[16] J. F. Corrigan, S. Balter, D. Fenske, *J. Chem. Soc., Dalton Trans.* **1996**, 729−738.
[17] S. Dehnen, D. Fenske, *Chem. Eur. J.* **1996**, *2*, 1407−1416.
[18] A. Deveson, S. Dehnen, D. Fenske, *J. Chem. Soc., Dalton Trans.* **1997**, 4491−4498.
[19] J. F. Corrigan, D. Fenske, *Angew. Chem.* **1997**, *109*, 2070−2071; *Angew. Chem. Int. Ed. Engl.* **1997**, *36*, 1981−1983.
[20] M. Semmelmann, D. Fenske, J. F. Corrigan, *J. Chem. Soc., Dalton Trans.* **1998**, 2541−2546.
[21] A. Eichhöfer, D. Fenske, *J. Chem. Soc., Dalton Trans.* **1998**, 2969−2972.
[22] M. Bettenhausen, A. Eichhöfer, D. Fenske, M. Semmelmann, *Z. Anorg. Allg. Chem.* **1999**, *625*, 593−601.
[23] N. Zhu, D. Fenske, *J. Chem. Soc., Dalton Trans.* **1999**, 1067−1075.
[24] A. Eichhöfer, J. F. Corrigan, D. Fenske, E. Tröster, *Z. Anorg. Allg. Chem.* **2000**, *626*, 338−348.
[25] N. Zhu, D. Fenske, *J. Clust. Sci.* **2000**, *11*, 135−151.
[26] H. Krautscheid, Ph. D. Thesis, University of Karlsruhe, **1991**.
[27] J. C. Steck, Ph. D. Thesis, University of Karlsruhe, **1992**.
[28] S. Balter, Ph. D. Thesis, University of Karlsruhe, **1994**.
[29] S. Dehnen, Ph. D. Thesis, University of Karlsruhe, **1996**.
[30] M. Semmelmann, Ph. D. Thesis, University of Karlsruhe, **1997**.
[31] A. Eichhöfer, D. Fenske, unpublished results.
[32] J. H. El Nakat, I. G. Dance, K. J. Fisher, G. D. Willet, *Inorg. Chem.* **1991**, *30*, 2957−2958.
[33] [33a] D. van der Putten, D. Olevano, R. Zanoni, H. Krautscheid, D. Fenske, *J. Electron. Spectrosc. Relat. Phenom.* **1995**, *76*, 207−211; [33b] A. Enderle, Diploma Thesis, University of Karlsruhe, **1993**; [33c] U. Stöhr, Diploma Thesis, University of Karlsruhe, **1993**.
[34] [34a] A. Schäfer, C. Huber, J. Gauss, R. Ahlrichs, *Theor. Chim. Acta* **1993**, *87*, 29−40; [34b] A. Schäfer, R. Ahlrichs, *J. Am. Chem. Soc.* **1994**, *116*, 10686−10692.
[35] S. Dehnen, A. Schäfer, R. Ahlrichs, D. Fenske, *Chem. Eur. J.* **1996**, *2*, 429−435.
[36] K. Eichkorn, S. Dehnen, R. Ahlrichs, *Chem. Phys. Lett.* **1998**, *284*, 287−292.
[37] A. Schäfer, Ph. D. Thesis, University of Karlsruhe, **1994**.
[38] [38a] *Structural Inorganic Chemistry* (Ed.: A. F. Wells), 5th ed., Clarendon Press, Oxford, **1984**; [38b] H. T. Evans, *Z. Kristallogr.* **1979**, *150*, 299−301.
[39] [39a] R. D. Heyding, R. M. Murray, *Can. J. Chem.* **1976**, *54*, 841−848; [39b] P. Rahlfs, *Z. Phys. Chem.* **1936**, *B31*, 157−159; [39c] W. Borchert, *Z. Kristallogr.* **1945**, *106*, 5−24; [39d] A. L. N. Stevels, *Philips Res. Rep. Suppl.* **1969**, *9*, 124; [39e] A. L. N. Stevels, F. Jellinek, *Recl. Trav. Chim.* **1971**, *90*, 273−283; [39f] A. Tonjec, Z. Ogorelec, B. Mestnik, *J. Appl. Crystallogr.* **1975**, *8*, 375−379.
[40] [40a] R. Blachnik, M. Lasocka, U. Walbrecht, *J. Sol. State Chem.* **1983**, *48*, 431−438; [40b] Y. G. Asadov, L. V. Rustamova, G. B. Gasimov, K. M. Jafarov, A. G. Babajev, *Phase Transitions* **1992**, *38*, 247−259.
[41] G. H. Aylward, T. J. V. Findlay, *Datensammlung Chemie*, VCH, Weinheim, **1986**, p. 125.
[42] C. A. Tolman, *Chem. Rev.* **1977**, *77*, 313−348.
[43] [43a] *Comprehensive Coordination Chemistry* (Ed.: G. Wilkinson), Vol. 5, Pergamon Press, Oxford, **1987**, p. 583f; [43b] M. G. B. Drew, A. H. B. Othman, D. A. Edwards, R. Richards, *Acta Crystallogr., Sect. B* **1975**, *31*, 2695−2697.
[44] [44a] R. Ahlrichs, M. Bär, M. Häser, H. Horn, C. Kölmel, *Chem. Phys. Lett.* **1995**, *242*, 652−660; [44b] O. Treutler, R. Ahlrichs, *J. Chem. Phys.* **1995**, *102*, 346−354; [44c] A. Schäfer, H. Horn, R. Ahlrichs, *J. Chem. Phys.* **1992**, *97*, 2571−2577.
[45] [45a] K. Eichkorn, O. Treutler, H. Öhm, M. Häser, R. Ahlrichs, *Chem. Phys. Lett.* **1995**, *242*, 652−660. [45b] K. Eichkorn, F. Weigend, O. Treutler, R. Ahlrichs, *Theor. Chim. Acta* **1997**, *97*, 119−124.
[46] C. Møller, M. S. Plesset, *Phys. Rev.* **1934**, *46*, 618.
[47] [47a] R. G. Parr, W. Yang, *Density Functional Theory of Atoms and Molecules*, Oxford University Press, New York, **1988**; [47b] T. Ziegler, *Chem. Rev.* **1991**, *91*, 651−667.
[48] [48a] G. Savelsberg, H. Schäfer, *Z. Naturforsch., Teil B* **1978**, *33*, 711−713; [48b] V. C. Burschka, *Z. Anorg. Allg. Chem.* **1980**, *463*, 65−71; [48c] R. S. Hall, J. M. Stewart, *Acta Crystallogr., Sect. B* **1973**, *29*, 579−581; [48d] J. E. Iglesias, K. E. Pachali, H. Steinfink, *J. Solid State Chem.* **1974**, *9*, 6−14.
[49] D'Ans, Lax, *Taschenbuch für Chemiker und Physiker*, Vol. 3 (Ed.: R. Blachnik), Springer, Berlin, Heidelberg, **1998**, p. 440.

[50] D'Ans, Lax, *Taschenbuch für Chemiker und Physiker*, Vol. 3 (Ed.: R. Blachnik), Springer, Berlin, Heidelberg, **1998**, p. 436.
[51] A. F. Hollemann, E. Wiberg, *Lehrbuch der Anorganischen Chemie*, W. de Gruyter, Berlin, **1985**, p.148.
[52] [52a] U. Müller, M.-L. Ha-Eierdanz, G. Kräuter, K. Dehnicke, *Z. Naturforsch., Teil B* **1990**, *45*, 1128−1132; [52b] J. Cusick, M. L. Scudder, D. C. Craig, I. G. Dance, *Polyhedron* **1989**, *8*, 1139−1141.
[53] [53a] M. G. Kanatzidis, Y. Park, *J. Am. Chem. Soc.* **1989**, *111*, 3767−3769; [53b] A. C. Sutorik, M. G. Kanatzidis, *J. Am. Chem. Soc.* **1991**, *113*, 7754−7755.
[54] G. Wedler, *Lehrbuch der Physikalischen Chemie*, VCH, Weinheim, **1987**, p. 168.
[55] D. Fenske, N. Zhu, T. Langetepe, *Angew. Chem.* **1998**, *110*, 2784−2788; *Angew. Chem. Int. Ed.* **1998**, *37*, 2640−2644.
[56] [56a] J. B. Foresman, M. Head-Gordon, J. A. Pople, M. J. Frisch, *J. Phys. Chem.* **1992**, *96*, 135−149; [56b] R. McWheeny, *Methods of Molecular Quantum Mechanics*, 2nd ed., Academic Press, London, **1992**.
[57] K. Raghavachari, G. W. Trucks, J. A. Pople, M. Head-Gordon, *Chem. Phys. Lett.* **1989**, *157*, 479−483.
[58] F. Schwabl, *Quantenmechanik*, Springer, Heidelberg, **1990**, p. 189f.
[59] A. A. Voskanyan, P. N. Inglizyan, S. P. Lalykin, I. A. Plyutto, Y. M. Shevchenko, *Fiz. Tekh. Poluprovodn.* **1978**, *12*, 2096−2099.
[60] E. J. D. Garba, R. L. Jacobs, *Physica B+C* **1986**, *138*, 253−260.
[61] S. N. Mostafa, S. A. Schiman, *Ber. Bunsenges. Phys. Chem.* **1983**, *87*, 113−119.
[62] P. Scherrer, *Göttinger Nachrichten* **1918**, *2*, 98f.
[63] Y. Park, Ph. D. Thesis, Michigan State University, **1992**.
[64] K. O. Klepp, *J. Less Common Met.* **1987**, *128*, 79−89.
[65] G. Savelsberg, H. Schäfer, *Mater. Res. Bull.* **1981**, *16*, 1291−1297.
[66] Y. Park, D. C. Degroot, J. Schindler, C. R. Kannewurf, M. G. Kanatzidis, *Angew. Chem.* **1991**, *103*, 1404−1407; *Angew. Chem. Int. Ed. Engl.* **1991**, *30*, 1325−1328.
[67] [67a] Y. Park, M. G. Kanatzidis, *J. Chem. Mater.* **1991**, *3*, 781−783; [67b] X. Zhang, Y. Park, T. Hogan, J. L. Schindler, C. R. Kannewurf, S. Seong, T. Albright, M. G. Kanatzidis, *J. Am. Chem. Soc.* **1995**, *117*, 10300−10310.
[68] M. Emirdag, G. L. Schimek, J. W. Kolis, *J. Chem. Soc., Dalton Trans.* **1999**, 1531−1532.
[69] D. Fenske, J. F. Corrigan, in *Metal Clusters in Chemistry* (Eds.: P. Braunstein, L. A. Oro, P. R. Raithby), Wiley-VCH, Weinheim, **1999**, Vol. 3, p. 1302.
[70] [70a] F. C. Frank, J. S. Kasper, *Acta Crystallogr.* **1958**, *11*, 184−190; [70b] F. C. Frank, J. S. Kasper, *Acta Crystallogr.* **1959**, *12*, 483−499.
[71] [71a] C. Kölmel, R. Ahlrichs, *J. Phys. Chem.* **1990**, *94*, 5536−5542; [71b] F. A. Cotton, X. Feng, M. Matusz, R. Poli, *J. Am. Chem. Soc.* **1988**, *110*, 7077−7083; [71c] K. M. Merz, R. Hoffmann, *Inorg. Chem.* **1988**, *27*, 2120−2127.
[72] U. Müller, *Anorganische Strukturchemie*, 2nd Ed., B. G. Teubner, Stuttgart, **1991**, p. 101f.
[73] [73a] F. Jellinek, in *MTP International Review of Science, Inorganic Chemistry Series One*, *Vol. 5* (Ed.: D. W. Sharp), Butterworths, London, **1972**, p. 339; [73b] C. W. Folmer, F. Jellinek, *J. Less Common Met.* **1980**, *76*, 153−162.
[74] R. Ahlrichs, J. Besinger, A. Eichhöfer, D. Fenske, A. Gbureck, *Angew. Chem.* **2000**, *112*, 4089−4099; *Angew. Chem. Int. Ed.* **2000**, *39*, 3923−3933.
[75] M. B. Robin, P. Day, *Adv. Inorg. Radiochem.* **1967**, *10*, 247−422.
[76] S. Kashida, J. Akai, *J. Phys. C: Solid State Phys.* **1988**, *21*, 5329−5336.

Received March 28, 2001
[I01112]